DISSERTATION

PASSIVATION STUDIES ON $Cd_{0.6}Zn_{0.4}Te$ FILMS USING $CdCl_2$, $MgCl_2$ and $ZnCl_2$ FOR TOP CELL APPLICATION IN A MULTIJUNCTION SOLAR CELL

Submitted by

Tushar M. Shimpi

Department of Mechanical Engineering

In partial fulfillment of the requirements

For the Degree of Doctor of Philosophy

Colorado State University

Fort Collins, Colorado

Summer 2018

Doctoral Committee

Advisor: W. S. Sampath

James R. Sites
Arun K. Kota
Ketul C. Popat

Copyright by Tushar Shimpi 2018

All Rights Reserved

ABSTRACT

PASSIVATION STUDIES ON $Cd_{0.6}Zn_{0.4}Te$ FILMS USING $CdCl_2$, $MgCl_2$ and $ZnCl_2$ FOR TOP CELL APPLICATION IN A MULTIJUNCTION SOLAR CELL

The passivation treatment with the chloride compounds is an important step in the fabrication of II-VI solar cells for improving the device performance. In the cadmium telluride solar cells, the cadmium chloride passivation treatment incorporates chlorine along the grain boundaries and helps in recrystallization, grain growth, removal of stacking faults and doping grain boundaries as n-type. In the cadmium zinc telluride solar cells, the retention of zinc after the cadmium chloride passivation treatment is one of the challenges incurred in fabricating the top cell in a multijunction solar cell. During the passivation treatment, the loss of zinc occurs in the form of volatile zinc chloride compound. The depletion or complete loss of zinc reduces the higher band gap ternary alloy into lower band gap binary compound of CdTe. This impedes the purpose of fabricating a high band gap top cell in a multijunction solar cell.

The focus of this study is on passivating $Cd_{0.6}Zn_{0.4}Te$ (CdZnTe) films using three different chloride compounds separately and understanding the effects by studying the material properties of the passivated films and electrical performance of the fabricated devices. In the preliminary experiments, the CdZnTe films were deposited by RF sputtering from a single target. Initial characterization of CdZnTe films deposited on plain glass indicated that the films had a strong preferred orientation along {111} plane with a band gap of ~1.72eV. In the cadmium chloride passivation treatment, loss of zinc from the surface and no chlorine along the grain boundaries was observed from transmission electron microscope images and X ray diffraction measurements. No loss of zinc was observed after the magnesium chloride and zinc chloride

passivation treatments. Increase in the grain size of the CdZnTe films after magnesium chloride treatment and decrease of the preferred orientation after zinc chloride treatment were the benefits of the individual passivation treatments. Modifying the test structure by adding a cadmium telluride film as a capping layer on the back of RF sputtered CdZnTe and then carrying out the cadmium chloride passivation treatment helped in retaining the zinc. Heavy diffusion of zinc into cadmium sulphide due to cadmium telluride deposition at high temperature and difficulty to isolate the photo current generated by cadmium telluride were few drawbacks of this test structure.

Based on the insights gained from the preliminary experiments, two sets of experiments were conducted. In the first set, cadmium sulphide cap as a barrier was deposited on the back of RF sputtered CdZnTe and co-sublimated cadmium telluride and zinc films with a band gap of 1.72 eV. The bulk composition was maintained after the cadmium chloride passivation treatment in the films deposited by both the methods. However the device performance of co-sublimated films was better than the RF sputtered CdZnTe devices. The transmission electron image obtained from the cross section of co-sublimated film fitted with cadmium sulphide cap and then treated with cadmium chloride showed presence of chlorine along the grain boundaries.

The zinc chloride passivation treatments with higher substrate temperature compared to the source were the second set of experiments. The zinc loss from RF sputtered CdZnTe films after the cadmium chloride treatment did not occur. The fabricated devices exhibited diode like behavior. The images under scanning electron microscopy showed that the grain size did not increase after the zinc chloride treatment.

ACKNOWLEDGEMENTS

I would like to thank my advisor Dr. Sampath for his support and guidance in my PhD. program. Dr. Sites' insights and suggestions on the project during the lab meetings were very helpful and would like to thank him. I would like to thank Dr. Popat and Dr. Kota for taking time to serve on the committee. I would like to thank Kurt Barth for helping me in the project and Lab manager Kevan Cameron for taking care of scheduling and lab supplies.

A special thanks to Dr. Munshi and researchers (Dr. Walls and Dr. Abbas) from Loughborough University for the help in material characterization using TEM. I would like to thank, Dr. Kephart and Dr. Swanson for installing the sputter chamber and answering my queries from time to time. Dr. Swanson also helped me in teaching co-sublimation process and would like to thank him again.

Most of the electrical characterization work was done in the Photovoltaic Lab in the physics department. I would like to thank Dr. Drayton, Dr. Raguse, Dr. Geisthardt, Dr. Moore, Anna Wojtowicz, Ramesh Pandey and Kahl Counts. I would like to thank Dr. Newell, Dr. McCurdy and Dr. Geiss from CIF, Chemistry department for their instructions in material characterization. I would also like to thank lab memebers: Marina, Christina, James and Kyle for their help. Special thanks to Carey Reich for regular maintenance of co-sublimation deposition chamber.

This project is funded by NSF I/UCRC Next Generation Photovoltaics and Accelerated Innovative Research program. I would like to express my gratitude. Thanks to the Industrial Advisor Board Members Dr. Rick Powell (First Solar), Dr. Alan Davies (First Solar), Jean-Nicholas Beaudry (5N Plus), Mandar Sunthankar (Ion Edge), Raju Jairam (MBI Corp.).

Last but not least; I would like to wholeheartedly thank my family members for their love and support.

DEDICATION

Passivation of polycrystalline CdZnTe absorber has been a challenge with minimal progress recorded in the literature for the last two decades.The graph shows the chronological progress since the inception of the project, in passivating CdZnTe and importantly, maintaining the composition after the $CdCl_2$ treatment.The passivation of CdZnTe is main focus of this dissertation.

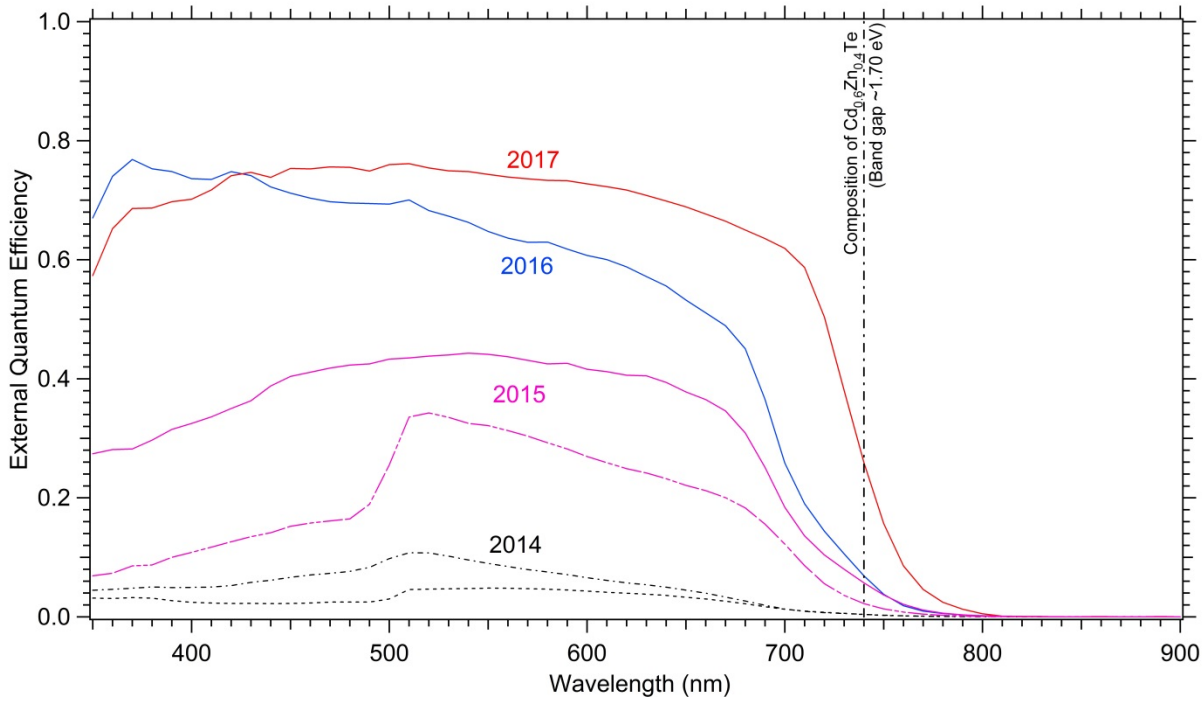

I dedicate this dissertation to my teachers who have inspired me to think out of the box.

TABLE OF CONTENTS

ABSTRACT ii

ACKNOWLEDGEMENTS iv

DEDICATION vi

LIST OF TABLES vii

LIST OF FIGURES viii

Chapter 1 1

Multi-junction Solar Cells 1

1.1 Single Junction Solar Cell 1

1.2 Thermalization Losses 1

1.3 Multijunction Solar Cells 3

1.4 Road Map for High Efficiency CdTe Based Devices 5

1.5 Literature Review 6

1.6 Motivation 9

Chapter 2 10

Sample Preparation and Characterization 10

2.1 Project Background 10

2.2 CdS Deposition in Advanced Deposition Research System 11

2.3 Passivation Treatment 12

2.4 Passivation treatment in ARDS 14

2.5 Copper Doping in ARDS and Tellurium Deposition Process 14

2.6 Small Area Device (SAD) Fabrication 15

2.7 RF Sputtering of CdZnTe Films 15

2.8 Characterization of CdZnTe films 17

2.9 Co-sublimation of CdTe and Zn 22

2.10 Characterization of co-sublimated Cd-Zn-Te films 23

Chapter 3 27

Preliminary Passivation Treatments on Sputtered CdZnTe with Chloride Compounds 27

3.1 $CdCl_2$ Passivation Treatment on RF sputtered CdZnTe 27

3.2 $CdCl_2$ Passivation on CdZnTe films with CdTe film capping 32

3.3 $MgCl_2$ Passivation Treatment on CdZnTe 37

3.4 $ZnCl_2$ passivation treatment of CdZnTe 40

Chapter 4 46

$CdCl_2$ Passivation Treatment on CdZnTe with CdS Capping Layer 46

4.1 Insights from the TEM/EDS of CdZnTe Cross Sections 46

4.2 Tested Hypothesis on RF Sputtered CdZnTe with CdTe Capping Layer During the $CdCl_2$ Passivation Treatment 47

4.3 Modified Device Structure Using CdS Capping Instead of CdTe 48

4.4 $CdCl_2$ Treatment on RF Sputtered CdZnTe with CdS Capping 49

4.5 Device Performance of RF sputtered CdZnTe with CdS capping treated with $CdCl_2$ 50

4.6 $CdCl_2$ treatement on co-sublimated CdZnTe with CdS capping 54

4.7 Device Performance of Co-Sublimated CdZnTe with CdS Capping Treated with $CdCl_2$ 55

Chapter 5 66

$ZnCl_2$ Passivation Treatment on RF Sputtered CdZnTe 66

5.1 Tested Hypothesis RF Sputtered CdZnTe with $ZnCl_2$ Passivation Treatment 66

5.2 Source Modification in the Horizontal Bell Jar 67

5.3 Graphite Source and Substrate Temperature Measurements 68

5.4 $ZnCl_2$ Passivation Treatment on RF Sputtered CdZnTe with New Source and Higher Substrate Temperature 71

5.5 Transmission Measurements on RF Sputtered CdZnTe After $ZnCl_2$ Passivation Treatment with New Source and Higher Substrate Temperature 72

5.6 Tape Test on RF Sputtered CdZnTe after the $ZnCl_2$ Passivation Treatment with New Source and Higher Substrate Temperature 73

5.7 Device Performance of RF Sputtered CdZnTe after $ZnCl_2$ Passivation Treatment with New Source and Higher Substrate Temperature 74

5.8 SEM Images of RF Sputtered CdZnTe after the $ZnCl_2$ Passivation Treatment with New Source and Higher Substrate Temperature 75

Chapter 6 76

Conclusions and Future Work 76

6.1 Summary 76

6.2 $CdCl_2$ Treatment of RF Sputtered CdZnTe 76

6.3 $CdCl_2$ Treatment on RF Sputtered CdZnTe with CdTe Cap Acting as a Capping 77

6.4 . $CdCl_2$ Treatment on RF Sputtered CdZnTe and Co-Sublimated CdTe and Zn with CdS Cap Acting as a Capping 77

6.5 $MgCl_2$ Treatment on RF Sputtered CdZnTe 78

6.6 $ZnCl_2$ Treatment on RF Sputtered CdZnTe 78

6.7 Overall Conclusions 78

6.8 Future Work 78

Bibliography 79

LIST OF TABLES

Table 1 Standard copper doping process 15

Table 2 Process Parameters for Characterization 17

Table 3 Deposition Rate Measurements 18

Table 4 CdZnTe Deposition Parameters 27

Table 5 CdZnTe deposition parameters for CdTe capping 33

Table 6 Passivation treatments with $MgCl_2$ 37

Table 7 $ZnCl_2$ passivation treatment conditions 41

Table 8 JV Testing on $ZnCl_2$ Passivated Devices 44

Table 9 Outline of process parameters varied 50

Table 10 List of RF sputtered CdZnTe samples fitted with CdS capping layer and treated with $CdCl_2$ 51

Table 11 Composition of contributing elements obtained from the line scans 60

Table 12 $ZnCl_2$ passivation treatment conditions with new graphite source 72

LIST OF FIGURES

Figure 1 Efficiency with varying Bandgap [7] 2

Figure 2 Thermalization Losses and Unutilized Photons below the Band Gap 3

Figure 3 Generic Structure of Multijunction Solar Cells 4

Figure 4 Efficiency vs Number of Junctions[10] 5

Figure 5 Generic Sample Structure 11

Figure 6 Horizontal Bell Jar Set Up 13

Figure 7 Temperature Profile for the Bottom Thermocouple 13

Figure 8 Schematic of RF Sputter Chamber 16

Figure 9 Deposition Time vs Measured Thickness 18

Figure 10 Countour plot 19

Figure 11 Transmission of CdZnTe deposited on glass 20

Figure 12 Transmission on CdZnTe deposited on CdS/Tec12D 20

Figure 13 X Ray Diffraction on CdZnTe deposited on Glass 21

Figure 14 Schematic of co-sublimation source for fabricating Cd-Zn-Te films 23

Figure 15 Transmission measurements on samples fabricated by varying the Zn source temperature 23

Figure 16 Increase in the band gap of deposited Cd-Zn-Te films with increase in the Zn source temperature 24

Figure 17 Glancing angle X-ray diffraction of Cd-Zn-Te films deposited with increasing Zn source temperature 25

Figure 18 Lattice parameter calculated as well as from the literature versus band gap 26

Figure 19 Transmission on the $CdCl_2$ Passivated Samples 28

Figure 20 X Ray diffraction of the $CdCl_2$ passivated samples 28

Figure 21 $CdCl_2$ passivated sample at 380^o C 29

Figure 22 $CdCl_2$ passivated sample at 400^o C 30

Figure 23 SEM images of CdZnTe surface Treated at Different Temperatures (a) As Deposited CdZnTe, (b)$CdCl_2$ Temperature 380^oC (c) $CdCl_2$ Temperature $400\ ^oC$ 31

Figure 24 JV Data on $CdCl_2$ passivated sample 32

Figure 26 CdZnTe with CdTe Cap passivated with $CdCl_2$ at 380C 34

Figure 27 CdZnTe with CdTe Cap passivated with $CdCl_2$ at 400C 34

Figure 28 JV Measurements on $CdCl_2$ treatment at different temperatures on the best CdS/CdZnTe/CdTe devices 35

Figure 29 QE Measurements on $CdCl_2$ treatment at different temperatures on the best CdS/CdZnTe/CdTe devices 36

Figure 30 Band Gap Deduced From QE Measurements 37

Figure 31 Transmission Measurements after $MgCl_2$ passivation 38

Figure 32 SEM image of $MgCl_2$ passivated CdZnTe for 20 minutes 39

Figure 33 Parameters from JV Testing of $MgCl_2$ passivated Sample 40

Figure 35 Transmission measurements on CdZnTe Films after $ZnCl_2$ treatment 41

Figure 36 X Ray diffraction of $ZnCl_2$ passivated sample 42

Figure 37 SEM images of the substrate passivated with $ZnCl_2$ 43

Figure 38 EDS Point analysis of the substrate passivated with $ZnCl_2$ 43

Figure 39 Delamination of CdZnTe after $ZnCl_2$ passivation at 380C 3minutes, No Spacers 44

Figure 40 JV Measurements On $ZnCl_2$ Passivated (380^o C, 15minutes and With Spacers) Substrates 45
Figure 41 JV Measurements On $ZnCl_2$ Passivated (380^o C,3 min and No Spacers) Substrates... 45
Figure 42 Modified device structure with CdS capping layer 48
Figure 43 Transmission measurements CdS etched from RF sputtered CdZnTe that had undergone $CdCl_2$ treatment 52
Figure 44 JV graph of devices fabrciated after etching CdS capping from RF sputtered CdZnTe treated with $CdCl_2$ 53
Figure 45 External quantum efficiency of devices fabrciated after etching CdS capping from RF sputtered CdZnTe treated with $CdCl_2$ 53
Figure 46 Co-sublimated CdZnTe samples used to test the efficacy of CdS capping layer during the $CdCl_2$ treatment 54
Figure 47 Transmission measurements on co-sublimated CdZnTe samples 55
Figure 48 Bright field image of the cross section of the CdZnTe sample fitted with CdS capping layer and treated with $CdCl_2$ treatment 56
Figure 49 Elemental maps collected from the cross section of co-sublimated CdZnTe sample fitted with CdS cap and treated with $CdCl_2$ 57
Figure 50 Line scans on the cross section of the co-sublimated CdZnTe sample fitted with CdS cap and treated with $CdCl_2$ 59
Figure 51 Glancing angle X-ray diffraction on the co-sublimated CdZnTe samples and Tec 10 glass 61
Figure 52 JV graphs of the devices fabricated from the co-sublimated CdZnTe samples. 63

Figure 53 External quantum efficiency measurement on the devices fabricated from the co-sublimated CdZnTe samples 64

Figure 54 a) Accumulated $ZnCl_2$ after the treatement in the grapite source without any pockets. b) non-uniform $ZnCl_2$ treatment on the substrate 67

Figure 55a) New graphite source with pockets was fabricated. b) $ZnCl_2$ was contained in the pockets after the treatment 68

Figure 56 Temperature measurements using the parameters in section 2.3 69

Figure 57 Temperature measurements with fixed top plate temperature fixed and the temperature of the graphite source was varied to a) 340^{o}C, b) 360^{o}C and c) 380^{o}C. 71

Figure 58 Transmission measurements on RF sputtered CdZnTe after $ZnCl_2$ passivation in the new graphite source and at higher substrate temperature. a) passivation treatment temperature varied. b) passivation treatment time varied 73

Figure 59 JV device performance of RF sputtered CdZnTe after $ZnCl_2$ passivation in the new graphite source and at higher substrate temperature. a) passivation treatment temperature varied. b) passivation treatment time varied 74

Figure 60 SEM images of CdZnTe (a) before and (b)(c)&(d) after the $ZnCl_2$ passivation treatment at for 3 minutes with the new source and higher substrate temperature 75

Chapter 1
Multi-junction Solar Cells

1.1 Single Junction Solar Cell

The earth receives solar energy in the form of electromagnetic radiations. The electromagnetic radiations can be quantified in small packets of different energies called photons [1] [2]. The single junction solar cell is made up of semiconductor material with a fixed band gap. When photons of higher energy or energy equal to the band gap are absorbed, electron hole pairs are created. An electric field present due to the dissimilar materials at the junction (n-type and p-type semiconductor), sweeps electrons and holes to the respective electrodes. The electrons flow through an external circuit to combine with the holes thereby performing work [2] [1].

The performance of the solar cells depends on how efficiently the incident light is converted into electric power. For a single junction Cadmium Telluride (CdTe) solar cell, the maximum theoretical efficiency is equal to ~33% derived from Shockley Queisser limit[3]. In the past five years, the efficiency of CdTe solar cell has increased by 23% [4]. First Solar is the largest CdTe module manufacturer and recently has reported world record CdTe cell efficiency of 22.1%[5]. As the fabricated device efficiency approaches theoretical efficiency, there is a need to maximize energy per unit area by utilizing the photons efficiently and minimize losses in the devices. A multijunction solar cell is one approach to maximize energy and minimize losses.

1.2 Thermalization Losses

In converting the incident light into electric power, there are intrinsic and extrinsic losses [6] which are quantified and presented graphically in the graph below.

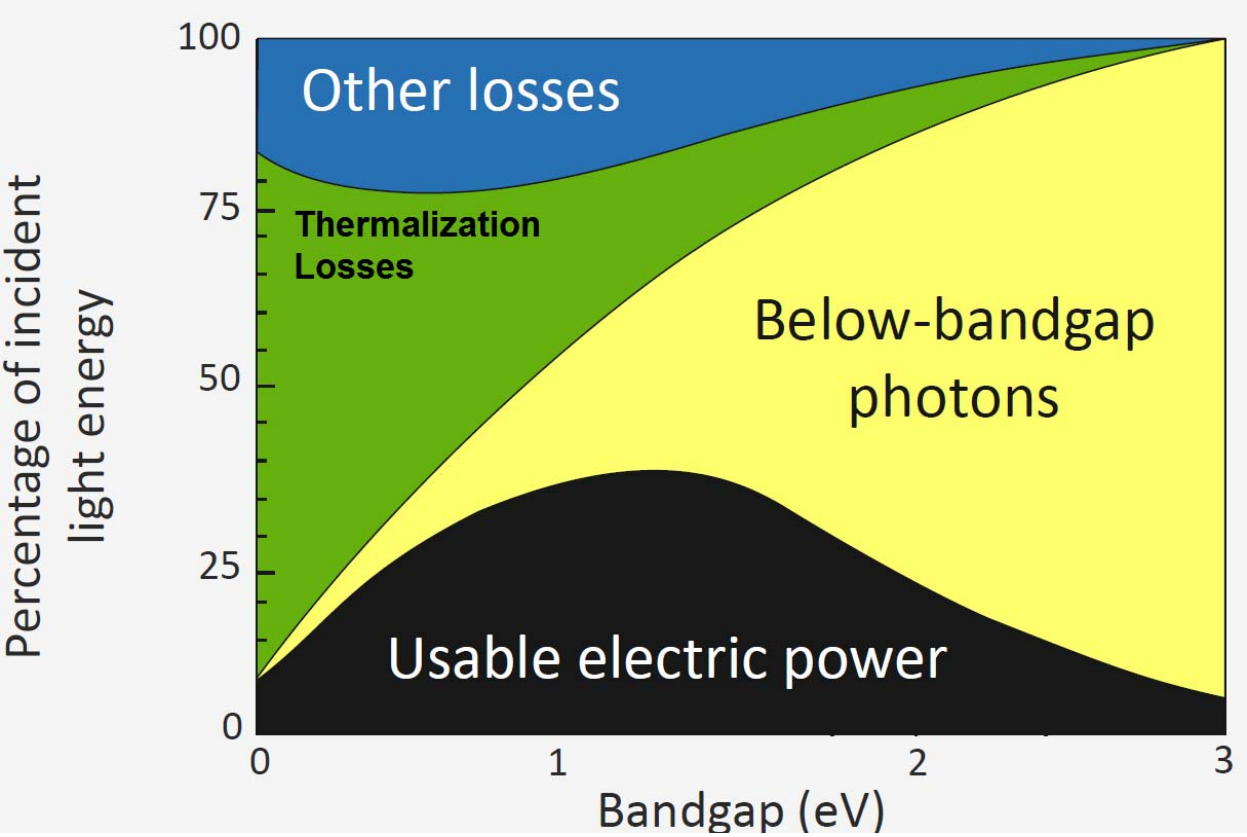

Figure 1 Efficiency with varying Bandgap [7]

As seen from the graph, two major losses are thermalization losses (highlighted in green region) and unutilized photons (highlighted in yellow region) below the band gap of the single junction solar cells. To understand both these losses, three cases are shown in the Figure 2 [8]

Case A. When a photon incident on the solar cell with a energy equal to the band gap, electron hole pairs are generated. Electrons are excited from valence band to conduction band edge. Due to the electric field, holes and electrons are swept to the respective electrodes.

Case B. When photon of higher energy than the band gap of the solar cell is incident on the solar cell, electron hole pairs are created. The electrons from the valence band are excited to the conduction band. After losing the energy in form of heat, electron relaxes to the conduction band edge. Due to electric field, electron is swept towards the respective electrode.

The energy loss in form of heat is transferred to the lattice as phonon energy and is not recoverable. This loss of energy is called thermalization loss.

Case C. In this case, photon energy is less than the band gap of the solar cell. Due to less energy, photon is not absorbed and no electron hole pair is created. This loss is term as unutilized energy.

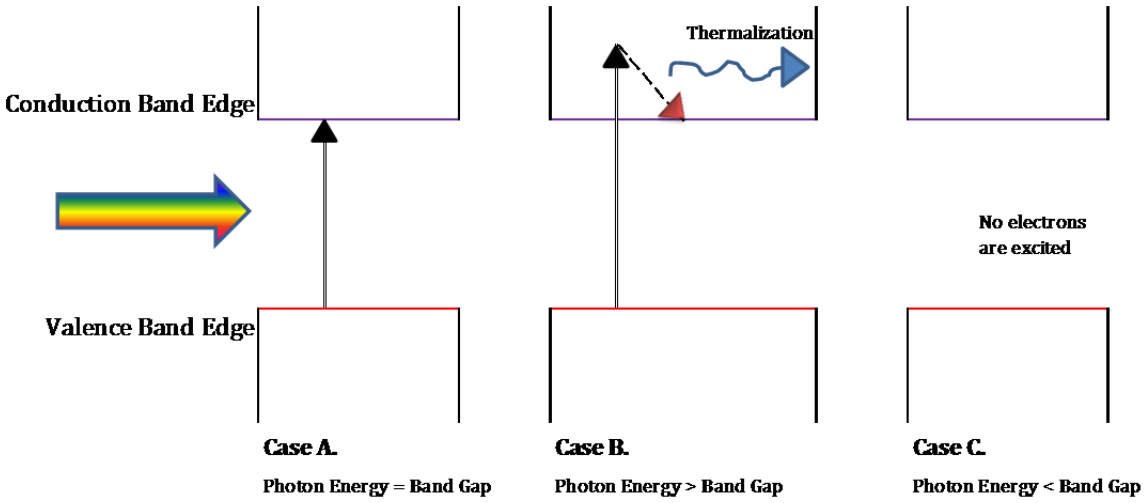

Figure 2 Thermalization Losses and Unutilized Photons below the Band Gap

1.3 Multijunction Solar Cells

To avoid thermalization losses, the solar cell needs to be fabricated with high band gap material. This high band gap solar cell will utilize short wavelength photons and thereby reduce the thermalization losses. But the low energy photons will be unutilized and photo current generated will be low. To utilize all the photons available, the solar cell needs to be fabricated with lower band gap material. This will increase the photo generated current but induce heavy thermalization losses with lower voltage. Since the power generated is product of voltage and current, the power produced by the solar cells will be low in both the circumstances. To efficiently utilize the photons from the sun's spectrum and minimize thermalization losses, multijunction solar cells are a promising alternative.

A generic structure of a multijunction solar cell is shown (Figure 3).

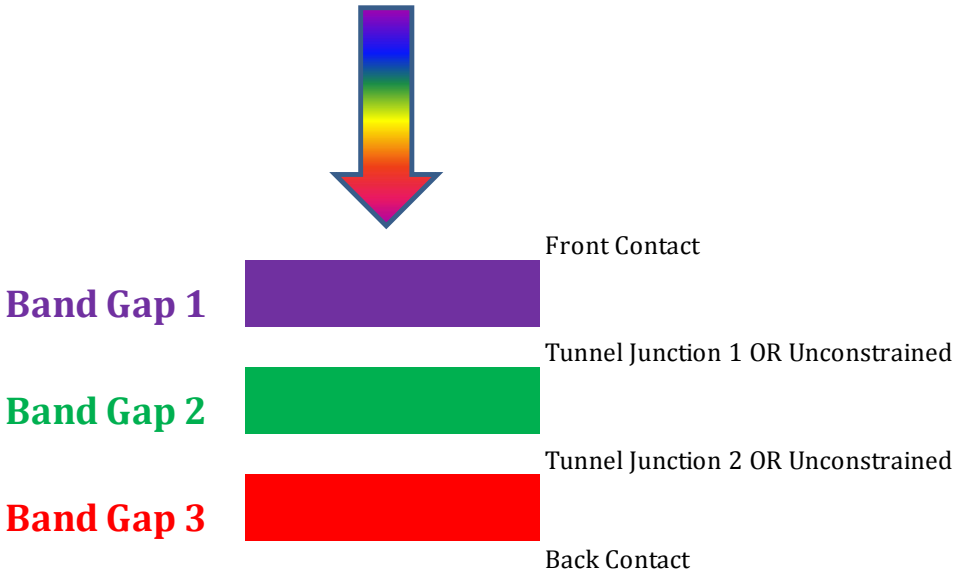

Figure 3 Generic Structure of Multijunction Solar Cells

The individual junctions are designed so that it would absorb a specific portion of the sun's spectrum. The top cell absorbs short wavelength photons and is transparent to photons with energies lower than the band gap. Similar process continues with the junctions stacked below the top cell [8]. If the junctions are connected through a tunnel junction (constrained), then the current passing through each junction must be the same. The individual junctions can be stacked mechanically on one over the other and connected separately (unconstrained). In this type of connection, current matching is not required but requires the contact electrodes to be extremely transparent [9].

The gain in the total efficiency is higher with two or three junctions as shown in the graph (Figure 4). Above three junctions, the gain in the efficiency is receded and substantially plateaus. Taking the practical considerations for fabrication and manufacturing of multijunction solar cells, 2 or 3 junctions is ideal.

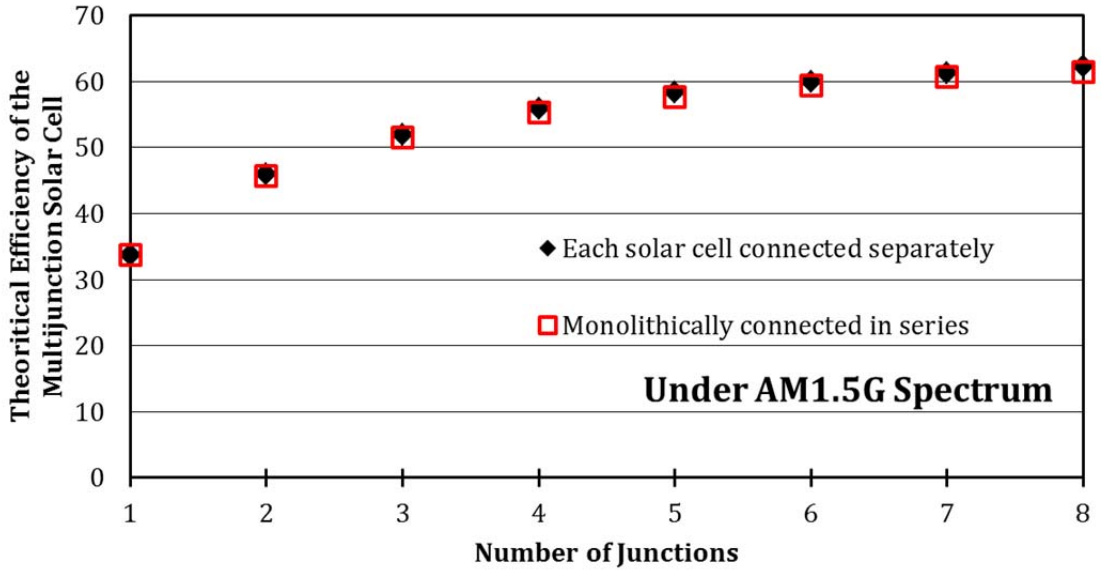

Figure 4 Efficiency vs Number of Junctions[10]

1.4 Road Map for High Efficiency CdTe Based Devices

The research on fabrication of CdTe devices started at Colorado State University (CSU) in 1991. Over the years, the device structure has changed and process parameters have been varied to produce high efficiency devices but the absorber material in all the devices has been CdTe based. In 2011, the lab became a part of I/UCRC Next Generation Photovoltaics (NGPV) Center supported by National Science Foundation. More information about the NGPV's goals and activites can be found on the website at http://www.nextgenpv.org/ .

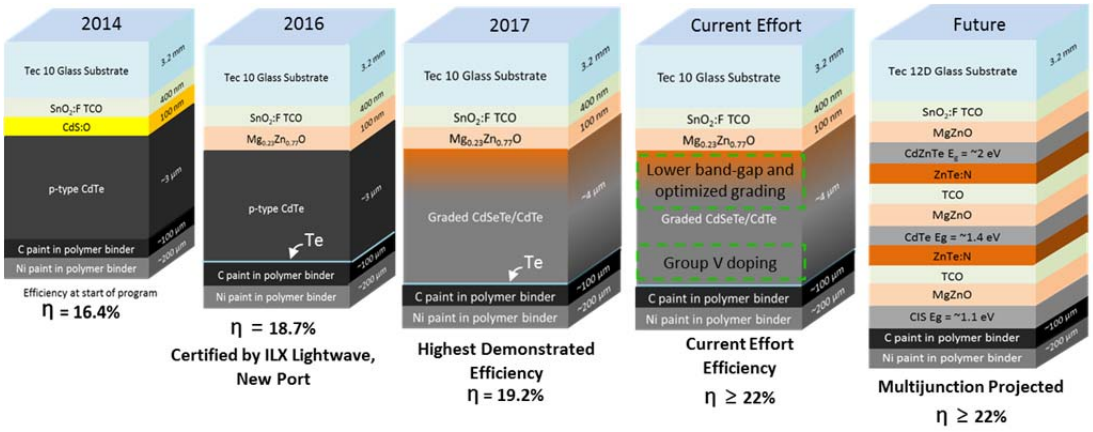

Figure 5 Roadmap for high efficiency CdTe based devices

The roadmap to obtain high efficiency CdTe based devices is shown in the Figure 5. Last year, team members working on the single junction CdTe demonstrated 19.1% efficient devices by lowering the band gap of the absorber. The on-going efforts are to optimized the band gap of the absorber and introduce doping at the back to further improve the efficiency of single junction CdTe based device. The final frontier on the roadmap is to fabricate a multijunction solar cell preferably made from CdTe based absorbers. The multijunction solar cell shown in the figure has three junctions. The top cell absorber in the multijunction solar cell is proposed to be fabricated using ternary alloy of CdZnTe. I joined CSU as a PhD student in 2012 and started working on the CdZnTe top cell project in 2014.

1.5 Literature Review

The passivation treatment is an important step in II VI solar cells and is carried out after the deposition of the absorber layer. The passivation treatment also called as post annealing or vapor treatment. The treatment is done in the presence of a halogen compound. Most commonly used halogen in this treatment is chlorine. The passivation of cadmium telluride (CdTe) solar cells with cadmium chloride ($CdCl_2$) compound is widely researched and frequently reported in the literature. Recently it has been shown that using magnesium chloride ($MgCl_2$) compound

which is less toxic than $CdCl_2$ compound can also improve the electrical performance of CdTe solar cells [11]. The improvements in the electrical performance of CdTe solar cells are due to following effects that happen after the $CdCl_2$ treatment.

- Chlorine along the grain boundaries [12][13]
- Recrystallization and grain growth in CdTe layer[14][15][16][13]
- Loss of preferred orientation along {111} plane and increase in random orientation [17]
- Elimination of stacking faults[18]

CdTe and CdZnTe have the same cubic zinc blende structure [19][20]. The band gap the ternary alloy can be varied from 1.48eV to 2.26eV by changing the amount of zinc [21]. Insights understood from the passivation of CdTe devices can be implemented on CdZnTe for better device performance.

Initial literature survey on CdZnTe material with 2.0 eV band gap for top cell absorber did not yield any results. So it was decided to focus on lower band gap CdZnTe absorber for which journal papers were available. The numerical simulations [22] for optimum band gap for the two junction solar cell indicate that the top cell can have a band gap in between the range of 1.65eV to 1.72eV. The bottom cell pairing with the top cell should have a band gap between 0.9eV to 1.1eV. The simulations are done on the assumptions that there are no internal losses, reflection losses are zero and the photo current generated from each solar cells is the same. $Cd_xZn_{1-x}Te$ [23] [24][25], $Cd_xMn_{1-x}Te$, [23][26] and $Cd_xMg_{1-x}Te$ [27] are different candidate materials whose band gap can be tuned to 1.72eV.

The compound selected for this study is a ternary alloy with composition of $Cd_{0.6}Zn_{0.4}Te$ and band gap of 1.72eV. Various research groups have investigated CdZnTe as an absorber layer for the top cell. CdZnTe with different compositions of zinc, have been deposited by vapor

transport method [28], closed space sublimation [29], co-sputtering [30], MOCVD [31] [32] , single target sputtering [33] [23], co-sputtering of CdTe and ZnTe [30] [34] and sequential layers of CdTe and ZnTe deposition with heat treatment for diffusion [35]. The deposited CdZnTe films with RF sputtering had preferred orientation along {111} plane [23][24].

McCandless [21] evaluated $CdCl_2$ and $ZnCl_2$ treatment on co-evaporated CdZnTe with ZnTe composition of 40%.The treatment temperature was 400^oC and time was for 15 minutes. Zinc loss was confirmed after $CdCl_2$ treatment. At lower pressure, no zinc loss was observed after treating with $ZnCl_2$. $ZnCl_2$ treatment in air forms ZnO. The photo current generated was low and fill factors were not mentioned.

Lee etal [23][24], RF sputtered CdZnTe from a single target. The deposited films had composition of 20% and 30% ZnTe from the individual targets containing 25% and 40% ZnTe. This indicates sputtering of the target material was not uniform. $CdCl_2$ treatment removed zinc and the films delaminated. The mixture of $CdCl_2$ + 0.05% $ZnCl_2$ was used to compensate the vapor pressure of the individual materials. Annealing in 2%H_2 + Ar gas at high temperature increased the crystalline quality of the CdZnTe films but did not improve the device performance. No loss of zinc occurred after the annealing treatment. On the best performing device, the zinc composition was x= 0.05.

Dheere etal [29] sublimated mixed powders of CdTe and ZnTe. But due to high vapor pressure of CdTe, the deposited films were entirely CdTe. It was also found that presence of oxygen at any processing step was a concern due to formation of zinc oxide. No devices were fabricated. Sivaraman [36] deposited CdZnTe with closed space sublimation and then treated with H_2 gas at 400^oC. The fabricated devices have open circuit voltage (V_{oc}) of 640mV and short circuit current (J_{sc}) of 4.5mA/cm^2. The fill factor was below 40 and no loss of zinc was observed.

McCandless etal [28] investigated $CdCl_2$ and $ZnCl_2$ treatment on CdZnTe film using vapor transport method. Using EDS and depth profiling, it was found that zinc loss happens through the surface. $ZnCl_2$ treatment at 400^oC for 20 minutes did not show any loss of zinc. The best device performance was V_{oc} = 775mV, J_{sc} = 20.8 mA/cm^2, FF = 54 with zinc composition equal to 0.27 at the start. The band gap deduced from the quantum efficiency measurements show that the band gap reduced to below 1.55eV after passivation.

1.6 Motivation

To improve the device performance some form of post deposition processing treatment is required on as deposited $Cd_{0.6}Zn_{0.4}Te$. From the literature, it is evident that there is a loss of zinc after $CdCl_2$ passivation treatment. The presence of chlorine plays an important role in CdTe device performance. For the top cell to work with CdZnTe as an absorber layer, there is a need to find a strategy to address the questions below:

- Whether chlorine gets incorporated in the grain boundaries of CdZnTe film?
- Is chlorine present in the residual CdTe after zinc loss?
- Where the recrystallization begins?

In the literature, $MgCl_2$ treated CdTe devices have shown a promising device performance for CdTe devices [11]. So it needs to be investigated whether $MgCl_2$ treatment is a viable option for treating CdZnTe film. The morphological studies on CdZnTe films after $ZnCl_2$ treatment can give insights on the decrease in the preferred orientation. Most importantly, there is a need to find a strategy to retain zinc after $CdCl_2$ treatment.

This study focusses on all these aspects.

Chapter 2
Sample Preparation and Characterization

2.1 Project Background

The passivation of RF sputtered CdZnTe project started in March 2014 and is funded and reviewed annually by National Science Foundation / Industry-University Coooperative Research Centers program. The passivation of co-sublimated CdTe and Zn project is funded and reviewed under National Science Foundation/ Accelerated Innovation Research program. This dissertation focusses on passivation of CdZnTe films with three different chloride compounds for the application as the top cell in the mulitjunction solar cells. The doping of the CdZnTe films, acid etching, hot probe measurements, Hall-effect measurements, chlorine outgassing, annealing, passivating with $CdCl_2$+$MgCl_2$, and annealing + $CdCl_2$ (also vice versa) experiments are not covered. The deposition process, film thickness measurements, passivation treatments, device fabrication and transmission measurements were carried out in the PV Manufacturing Laboratory at Engineering Research Center, CSU. Electrical characterization (JV and QE measurements) was done in PV Manufacturing Lab and Photovoltaics Lab, Physics department, CSU. Surface imaging under Scanning Electron Microscope (SEM), Energy Dispersive Spectroscopy (EDS) and X Ray Diffraction (XRD) measurements and contour thickness plots were carried out at CIF, Chemistry department, CSU. Most of the work on specimen preparation and imaging under Transmission Electron Microscope (TEM) was done at CREST facility, Loughborough University. Some part of TEM imaging was also done at CIF.

Until now more than 300 RF sputtered substrates have been fabricated and tested. The processing of each RF sputtered CdZnTe substrate takes around on an average of five hours in

addition to characterization and testing. The different steps for the fabrication are discussed in details. The deposition of CdZnTe films and characterization topics are covered in separate sections (*sections 2.6 and 2.7*). Out of 450 substrates fabricated with co-sublimated CdZnTe films, ~200 substrates were dedicated for the passivation experiments. The deposition of co-sublimated CdZnTe films takes around 10 minutes and passivation with cadmium chloride treatment is usually for 2 minutes.

A generic sample structure is shown (Figure 6).

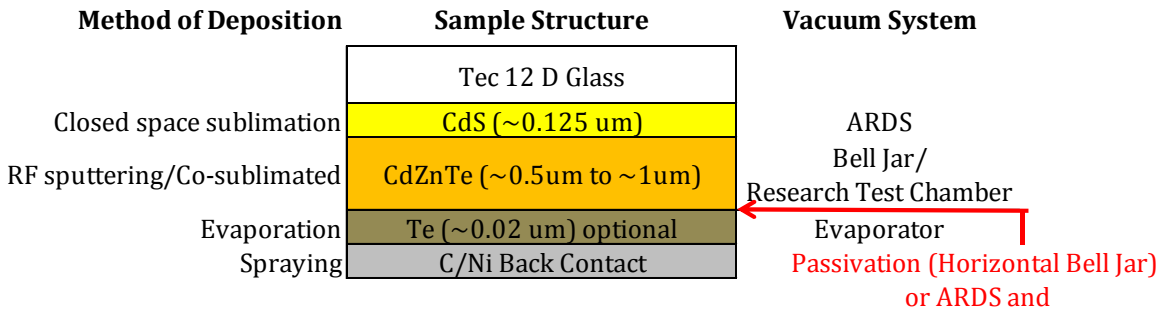

Figure 6 Generic Sample Structure

2.2 CdS Deposition in Advanced Deposition Research System

The Tec 12D glass (3" by 3") samples from Pilkington Corp. are coated with SnO_2:F on one side. SnO_2:F is deposited by Chemical Vapor Deposition on glass through a substrate configuration. In this dissertation, glass samples coated with SnO_2:F are referred as glass substrates even though deposition of semiconductor materials is done in superstrate configuration. Before the Cadmium Sulphide (CdS) deposition, the glass substrates were cleaned ultrasonically for 30 minutes.

The CdS deposition was carried out in Advanced Research Deposition System (ARDS) [37]. ARDS has a total of nine stations and a separate vacuum chamber attached to the main chamber for plasma cleaning of glass. The nine stations can be altered for closed spaced sublimation or for processing (annealing or cooling). A magnetic arm transfers the glass samples

to different stations according to a user defined program. The stations are independently heated and deposition time on each station can be individually programmed.

Before CdS deposition, glass substrate was plasma cleaned for 30 seconds, 450V, 15mA, Ar/ 2%O_2 mixure at 200 mTorr. Without breaking the vacuum, the glass substrate was preheated in the first station for 110 seconds with SnO_2:F side facing down. The top and bottom heaters were maintained at 620^{o}C. The exit temperature was measured under pyrometer and was roughly around 480^{o}C. Then the glass substrate was transferred for CdS deposition. The top and bottom heaters were maintained at around 500^{o}C and 626^{o}C. The deposition time was for 110 seconds. After the deposition process, the glass substrate was cooled for few minutes in the chamber. A stock 12 to 15 CdS deposited substrates were made in each run. CdS thickness was measured using a calibrated UV laser absorption. The thickness of CdS film was usually between 0.1um to 0.13 um. $Cd_{0.6}Zn_{0.4}Te$ films were then deposited on CdS samples and the details are covered in separate section *(section 2.6)*.

2.3 Passivation Treatment

The stacked CdS/ $Cd_{0.6}Zn_{0.4}Te$ films on the glass substrates were then passivated individually in the horizontal bell jar. The experiment setup is shown in the Figure 7.

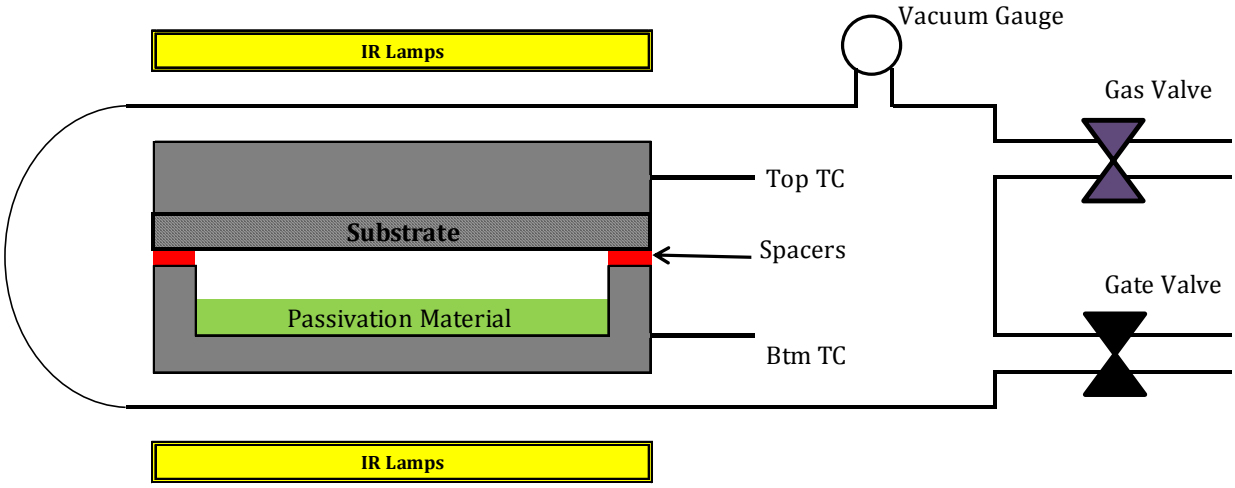

Figure 7 Horizontal Bell Jar Set Up

The material for passivation was weighted and placed in the graphite boat. The substrate was placed on the boat with spacers in between. To contain the vapors and create a high flux of passivation material, spacers were not used in some experiments. The graphite top plate was placed on the substrate. The temperatures (top and bottom) were controlled separately using two thermocouples as shown. The horizontal bell jar was pumped down below 50mTorr and then baked at 200^{o}C for 5 minutes with Argon gas purging. Afterwards temperatures were set to passivation treatment temperatures with gate valve and gas valve closed. The pressure in the horizontal bell jar was ~50 torr of argon gas. Typical passivation treatment cycle is shown in the Figure 8.

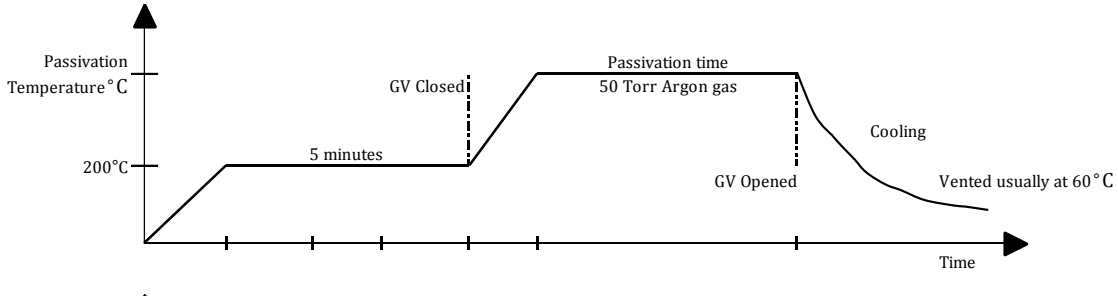

Figure 8 Temperature Profile for the Bottom Thermocouple

The passivation treatment time started when the bottom thermocouple reading reached the specified temperature. In all the experiments, top plate lagged in reaching the specified temperature by ~30seconds. Currently, there is no setup to measure the substrate temperature during the passivation treatment. The substrates were cooled by switching OFF the IR lamps and sliding away the heater setup. The substrates were then rinsed with deionized water and air dried.

2.4 Passivation treatment in ARDS

For passivation treatment in the ARDS, the substrate with co-sublimated CdZnTe film was heated to 480^{o}C in the heater station. A layer of CdS as capping was deposited on the back of CdZnTe. The transfer arm moved the substrate to the $CdCl_2$ station for the passivation treatment.The $CdCl_2$ source was maintained at 437^{o}C and the treatment time was for 20 seconds. After the treatment, substrate was annealed for 2 minutes at station maintained at 400^{o}C. The $CdCl_2$ on the back of the substrate was rinsed using deionized water.

2.5 Copper Doping in ARDS and Tellurium Deposition Process

Other ongoing projects in the lab have shown that deposition of tellurium (Te) on the back creates a better back contact in CdTe devices. So in some experiments, tellurium was evaporated on the back of passivated films at room temperature. Thickness of the Te film was ~0.02um.

The copper doping was done in ARDS after the passivation treatment. The standard copper doping process parameters are given in Table 1. The substrates were rinsed with deionized water and air dried after doping process.

Table 1 Standard copper doping process

	Preheat	Pyrometer	$CuCl_2$	Annealing
Time (seconds)	75	2	110	220
Top (°C)	330	~125	170	220
Bottom (°C)	330		190	220

2.6 Small Area Device (SAD) Fabrication

The carbon and nickel paint were sprayed on the back. The small area devices were made by masking, blasting and soldering an indium ring around the area. In some experiments, total of nine devices were fabricated and some experiments, the substrate was cut into half and three devices were prepared on each side. The area of the fabricated devices were prepared from masking and blasting [37].

2.7 RF Sputtering of CdZnTe Films

The sputtering is a process of ejecting atoms from the target material using high energy ions. The target is the material to be deposited and is set at negative potential (cathode) which attracts the positively charged gaseous ions. In RF sputtering, AC power is applied at high frequency (13.56 MHz). Due to the AC power, positive ions are not built up on the resistive target. The magnets placed under the target with certain orientation helps to direct the secondary electrons which increase the plasma density [38].

CdZnTe material is highly resistive. So RF sputtering was used to deposit CdZnTe films from a single target. The target was fabricated by Plasmaterials Inc. The initial powder composition of the target was (CdTe) 60% and (ZnTe) 40% by weight. The powder was hot pressed in to a circular disc of size 4" diameter by 0.125" thick. The target was then bonded to oxygen free copper plate as a backing plate. The schematic of sputter chamber is shown in the Figure 9.

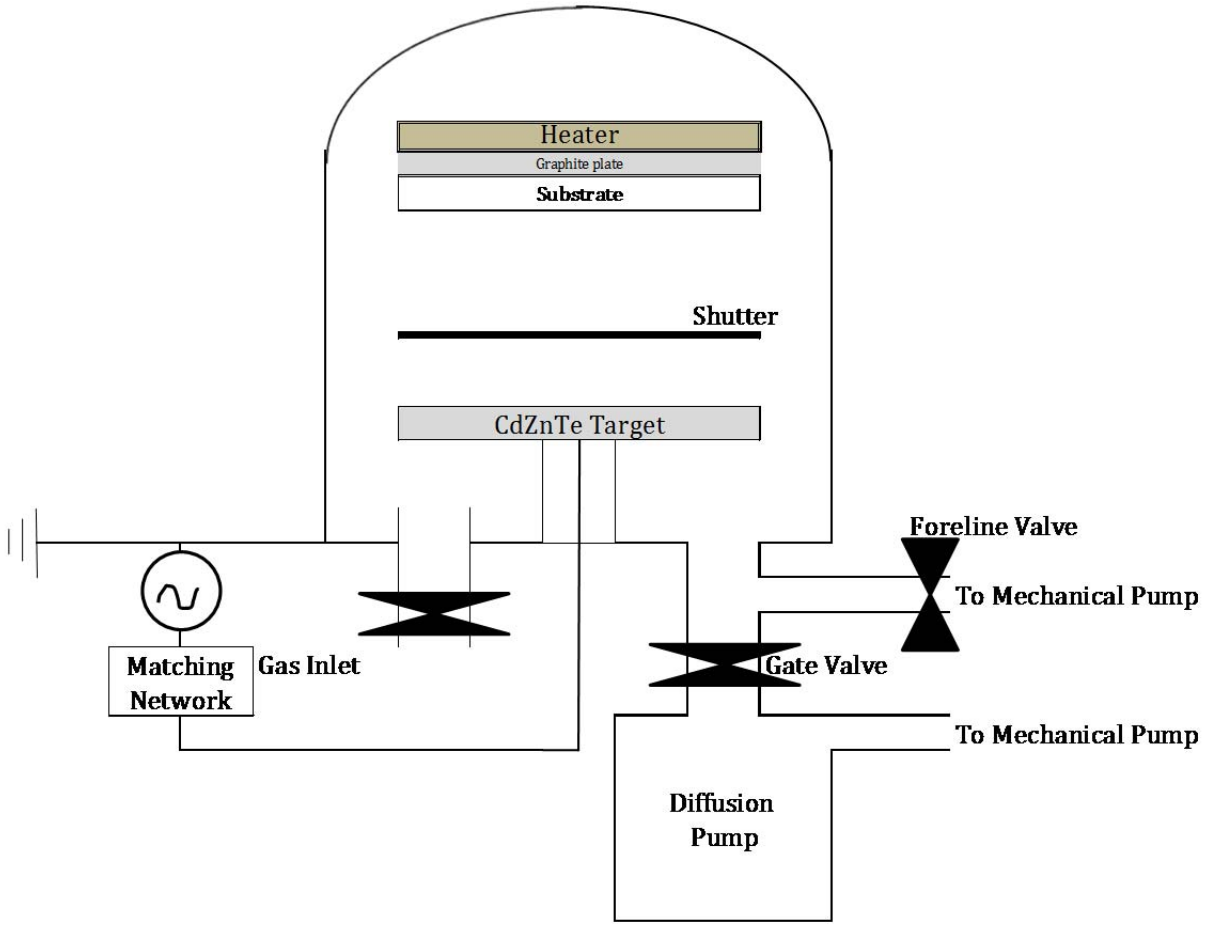

Figure 9 Schematic of RF Sputter Chamber

The CdZnTe target was bolted to the cathode which was continuously water cooled. Substrate was mounted on the substrate holder which was directly over the target. For the each run, the chamber was pumped down to the base pressure of 1E-5Torr. After reaching the base pressure, sputter chamber was purged five times with argon gas to minimize residual oxygen. The substrate heater was started and substrate was baked for 15 min after the specified temperature was reached. Three thermocouples were attached to graphite plate for temperature reading. The operating pressure varied between 3mTorr to 18mTorr depending upon the selected pressure conditions. The matching network was used to minimize reflected power. At the start of the deposition process, target surface was cleaned for three minutes after igniting the plasma.

The shutter prevented the exposure of the substrate during target cleaning. After target surface cleaning, shutter was opened for CdZnTe deposition. The power was switched OFF once the required film thickness was deposited based on the deposition time. The substrate was cooled by filling the chamber by argon gas up to ~100Torr. Normally after two hours of cooling, temperature reached below 60^{o}C. To prevent oxide formation, the chamber was always vented below 60^{o}C.

2.8 Characterization of CdZnTe films

CdZnTe films were characterized by depositing on plain glass. The process parameters that can be varied are shown below:

Table 2 Process Parameters for Characterization

A.	Deposition Time
B.	RF Power
C.	Distance Between the Target and Substrate
D.	Carrier Gas
E.	Operating Process Pressure
F.	Substrate Temperature

The deposition Rate was measured by varying the deposition time and keeping the rest of the parameters unchanged.

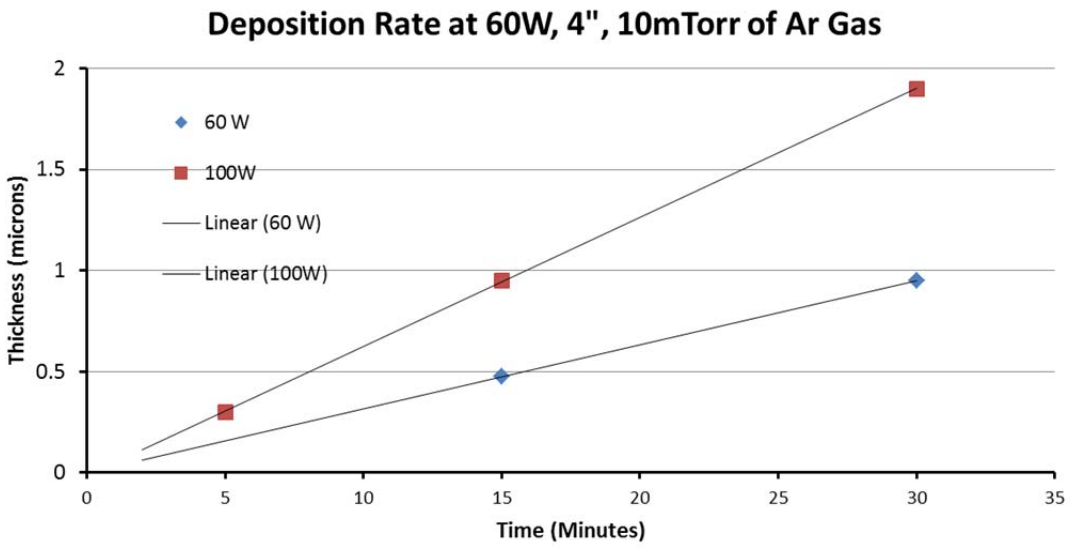

Figure 10 Deposition Time vs Measured Thickness

From the graph (Figure 10), as the deposition time increased, film thickness also increased linearly. For the same amount of time, film thickness was more with higher RF power. The deposition rate for the different powers were calculated by drawing a trend line and calculating the slope of the trend line.

Table 3 Deposition Rate Measurements

Power	Deposition Rate
60W	~32 nm/min
100W	~63 nm/min

If any of the process parameters were changed during the experiments, film thickness was remeasured for that particular condition.

The contour plot was graphed by measuring film thickness at 25 different positions on the substrate. The deposition conditions were 60W, 4", 10mTorr of Ar gas for 15 minutes.

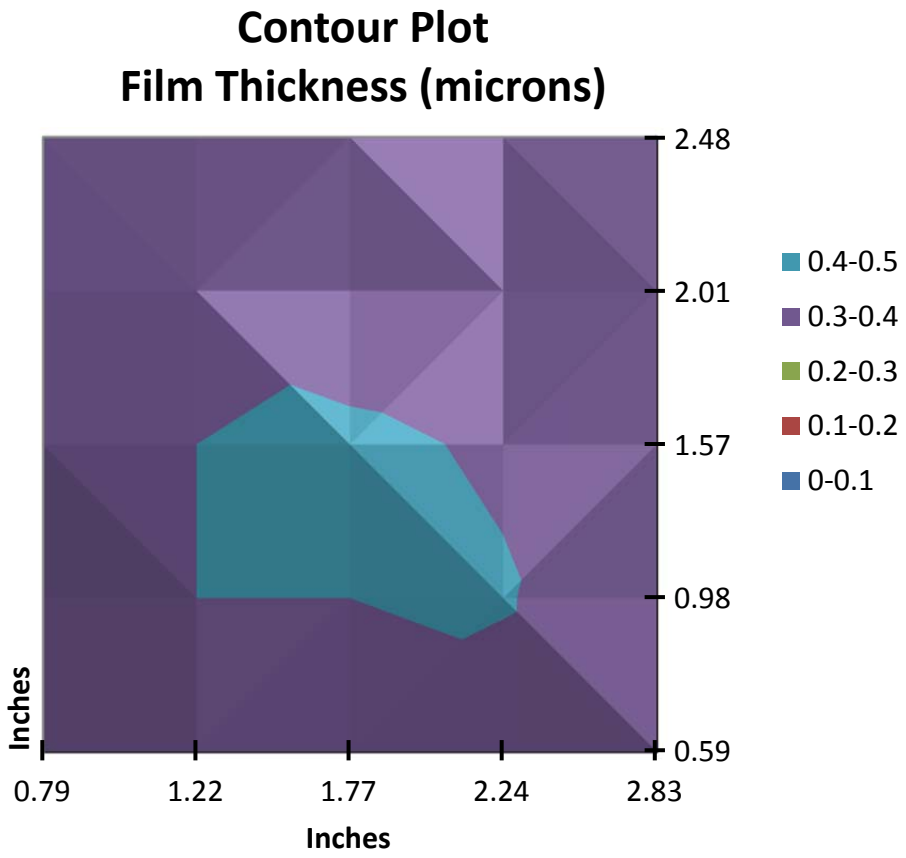

Figure 11 Countour plot

From the contour plot (Figure 11), the deposited film was slightly thicker at the center and the thickness decreased gradually towards the substrate edges. This is typical result of sputter deposited films which follows the cosine law of distribution [38]

The transmission measurements were carried out at nine different positions on the substrate. The nine positions selected are the points where SAD's are fabricated. The optical transmission was measured by UV-Vis spectrometer. The wavelength was scanned from 350nm to 1000nm. The substrates selected were CdZnTe deposited on plain glass and on CdS deposited on glass substrates. The light passing through the plain glass and Tec12D glass was taken as a reference (100%).

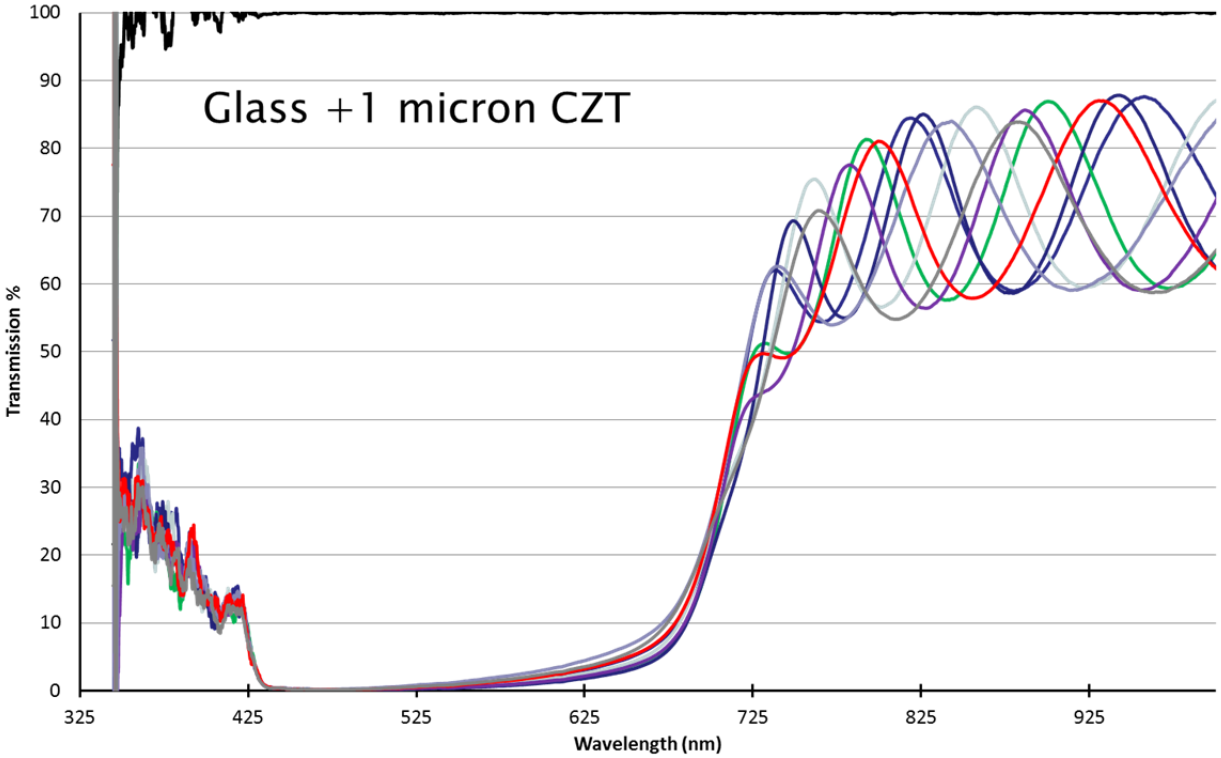

Figure 12 Transmission of CdZnTe deposited on glass

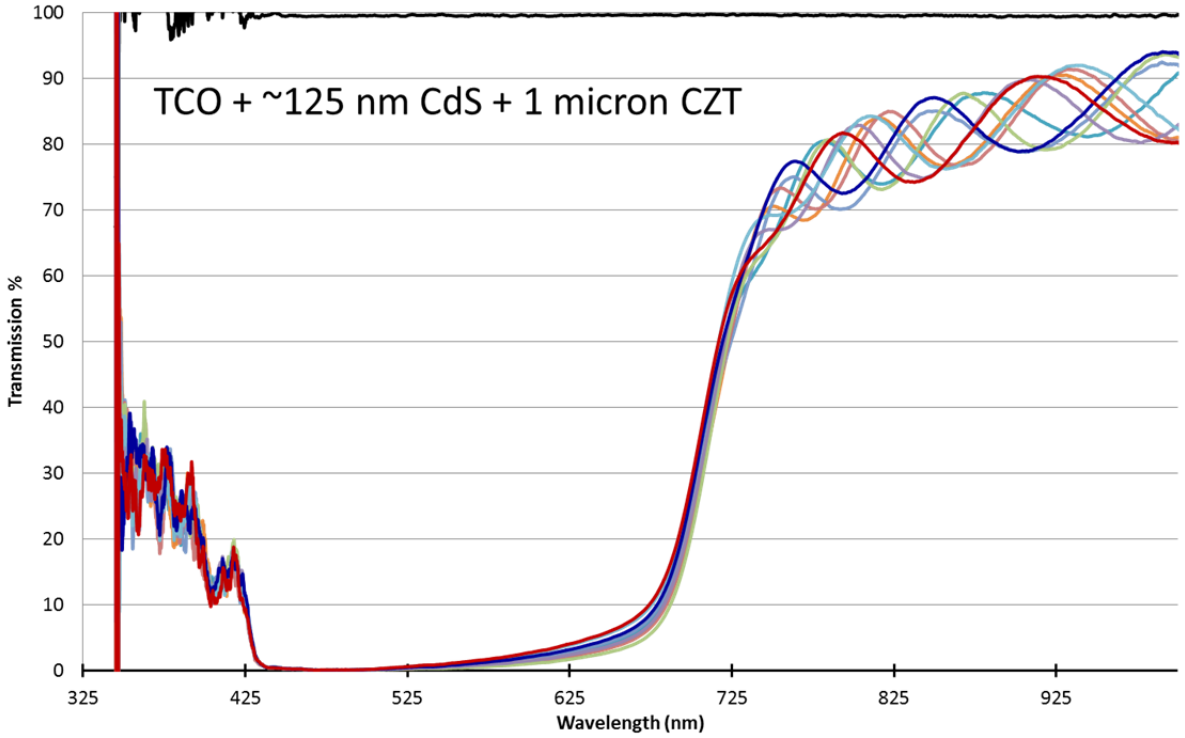

Figure 13 Transmission on CdZnTe deposited on CdS/Tec12D

The transmission measurements indicated that the deposited CdZnTe film had a uniform stoichiometry (Figure 12 and Figure 13). The band gap of the deposited film was calculated using Tauc plot and n=2 for direct band gap semiconductor. The average band gap was 1.72 eV and that corresponded to $Cd_{0.6}Zn_{0.4}Te$ composition of the film.

To understand the structural properties, X ray diffraction was carried out on CdZnTe films deposited on plain glass at two different temperatures (150C and 400C) is shown in the Figure 14. The 2Θ angle was scanned from 10^{o} to 80^{o}. The measured diffraction spectrum was then compared to standard ICDD card for $Cd_{0.6}Zn_{0.4}Te$ [39].

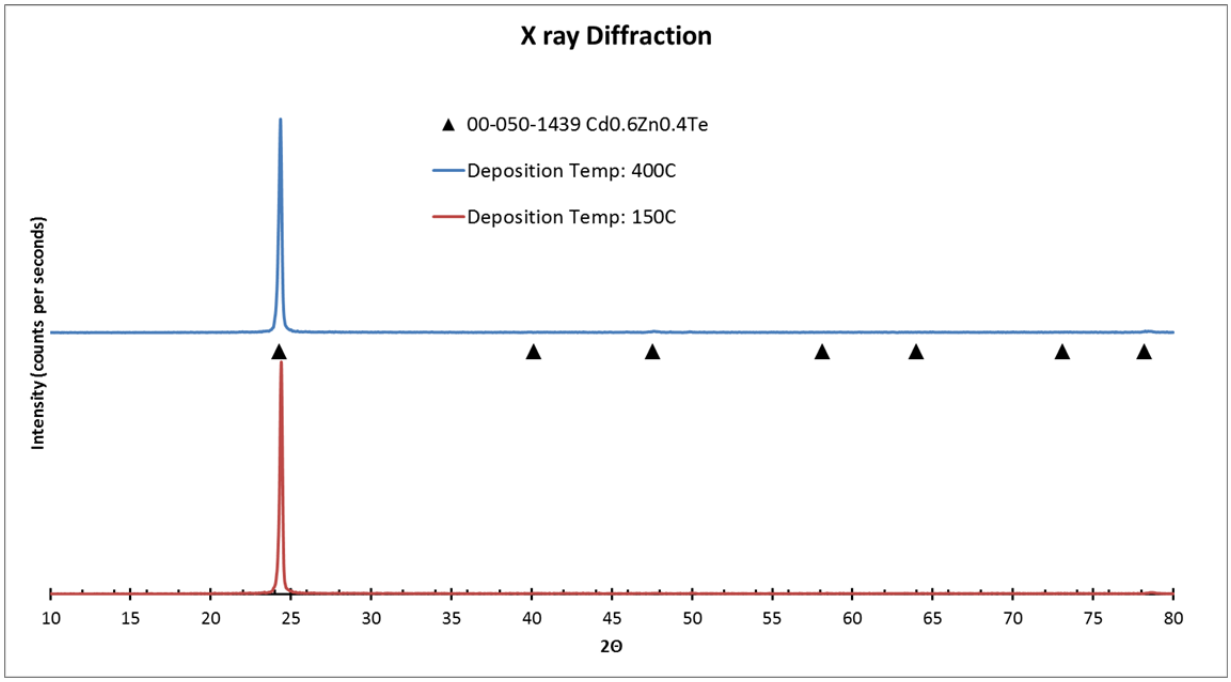

Figure 14 X Ray Diffraction on CdZnTe deposited on Glass

From the X ray diffraction results, the peak pattern of the deposited films was close match with the ICDD card for $Cd_{0.6}Zn_{0.4}Te$. Also the composition of the deposited film was same the target material. The diffraction peaks linked to binary compounds, CdTe [40] and ZnTe [41] were absent indicating that there was no preferentially sputtering. The diffraction peak intensity

was strong at 24.35^{o} {111} and relatively low at 40.14^{o} {220} and 47.56^{o} {311} suggesting that deposited film has a strong {111} preferred orientation.

2.9 Co-sublimation of CdTe and Zn

The co-sublimation is a process in which a compound is formed by subliming elements/compounds independently. This technique is commonly used when the subliming elements/compounds have vastly different vapor pressures. The co-sublimation of CdTe and Zn was carried out in Research Test Chamber (RTC) to form ternary alloy of Cd-Zn-Te. The RTC system has a vaccum chamber with an extended load lock. The vacuum chamber has two stations in line. A manually controlled transfer arm is used to move the samples in the two stations located in the vacuum chamber. The Cd-Zn-Te films were deposited on Mg-Zn-O/SnO_2:F/Glass in a superstratre configuration. On the first station, the sample is preheated to ~500^{o}C and then moved to a second station for depositing Cd-Zn-Te films.

The second station comprises of two graphite sources stacked vertically and heated independently (Figure 15). Prior to fabrication, CdTe material is loaded in the primary source and Zn material is loaded in the bottom source. During the fabrication process, CdTe source is operated at a fixed temperature. The stoichiometry of the deposited Cd-Zn-Te films can be varied by varying the Zn source temperature

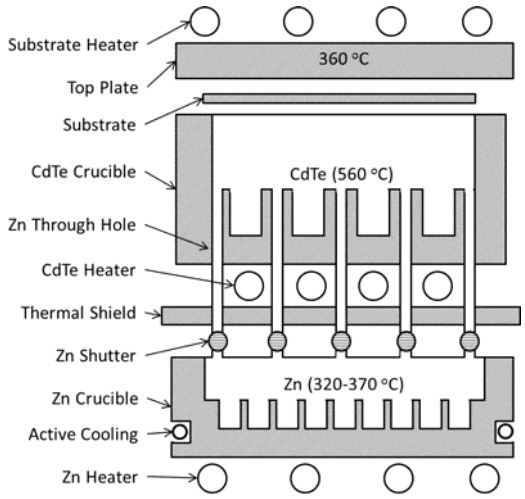

Figure 15 Schematic of co-sublimation source for fabricating Cd-Zn-Te films

2.10 Characterization of co-sublimated Cd-Zn-Te films

The Cd-Zn-Te films with different stoichiometry were prepared separately on the different Mg-Zn-O/SnO_2:F/Glass samples. The concentration of Zn was varied by changing the Zn source temperature from 300°C to 370°C in small increments.

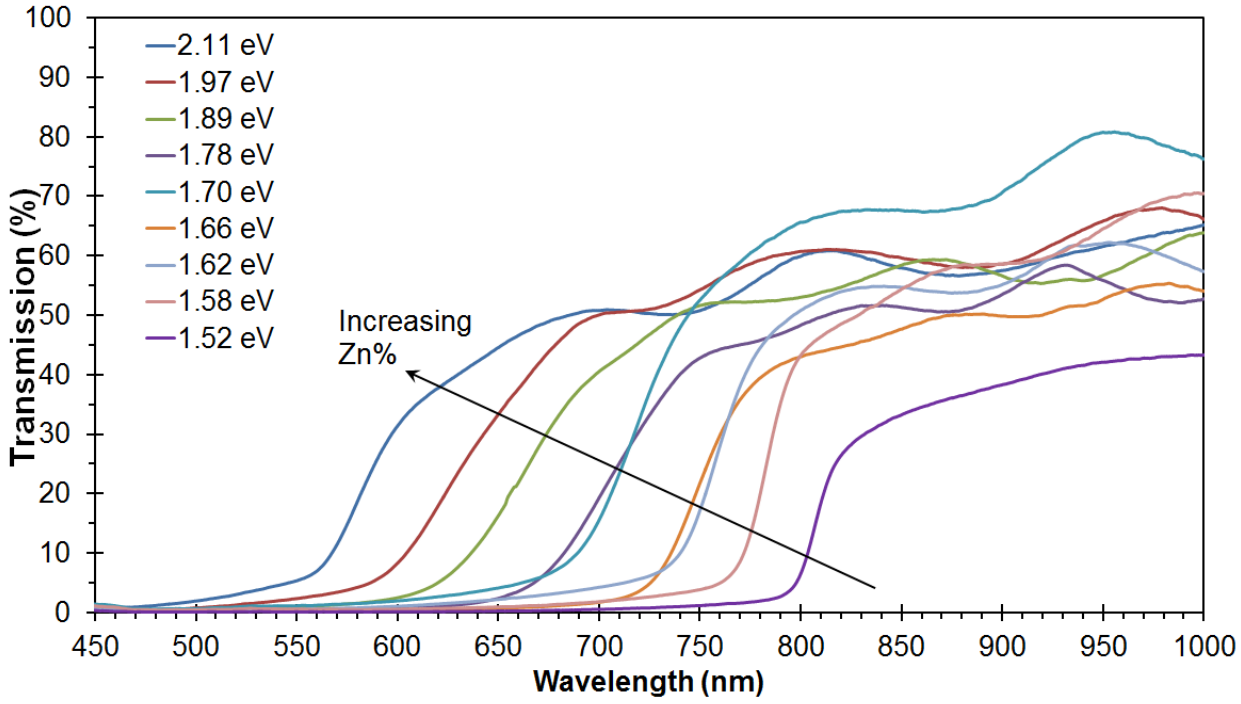

Figure 16 Transmission measurements on samples fabricated by varying the Zn source temperature

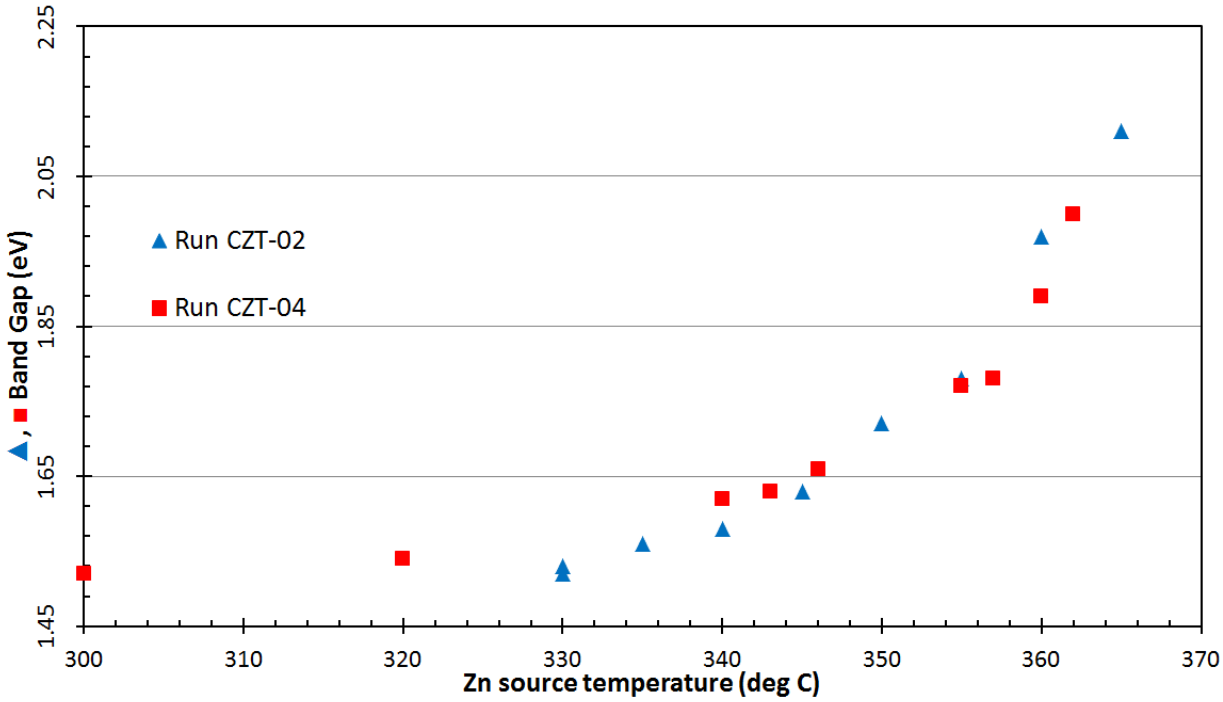

Figure 17 Increase in the band gap of deposited Cd-Zn-Te films with increase in the Zn source temperature

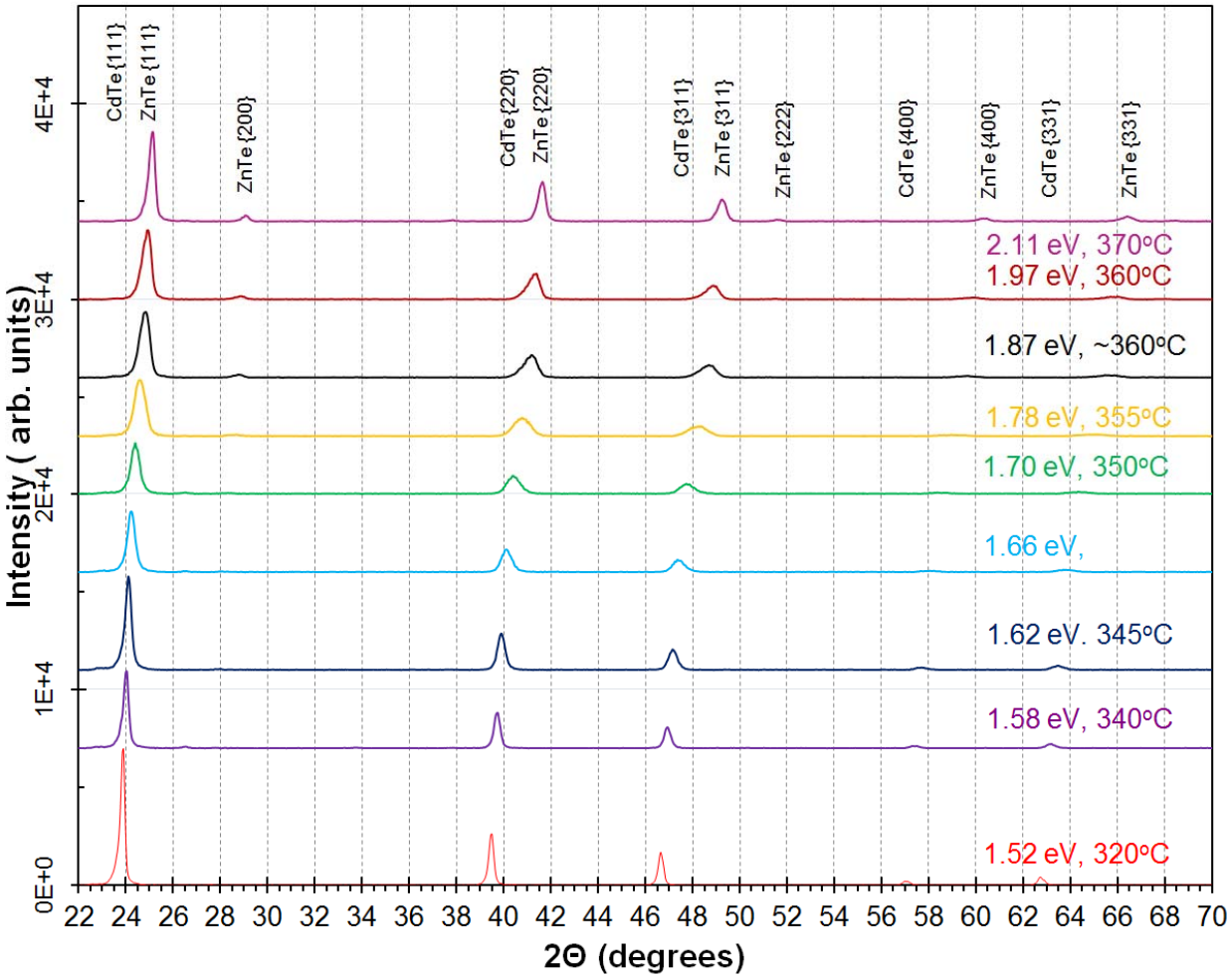

Figure 18 Glancing angle X-ray diffraction of Cd-Zn-Te films deposited with increasing Zn source temperature

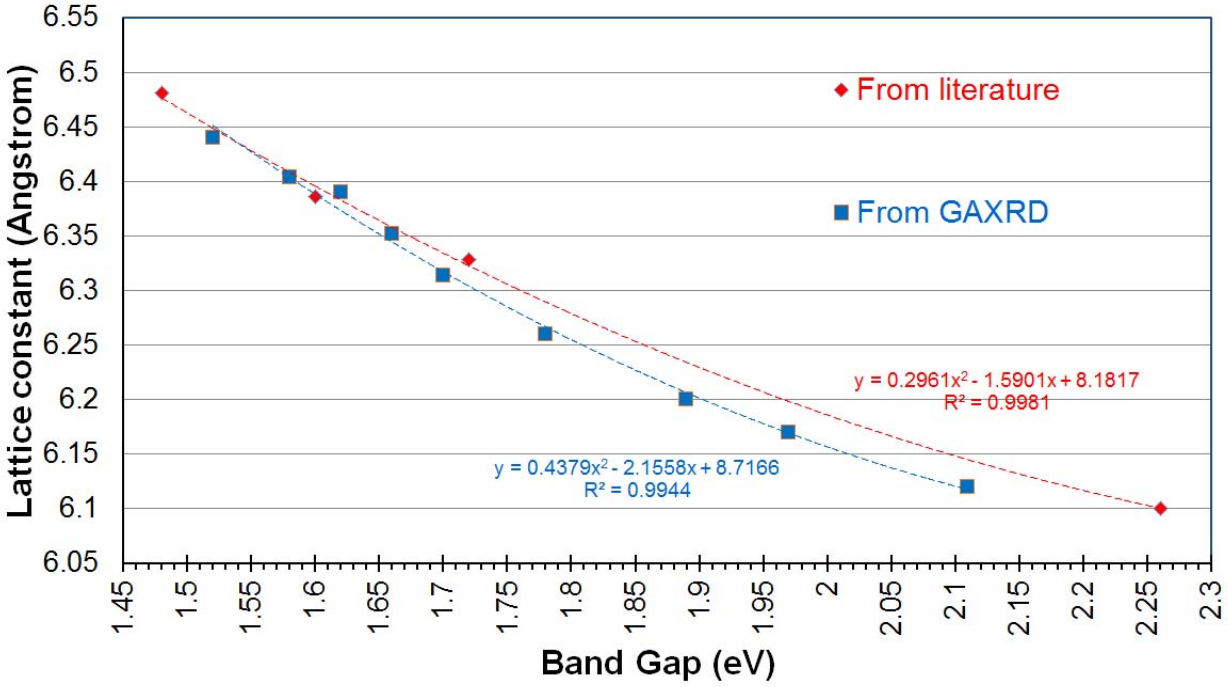

Figure 19 Lattice parameter calculated as well as from the literature versus band gap

The transmission measurements shown in the Figure 16 indicated that the band edge of the deposited Cd-Zn-Te films shifted towards the shorter wavelength region with the increase in the Zn source temperature (Figure 17).

The glancing angle X-ray diffraction conducted on the different samples with increasing Zn content exhibited shift in the diffracted peaks towards to higher 2Θ angle (Figure 18). The deposited films were single phase with zinc blende structure. The orientation of the films was along {111} plane. The lattice parameter of each individual film deposited with varying Zn source temperature was calculated based on the peak loction at {111} plane and was in good agreement with the values in the literature [21], [24], [31] (Figure 19).

Chapter 3
Preliminary Passivation Treatments on Sputtered CdZnTe with Chloride Compounds

3.1 $CdCl_2$ Passivation Treatment on RF sputtered CdZnTe

The CdZnTe film was deposited on two substrates pre-deposited with CdS film. The deposition steps are described in the section 2.6. The process parameters for the RF sputtered CdZnTe films deposition is given below.

Table 4 CdZnTe Deposition Parameters

Power	60W	**Gas**	Ar
Dep. Time	36 minutes	**Pressure**	10mTorr
Dep. Temp.	400C	**Distance**	4 inches

The $CdCl_2$ material (10 gms) was uniformly spread in the graphite boat and then placed in the horizontal bell jar. The passivation treatment cycle was similar to the process described in section 2.3. The passivation treatment time was kept for 3 minutes and the temperature was set to 380^{o}C and 400^{o}C. The transmission measurements were carried out on the same points on the substrates before and after the passivation treatments. After the treatment, the substrates were cut into two halves. On one half, material properties were studied using X ray diffraction, and imaging under TEM. On the other half, SAD's were fabricated for JV testing.

From the transmission measurements (Figure 20), the as-deposited CdZnTe films had a sharp absorption edge. The calculated band gap from the Tauc plot was ~1.72eV. After the $CdCl_2$ passivation treatment, the absorption edge was less pronounced indicating that the crystalline quality of the film has decreased. Also there was an absorption edge shift towards

longer wavelength suggesting that the overall band gap of the film has decreased. The decrease in the band gap points out that there is a zinc loss from the films.

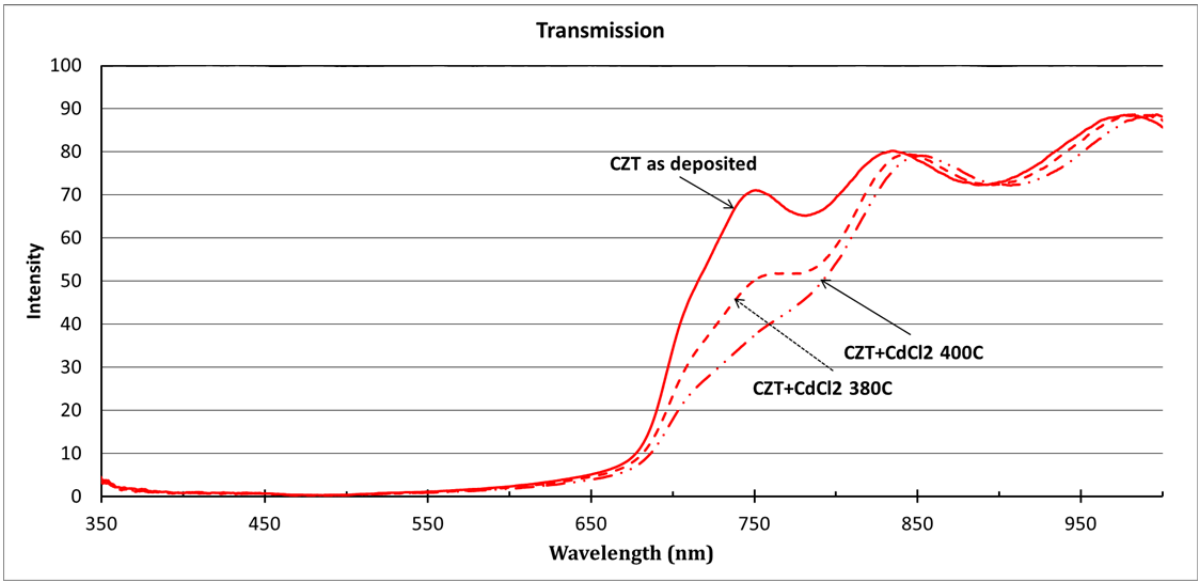

Figure 20 Transmission on the $CdCl_2$ Passivated Samples

The X ray diffraction spectrum of $CdCl_2$ passivated samples were measured (Figure 21) and compared with the diffraction spectrum of CdS/Tec12D and with ICDD cards of CdTe [40] and ZnTe [41].

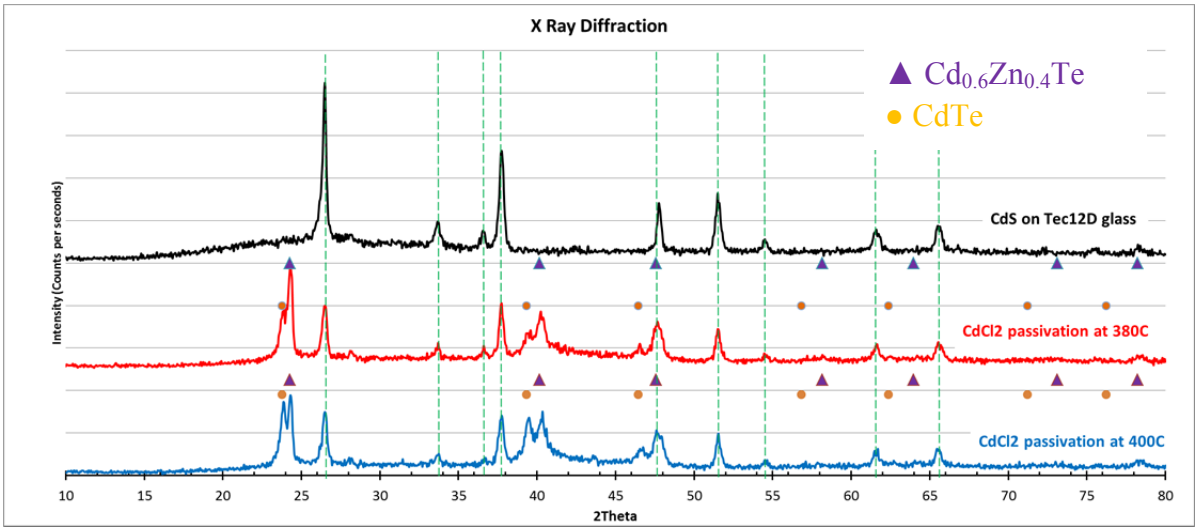

Figure 21 X Ray diffraction of the $CdCl_2$ passivated samples

To analyze the diffraction spectrum, the vertical dotted green lines are drawn from the diffraction peaks of CdS/Tec12D to distinguish the CdS/Tec12D peaks in the $CdCl_2$ passivated samples. The peaks with purple triangles are associated with $Cd_{0.6}Zn_{0.4}Te$ compound [39]. At 380^{o}C passivation temperature, new peaks started to emerge to the left of $Cd_{0.6}Zn_{0.4}Te$ peaks. At 400^{o}C passivation temperature, new peaks are clearly visible. The orange dots are linked to peak angles of CdTe. After finding the *d* values for the new unassigned peaks and applying Vegards Law [31], the composition of the compound was found to be $Cd_{0.94}Zn_{0.06}Te$. This clearly indicates that there is a depletion of zinc from the original material after $CdCl_2$ passivation. Passivated film is no longer a single phase CdZnTe material.

The TEM specimens and cross section imaging was done on the samples passivated with $CdCl_2$ at different temperatures. EDS was conducted to analyze elemental composition.

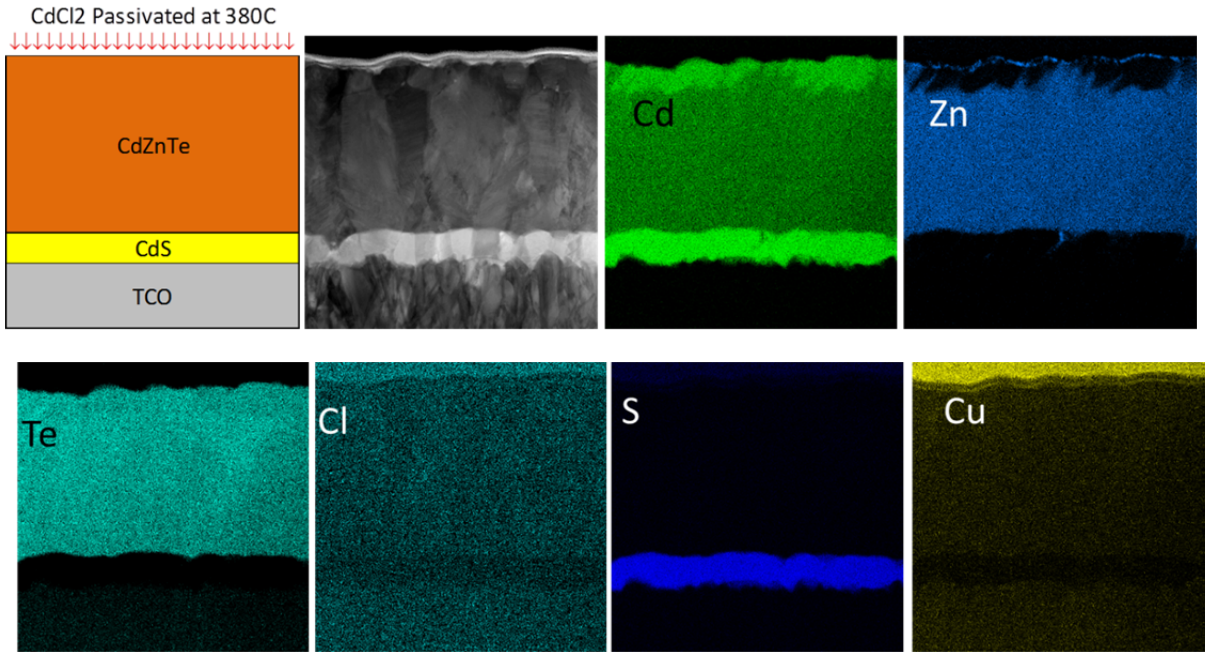

Figure 22 $CdCl_2$ passivated sample at 380^{o} C

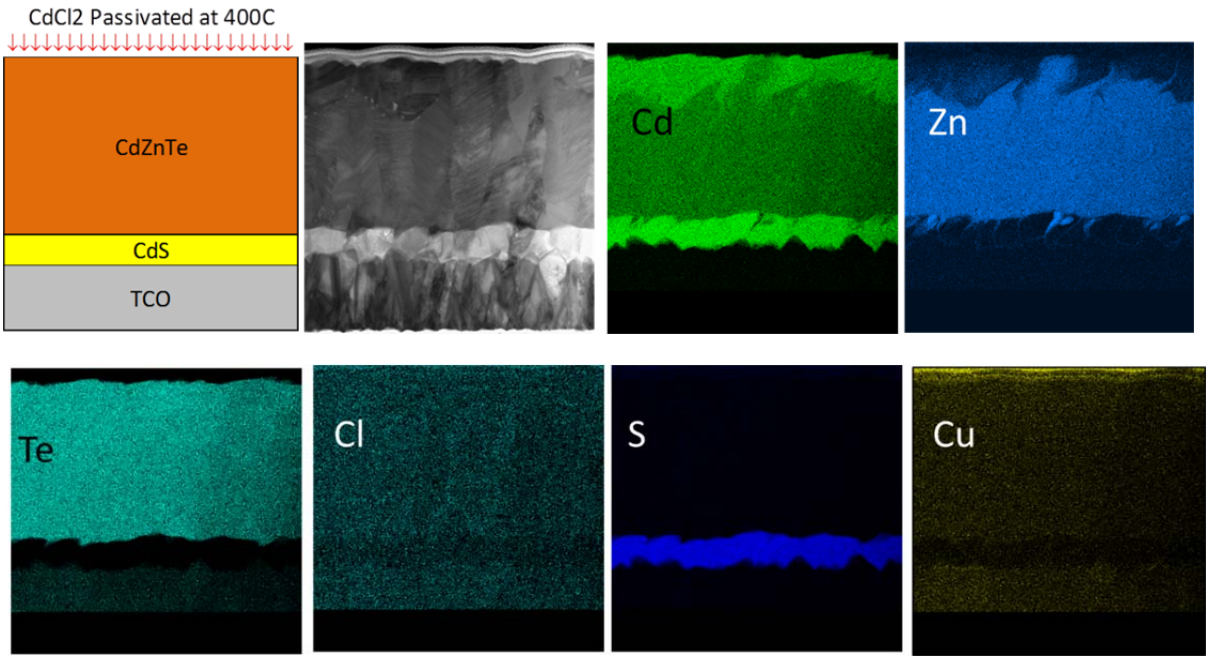

Figure 23 $CdCl_2$ passivated sample at 400^o C

In Figure 22 and Figure 23, the first image is the schematic of the device structure and the second image adjacent is the bright field image under TEM. The rest of the images are the elemental maps collected from each cross section. In the zinc map, it can be clearly observed that there is a loss of zinc from the surface as reported by McCandless [28] who did the passivation at high temperature. This is due to the formation of volatile $ZnCl_2$ which occurs when it is exposed to $CdCl_2$ at high temperatures [29] [21]. The loss of zinc is more when the passivation treatment temperature is higher. At front interface of CdZnTe, zinc leaches into CdS forming CdZnS or ZnS. In the chlorine maps, the signal is below the detection limit in the region where zinc loss has occurred. Also the chlorine signal is below the detection limit at the grain boundaries and at the front interface of CdZnTe. The overall absence of strong chlorine signal in CdZnTe indicates that CdZnTe is not well passivated. In the bright field images, grain growth is observed at the outer edge of CdZnTe. This is contradictory to the phenomenon observed in DC sputtered CdTe films passivated with $CdCl_2$ [16].

The SEM images and EDS spot analysis is shown below (Figure 24).

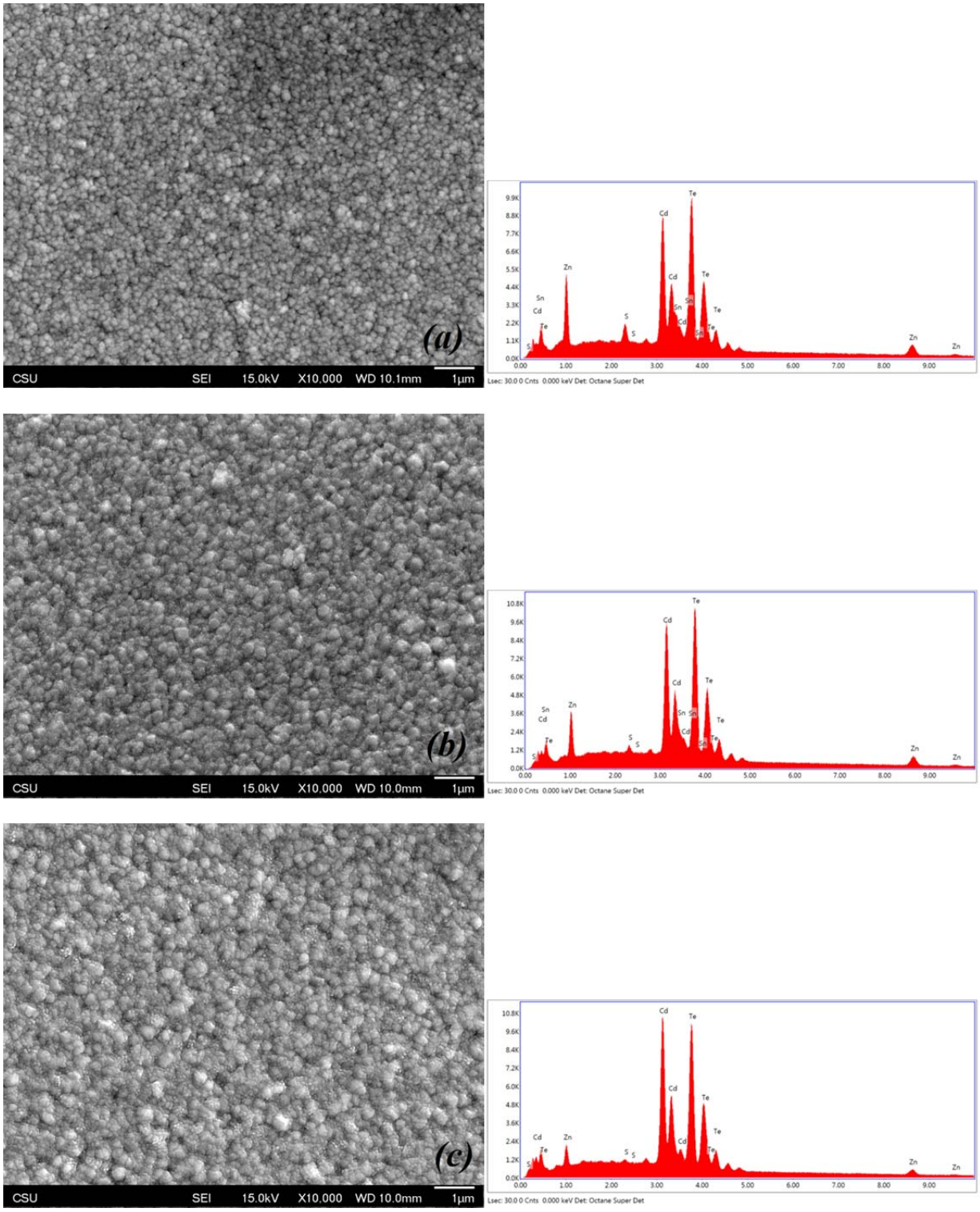

Figure 24 SEM images of CdZnTe surface Treated at Different Temperatures (a) As Deposited CdZnTe, (b)$CdCl_2$ Temperature 380^oC (c) $CdCl_2$ Temperature 400 ^oC

On the as-deposited CdZnTe, the grains are spherical shaped and uniformly distributed over the surface. As the $CdCl_2$ passivation temperature increases, coalescence of the grains is observed indicating recrystallization. The EDS spot analysis on thick materials is a coarse indication of composition of each elements present. From the EDS graphs, the decrease in the $L_{\alpha 2}$ peak of zinc at 1.0118eV is an indication of zinc depletion.

After the copper doping, three SAD's were fabricated on each of $CdCl_2$ passivated samples and JV testing was performed (Figure 25).

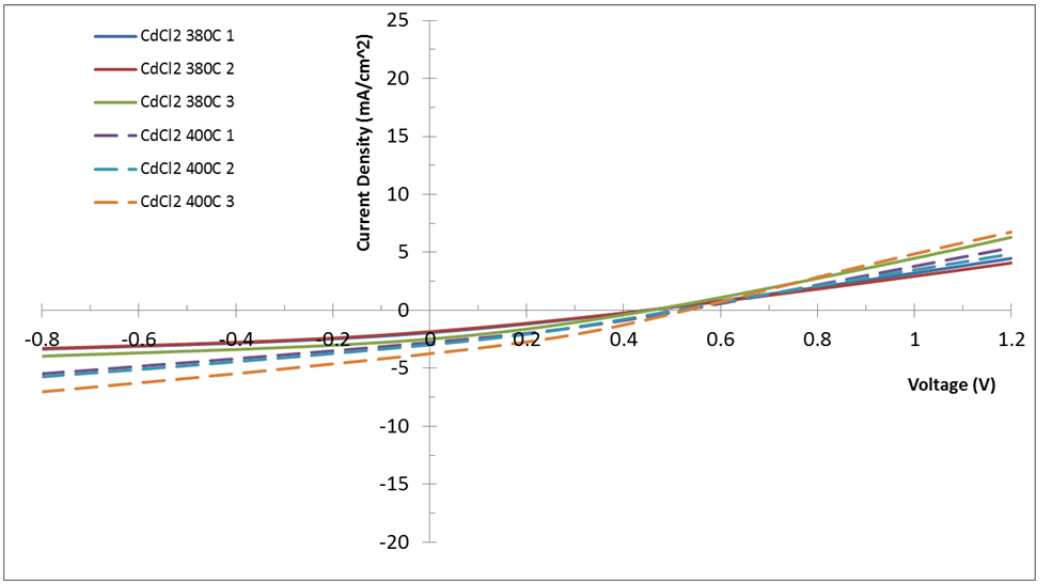

Figure 25 JV Data on $CdCl_2$ passivated sample

Due to the incomplete passivation of CdZnTe, the device performance was below expected. The photo generated current and fill factors were low and light JV did not exhibit a diode shape curve.

3.2 $CdCl_2$ Passivation on CdZnTe films with CdTe film capping

To prevent the zinc loss from the CdZnTe surface during passivation, 200nm of CdTe film was deposited as a capping layer. The deposition of CdS and CdZnTe were done as described in the section 2.2 and 2.6. The CdTe film was deposited in ARDS after preheating the

CdZnTe deposited substrate to 480C in the first station for 110 seconds. The CdTe deposition time was for 110 seconds. Total of four substrates were prepared for this study out of which results of two samples are presented in this proposal. The deposition parameters for CdZnTe are different from the previous experiment and are given below. The thickness of CdZnTe films was around ~0.6 to 0.7um. The passivation time was kept constant for 3 minutes and temperatures were set to 380C and 400^{o}C. After the passivation, tellurium film of 0.02nm was deposited and then copper doping was done.

Table 5 CdZnTe deposition parameters for CdTe capping

Power	60W	**Gas**	Ar/H2
Dep. Time	~17 minutes	**Pressure**	3mTorr
Dep. Temp.	440C	**Distance**	2.5 inches

The CdZnTe film treated with $CdCl_2$ at 400^{o}C, 3 minutes appeared greenish in color from the glass side with some signs of delamination.

The TEM images and EDS mapping of the two substrates capped with CdTe and then passivated with $CdCl_2$ at two different temperatures are shown in Figure 26 and Figure 27.

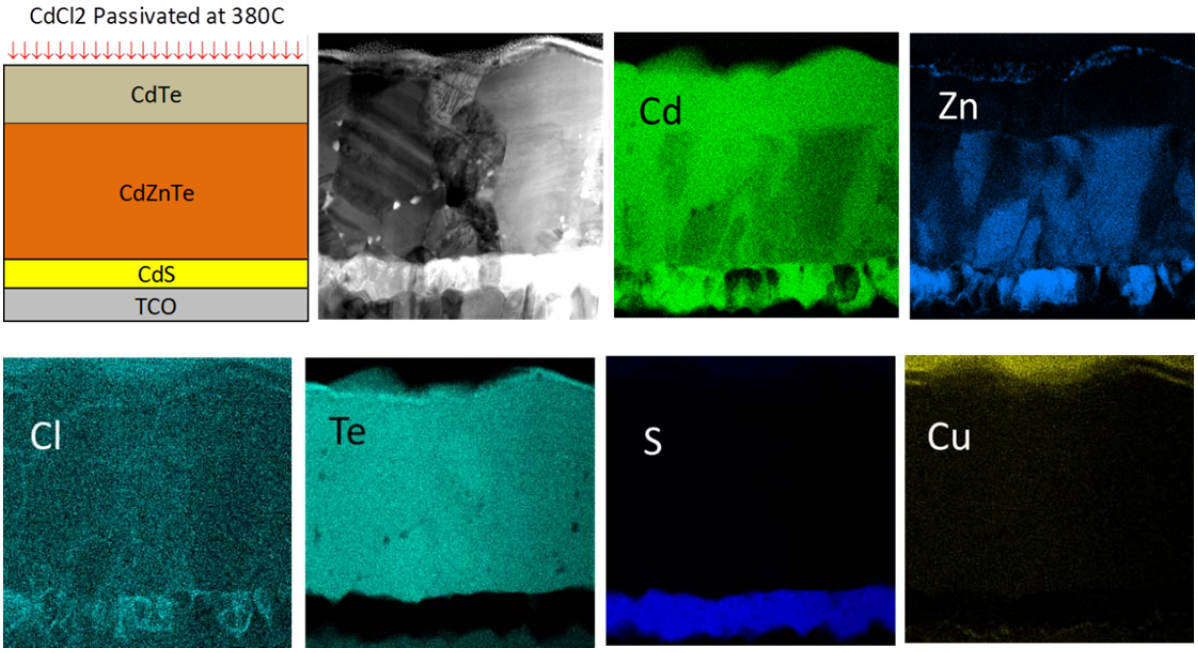

Figure 26 CdZnTe with CdTe Cap passivated with $CdCl_2$ at 380C

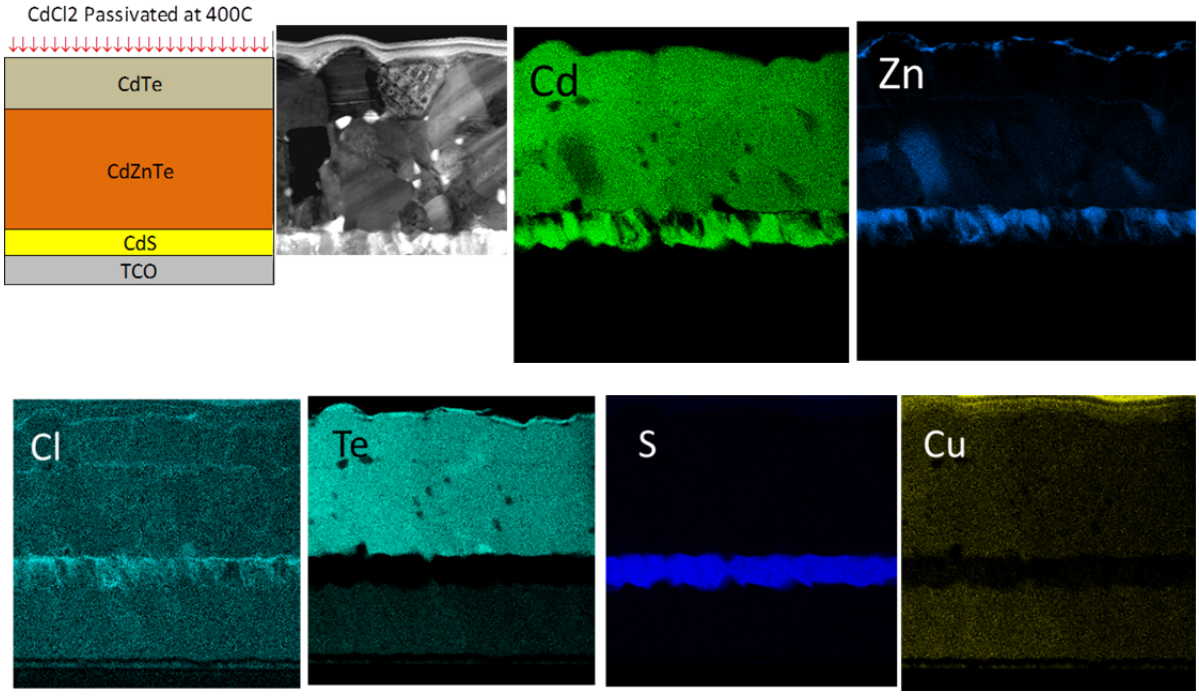

Figure 27 CdZnTe with CdTe Cap passivated with $CdCl_2$ at 400C

The observations and results from the TEM images are listed below:

- Heavy zinc diffusion into CdS is observed. When compared it with the previous $CdCl_2$ passivation treatment, it can be concluded that heavy zinc diffusion occurs when the sample is reheated during CdTe deposition.
- Zinc retention is observed in the sample treated with lower passivation temperature (380^{o}C).
- Chlorine is observed along the grain boundaries of CdTe, CdZnTe and CdS.
- CdZnTe grain growth is observed along with the formation of voids.

The JV and QE measurements on the best devices are shown (Figure 28 and Figure 29).

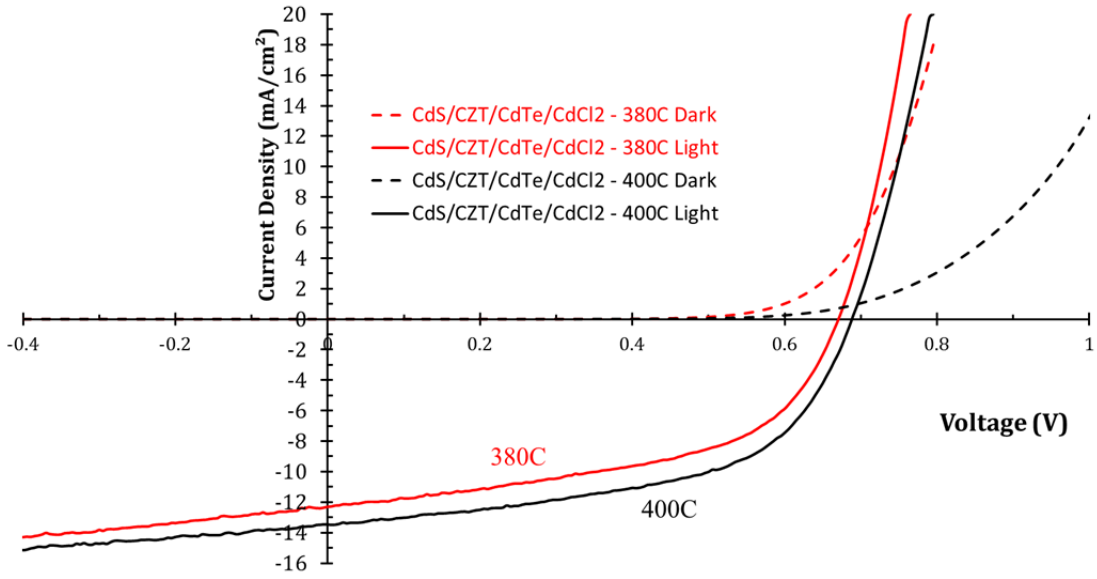

Figure 28 JV Measurements on $CdCl_2$ treatment at different temperatures on the best CdS/CdZnTe/CdTe devices

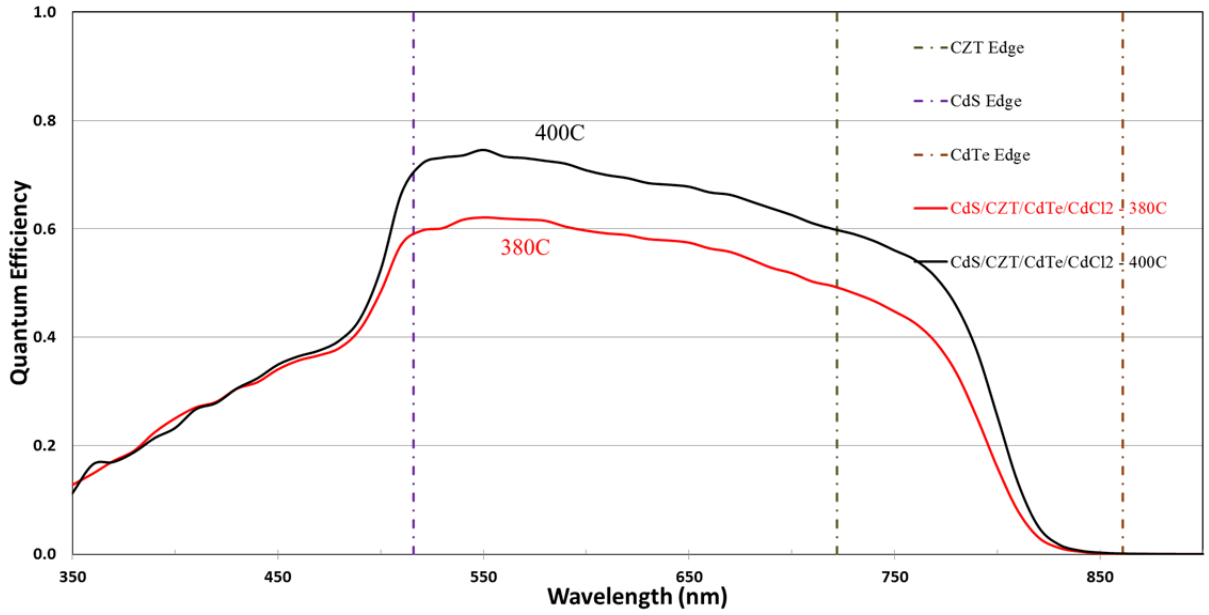

Figure 29 QE Measurements on $CdCl_2$ treatment at different temperatures on the best CdS/CdZnTe/CdTe devices

From the JV and QE measurements, the devices have better electrical performance when compared to the devices with no CdTe capping layer. The photo generated has increased as well as the fill factor which indicates that the devices are passivated. However, the band edge has shifted towards longer wavelength which indicates that the photo current is also generated in CdTe. It is difficult to calculate exactly how much photo current is generated in each of the layer (CdTe and CdZnTe). The calculations are complicated by the loss of zinc into CdS. The band gap deduced from the QE measurements comes out to be around ~1.57eV (Figure 30).

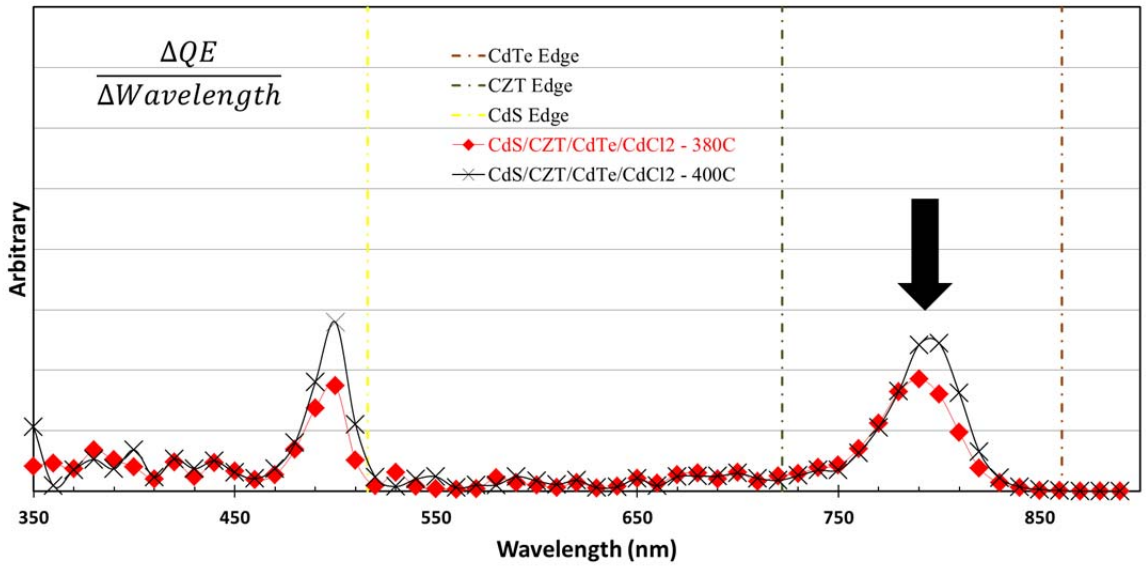

Figure 30 Band Gap Deduced From QE Measurements

3.3 $MgCl_2$ Passivation Treatment on CdZnTe

For the $MgCl_2$ passivation, the CdZnTe films were deposited on the CdS/Tec12D substrates. Two different passivation treatment conditions in the horizontal bell jar were investigated. $MgCl_2$ was weighted (~8gms) and place in the graphite boat. The passivation treatment process was similar to the process described in section 2.3. For the first treatment, the passivation temperature was set to 430^{o}C for the top plate and the bottom graphite boat. The passivation time was kept at 20min. In the second treatment process, different temperatures were set on the top plate (400^{o}C) and the graphite boat (430^{o}C). The passivation treatment time was 30 minutes. Below is table describing the two treatments in details:

Table 6 Passivation treatments with $MgCl_2$

Prassivation Material	Temperature		Gas	Pressure	Time
	Bottom (C)	Top (C)	Ar	(Torr)	(minutes)
MgCl2	430	430	Ar	50	20
MgCl2	430	400	Ar	50	30

The transmission measurements, imaging under SEM and JV testing were carried to understand the material properties and electrical performance.

The transmission measurements are given below (Figure 31).

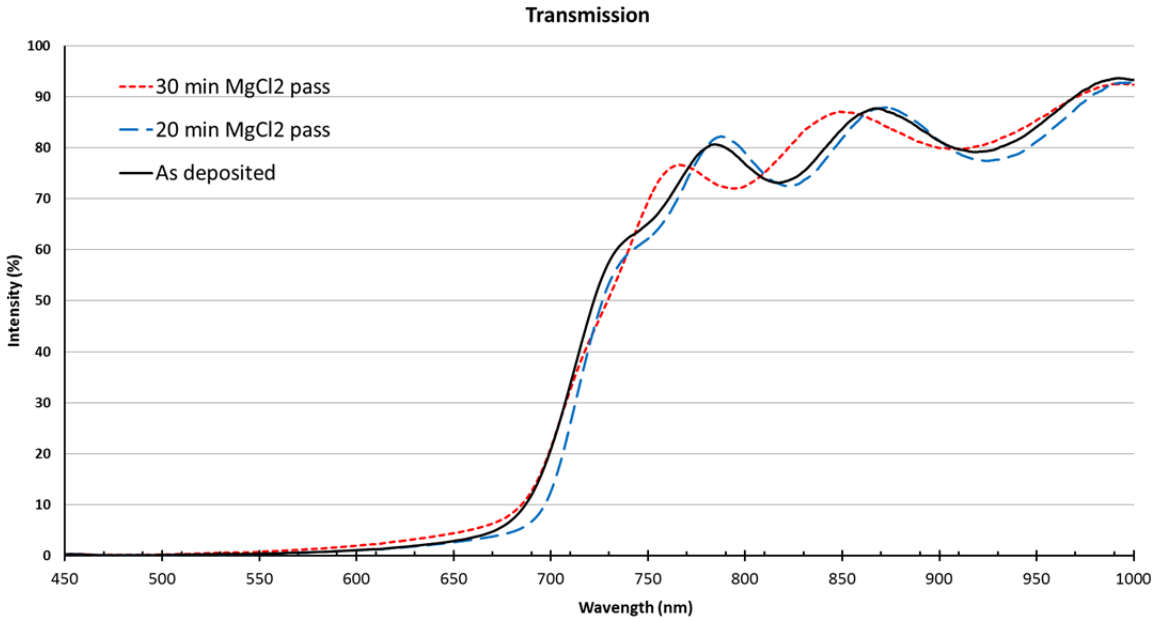

Figure 31 Transmission Measurements after $MgCl_2$ passivation

After 20 minutes and 30 minutes of $MgCl_2$ passivation treatments, the absorption edge did not shift towards the longer wavelength. This indicates that the zinc in the CdZnTe material has been retained. At this high temperatures and longer time, there is a probability that zinc would be diffusing from CdZnTe into CdS.

In the SEM image (Figure 32), after 20 minutes of $MgCl_2$ passivation, the grains were more faceted improved and the surface exhibited granular morphology with varying grain size.

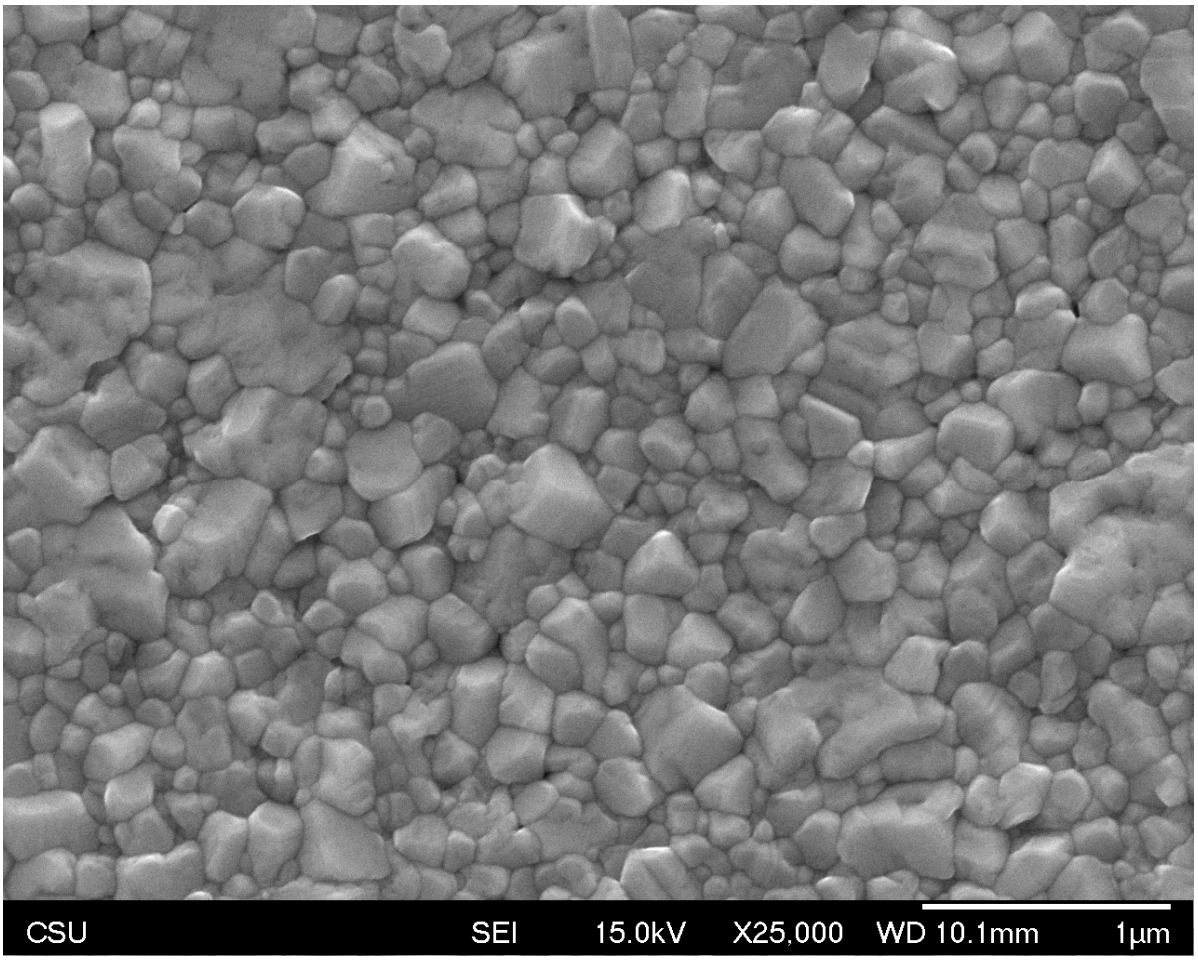

Figure 32 SEM image of $MgCl_2$ passivated CdZnTe for 20 minutes

JV measurements on the different passivated devices are shown below (Figure 33).

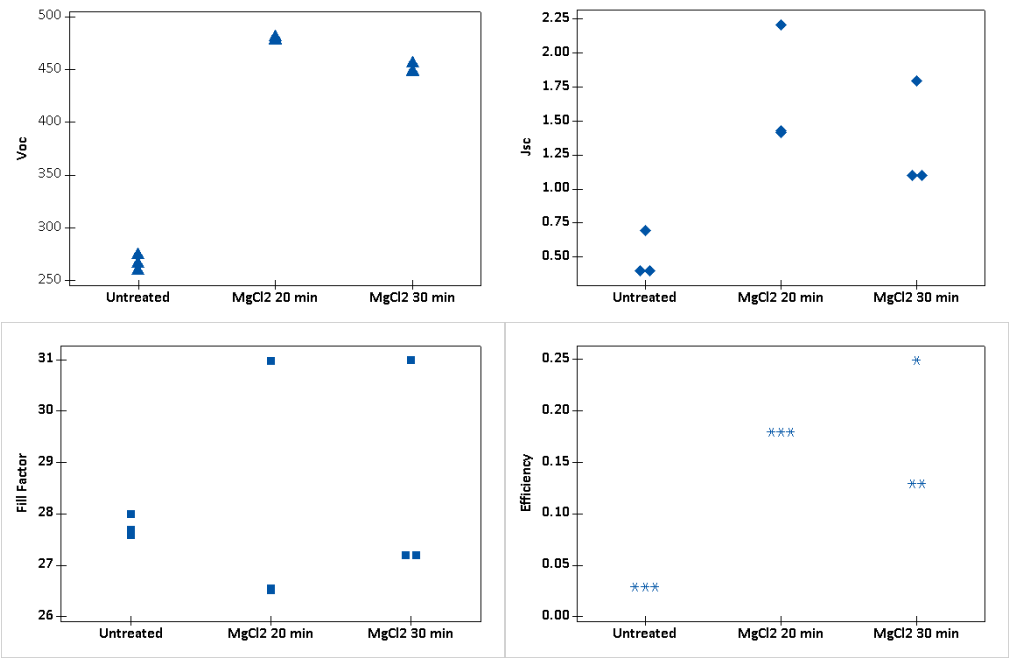

Figure 33 Parameters from JV Testing of $MgCl_2$ passivated Sample

From the above plots, there is an increase in the open circuit voltage for devices passivated with $MgCl_2$ when compared to the devices not passivated. The photo generated current is low in all the devices which indicates that the devices are not completely passivated. That affects the fill factor and efficiency values.

3.4 $ZnCl_2$ passivation treatment of CdZnTe

The $ZnCl_2$ passivation treatment was carried out on CdZnTe films deposited on CdS/Tec12D substrates along with CdTe films deposited on CdS/Tec12D. CdTe films were deposited in ARDS. The passivation treatment was carried out in the horizontal bell jar and process treatment is described in section 2.3. $ZnCl_2$ at 380^{o}C has a high vapor pressure of ~200mTorr. This temperature was kept constant in the passivation experiments. The passivation treatment time along with the spacing between the substrate and the graphite boat were varied. Details of the $ZnCl_2$ passivation treatment are given below.

Table 7 $ZnCl_2$ passivation treatment conditions

Passivation Temperature	Time	Spacers between the graphite boat and the substrate	Substrates	
(C)	Minutes	Yes/No	Half	Half
380	15	No	CdTe	CdZnTe
380	15	Yes	CdTe	CdZnTe
380	3	No	CdTe	CdZnTe

The purpose of not using the spacers was to contain $ZnCl_2$vapors in the region between the substrate and the boat. The intensity of the flux would be higher when not using the spacers.

The transmission was measured on the passivated substrates to check for zinc loss. The X ray diffraction study on one of the substrate (380^{o}C, 3 minutes, and no spacers) was conducted. The imaging under SEM, and EDS analysis was performed to understand the morphology and elemental composition at the surface. The tape test was conducted to check for delamination.

The transmission measurements are given below (Figure 34):

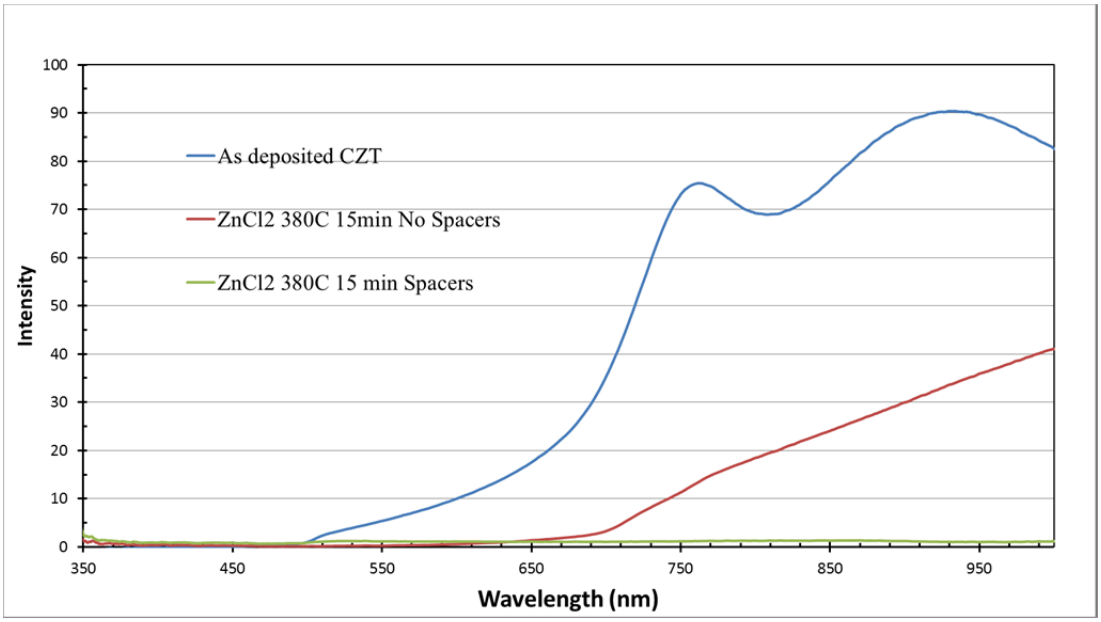

Figure 34 Transmission measurements on CdZnTe Films after $ZnCl_2$ treatment

In all the $ZnCl_2$ passivated substrates, severe decrease in the transmission was observed at the longer wavelengths.

The X ray diffraction result (Figure 35) on substrate with condition 380^oC, 3min and no spacers was compared with CdS/Tec12D substrate.

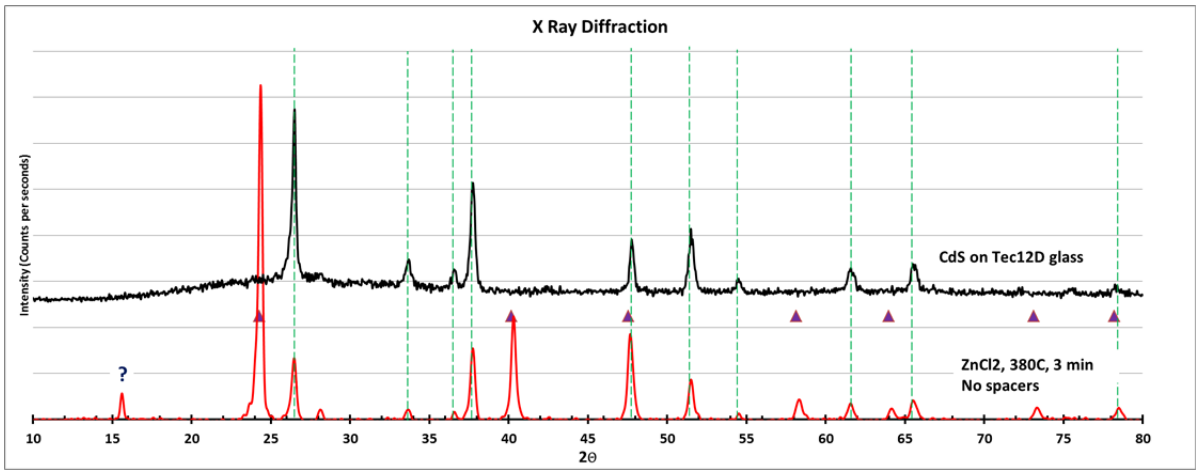

Figure 35 X Ray diffraction of $ZnCl_2$ passivated sample

After cross checking the peak pattern with standard CdZnTe ICCD card[40], no loss of zinc from CdZnTe film was observed. No new phases were detected. The intensity of the {111} decreased and other peaks related CdZnTe appeared with stronger intensity. This indicates that preferentially orientation along {111} has decreased and recrystallization has occurred. One of the peaks appeared at an angle 15.65^o. It was compared with peak patterns of CdTe, ZnTe, $ZnCl_2$, Zn, Te, Cd, Cd_xZn_xS and ZnO. No match was found.

The surface morphology of the same substrate was studies under SEM (Figure 36).

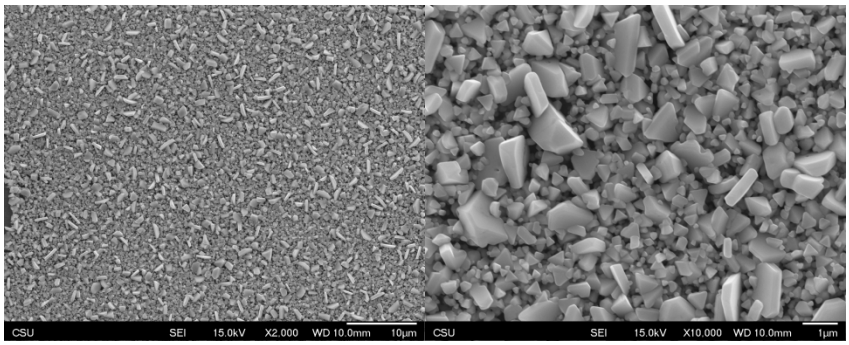

Figure 36 SEM images of the substrate passivated with $ZnCl_2$

The surface morphology of CdZnTe film changed from a coarse grain structure to loosely attached fine grain structure with large grains randomly distributed. The EDS point analysis showed (Figure 37) presence of zinc and chlorine on the surface.

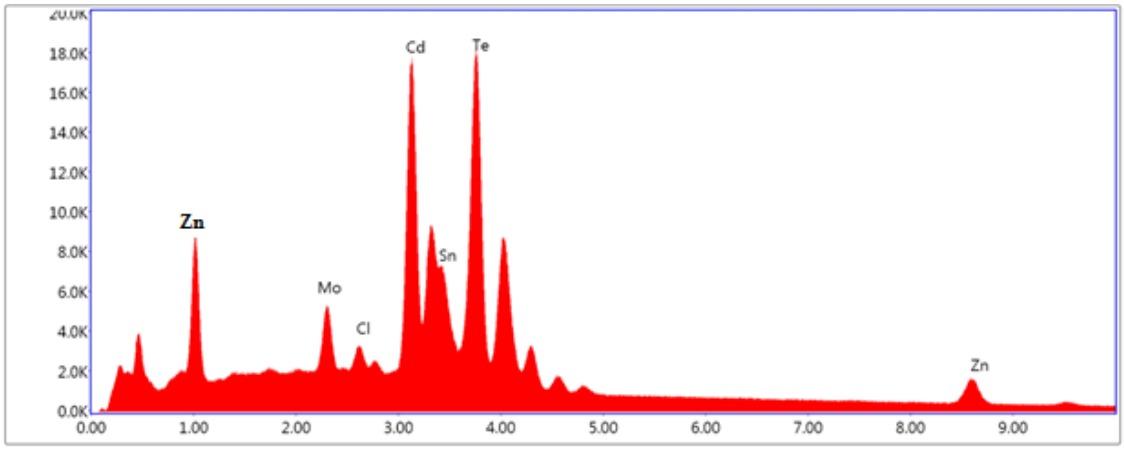

Element	Weight %	Atomic %	Net Int.	Error %	Kratio	Z	R	A	F
MoL	4.17	4.58	313.84	4.86	0.0386	0.0385	1.0458	0.9807	0.8503	1.0381
ClK	1.30	3.85	176.46	5.77	0.0139	0.0139	1.3027	0.8448	0.7941	1.0334
CdL	27.33	25.63	1655.24	2.33	0.2730	0.2730	1.0039	1.0095	0.9604	1.0361
SnL	10.19	9.05	486.34	3.76	0.0980	0.0987	0.9849	1.0177	0.9538	1.0310
TeL	44.58	36.83	1629.41	2.86	0.3936	0.3935	0.9473	1.0251	0.9143	1.0192
ZnK	12.44	20.06	180.73	5.95	0.1566	0.1566	1.1907	0.9649	0.9661	1.0946

Figure 37 EDS Point analysis of the substrate passivated with $ZnCl_2$

The delamination occurred in tape test conducted on all the CdZnTe substrates undergone $ZnCl_2$ passivation treatment (Figure 38). The delamination was at the interface of CdS and

CdZnTe. In CdTe films, the delamination occurred only in the film subjected to 15 minutes of $ZnCl_2$ at 380^oC with no spacers. This indicates that were aggressive and not suitable for passivation.

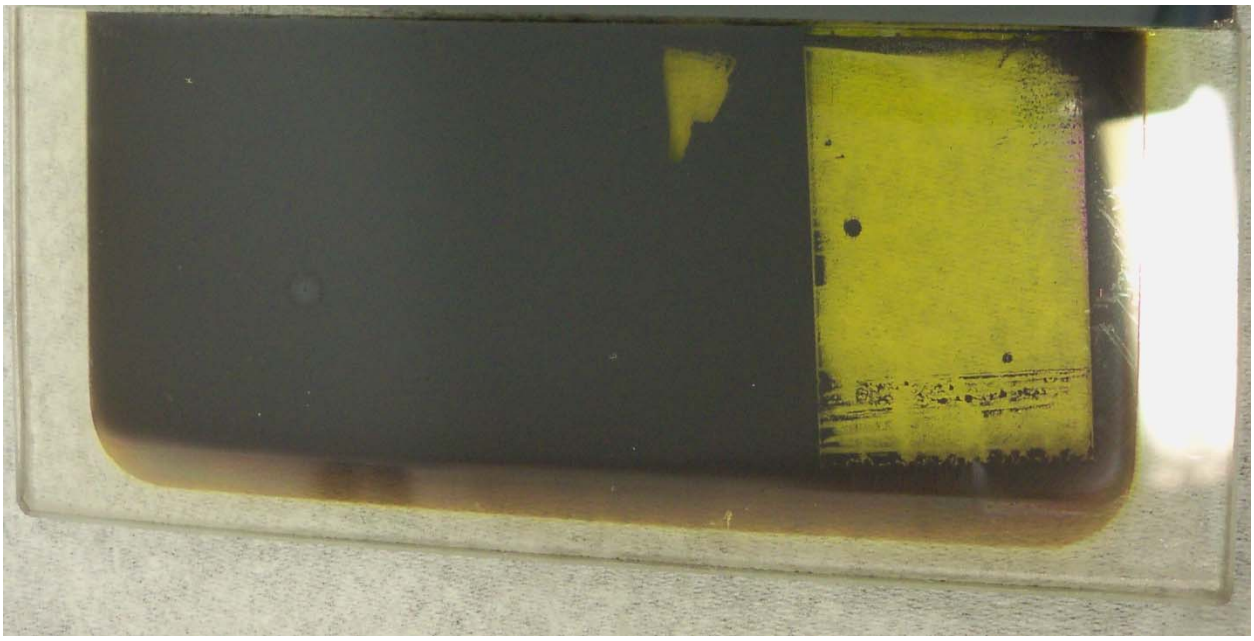

Figure 38 Delamination of CdZnTe after $ZnCl_2$ passivation at 380C 3minutes, No Spacers

The JV Testing was conducted on the following devices.

Table 8 JV Testing on $ZnCl_2$ Passivated Devices

Passivation Temperature	Time	Spacers between the graphite boat and the substrate	Substrates	
(C)	Minutes	Yes/No	Half	Half
380	15	Yes	CdTe	CdZnTe
380	3	No	CdTe	CdZnTe

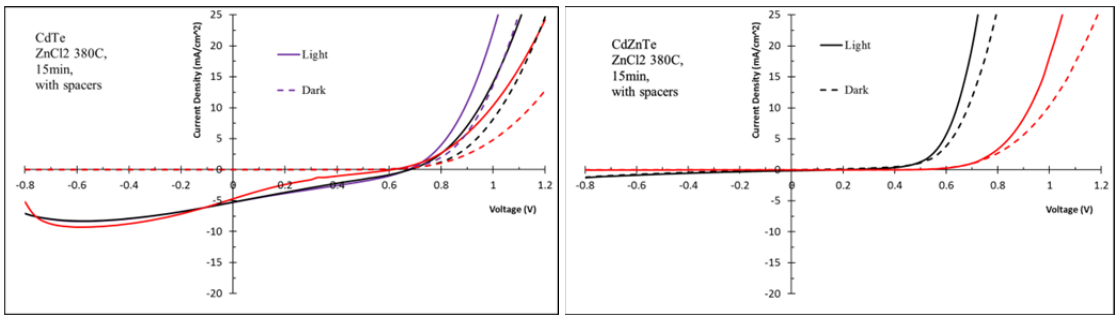

Figure 39 JV Measurements On $ZnCl_2$ Passivated (380^o C, 15minutes and With Spacers) Substrates

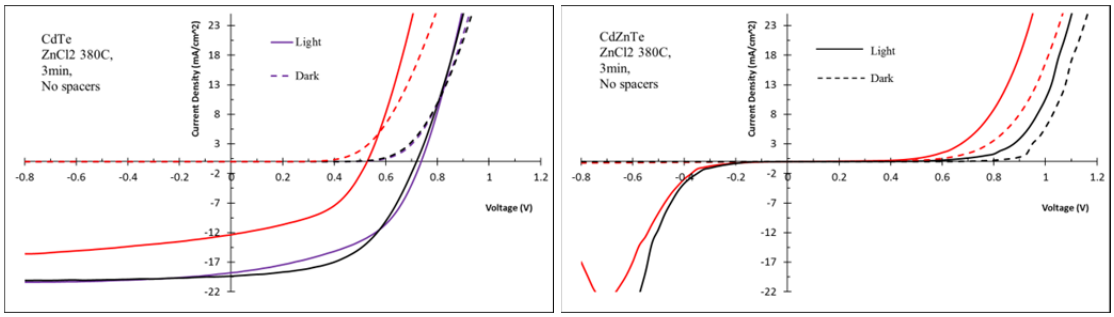

Figure 40 JV Measurements On $ZnCl_2$ Passivated (380^o C,3 min and No Spacers) Substrates

From the JV measurements, shorter $ZnCl_2$ treatment helps in improving the CdTe device performance. In both the cases for CdZnTe films, the devices are shunted.

The melting point of $ZnCl_2$ is 293^{o}C [42]. When the passivation treatments were conducted in the bell jar, graphite bottom and top plates would have been at 380^{o}C. But the glass substrate would be at slightly lower temperature. This would have caused condensation of $ZnCl_2$ on the substrate and led to undercutting of CdZnTe films. Determining correct parameters for $ZnCl_2$ treatment on CdZnTe is required.

Chapter 4
$CdCl_2$ Passivation Treatment on CdZnTe with CdS Capping Layer

4.1 Insights from the TEM/EDS of CdZnTe Cross Sections

Until now, 18 cross sectional specimens of CdZnTe deposited by RF sputtering or co-sublimation process on different window layers and processed at different conditions of $CdCl_2$ with or without different cappings have been viewed and mapped under TEM/EDS. The specimens were fabricated using focused ion beam. In this dissertation, results of 5 specimens are presented in total. The reaction mechanism proposed during the $CdCl_2$ treatment is based on the TEM/EDS results and other characterization techniques conducted on the CdZnTe samples.

During the $CdCl_2$ treatment on CdZnTe, two reactions initiate at the surface. The chlorine from $CdCl_2$ attacks the Zn atoms on the surface to form $ZnCl_2$ is the first reaction. After the surface layer of Zn is consumed, the reaction moves forward by converting Zn present in the grains to $ZnCl_2$. The second reaction is the chlorine migrating through the grain boundaries. Since large amount of Zn atoms available for chlorine to react, the Zn consumption from the grains to form $ZnCl_2$ dominates and the chlorine migration through the grain boundaries is retarded.

The capping layer which acts as a barrier layer on the back of the CdZnTe stalls the chlorine from reacting with Zn present on the surface. It allows the chlorine atoms to diffuse through the grain boundaries of capping layer and CdZnTe more rapidly than Zn escaping from the surface. If the $CdCl_2$ treatment is carried out for a longer amount of time, a localized loss of Zn from the surface occurs and heavy accumulation of chlorine along the CdZnTe/window layer

follows. For a extensively longer amount of $CdCl_2$ treatment time, the capping layer would be ineffective and complete loss of Zn would occur.

To minimize Zn escaping during the $CdCl_2$ treatment, the effective capping layer should have the following properties:

a) Deposition of the capping layer should be conformal and uniform on the CdZnTe surface
b) Efficacy of the $CdCl_2$ treatment should not be reduced by the prescence of the capping layer layer
c) Capping layer should not react with the underlying CdZnTe and be stable at high temperatures (500^{o}C)
d) Capping layer layer should be easily removed without hurting the underlying CdZnTe layer

4.2 Tested Hypothesis on RF Sputtered CdZnTe with CdTe Capping Layer During the $CdCl_2$ Passivation Treatment

Based on the material and electrical characterization results on RF sputtered CdZnTe with CdTe capping and then treated with $CdCl_2$, showed

a) Partial retention of zinc in the bulk CdZnTe at lower $CdCl_2$ passivation temperatures
b) Chlorine along the grain boundaries of CdTe, CdZnTe and CdS
c) Diffusion of Zn in the CdS window layer
d) CdZnTe grain growth was observed
e) Photo generated current was not observed in the short wavelength region corresponding to CdS

The improvement in the device performance was observed. But CdTe as a capping film had following disadvantages:

a) The CdTe capping layer contributed to the photo generated current
b) The CdTe capping layer was not effective to minimize loss of Zn from the bulk CdZnTe

c) The etching of CdTe using bromine methonal solution without damaging underlying CdZnTe is difficult

d) Additional resources such as ion beam etching would be required to etch CdTe film instead of wet etching process

4.3 Modified Device Structure Using CdS Capping Instead of CdTe

To overcome the drawbacks of CdTe as a capping film and Zn diffusion in CdS window layer, a modified device structure with CdS film as a capping layer and Mg-Zn-O as a buffer was fabricated (Figure 41)

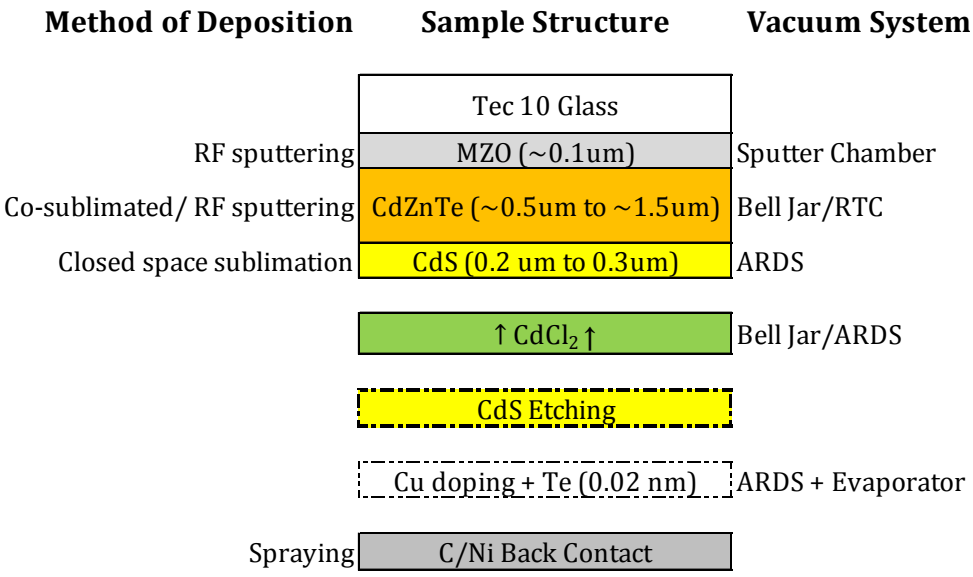

Figure 41 Modified device structure with CdS capping layer

The advantages of the modified structure are as follows:

a) The chlorine from the $CdCl_2$ can penetrate through the CdS layer and dope the CdZnTe grain boundaries as n-type

b) The CdS film can be etched without damaging the underlying CdZnTe layer

c) The etching process involves the use of diluted hydrochloric acid

d) The time for etching CdS (0.5 micron) is less than a minute

e) The CdS capping layer will not contribute to photo generated current

f) If CdS capping film is not etched properly, it will obstruct the current flow from the CdZnTe to the back contact and can be easily detected in JV testing

g) Mg-Zn-O is a wide band gap material and has low absorption coefficient in short wavelength region of the spectrum when compared to CdS

h) Zn diffusion in Mg-Zn-O layer will insignificant when compared to the diffusion in CdS

To investigate the efficacy of the CdS film as a capping layer, RF sputtered CdZnTe and co-sublimated CdZnTe as an absorber layer were used in the experiments. The band gap of the CdZnTe in both the cases was kept at 1.72 eV. The material and electrical characterization was conducted to determine the overall effectiveness of CdS film as capping layer during the $CdCl_2$ treatment.

4.4 $CdCl_2$ Treatment on RF Sputtered CdZnTe with CdS Capping

The samples were prepared with RF sputtered CdZnTe on MgZnO followed by CdS cap and then $CdCl_2$ treatment. The RF sputtered CdZnTe film thickness, $CdCl_2$ process temperature and CdS film thickness on RF sputtered CdZnTe were varied. The outline of the various parameters is listed (Table 9).

Table 9 Outline of process parameters varied

RF sputtered CdZnTe	*Thickness*	0.75 um, 1.0 um
CdS Capping Film	*Thickness*	0.1 um, 0.2 um
Bell jar $CdCl_2$ Passivation	*Temperature*	360°C, 380°C, 400°C
	Time	1 minute to 8 minutes
ARDS $CdCl_2$ Passivation	*Temperature*	380°C
	Time	2 minute to 3.5 minutes

4.5 Device Performance of RF sputtered CdZnTe with CdS capping treated with $CdCl_2$

The summary of RF sputtered CdZnTe undergon $CdCl_2$ passivation treatment with CdS capping is shown in Table 10.

Table 10 List of RF sputtered CdZnTe samples fitted with CdS capping layer and treated with $CdCl_2$

Sample#s	Cd-Zn-Te thickness on MgZnO	$CdCl_2$ passivation treatment in Horizontal Bell Jar		CdS cap	Zinc loss after CdCl treatment (Transmission Measurements)	JV	
		temperature	time			Dark	Light
	microns	deg C	minutes	nanometers			
106-3R	1	380	5	200	Significant loss	rectifying	poor diode
106-3l	1	400	5	200	huge loss with shift in band edge	Delaminated	
105-2R	2	400	3	200	No loss (pinholes)	rectifying	poor diode
105-2L	2	360	8	200	No loss	rectifying	poor diode
106-4lQE	1	400	2	200	minor loss at the back	rectifying	poor diode
106-4r	1	-	-	200			
106-2L	1	435^{ARDS}	1	200	minor loss at the back	flat	poor diode
106-2R	1	435^{ARDS}	0.75	200	minor loss at the back	rectifying	poor diode
94-8L	1	380	1	200	No loss	rectifying	good diode
94-8R	1	380	2	200	No loss	rectifying	good diode
94-9R	1	380	3	150	minor loss at the back (pinholes)	-	-
94-9L	1	380	5	150	minor loss at the back (pinholes)	-	-
94-11L	0.75^{CdS}	380	1	100	No loss	rectifying	good diode
94-11R	0.75^{CdS}	380	2	100	No loss	rectifying	good diode
105-4l	1	$380^{ARDS, intlet temp 325C}$	2.5	200	No loss	flat	poor diode
105-4R	1	$380^{ARDS, intlet temp 325C}$	3.5	200	No loss	flat	poor diode
105-3l	1	$380^{ARDS, intlet temp 325C}$	2	200	No loss	flat	poor diode
105-3R	1	$380^{ARDS, intlet temp 300C}$	2	200	No loss	flat	poor diode

^{ARDS} $CdCl_2$ passivation treatment conducted in ARDS

^{CdS} CdS window layer used instead of MgZnO

Although no strong correlation was observed, some of the promising results are discussed. At higher passivation temperature accompanied by longer treatment time caused significant loss of Zn from the CdZnTe. The shift in the band edge towards the longer wavelength region measured in the transmission was an indication of significant loss of zinc.

In the passivation treatments conducted at 380^{o}C with varied time suggested a trend in the overall device performance. After etching the CdS capping layer from the CdZnTe treated with the $CdCl_2$, no significant change in the band gap was observed (Figure 42). However, with the passivation treatment time of 5 minutes, there was an increase in the transmission intensity. Close examination of the samples treated for 3 minutes and 5 minutes revealed lot of pinholes in

the CdZnTe absorber. The prescence of pinholes in the CdZnTe absorber is detrimental to the device performance.

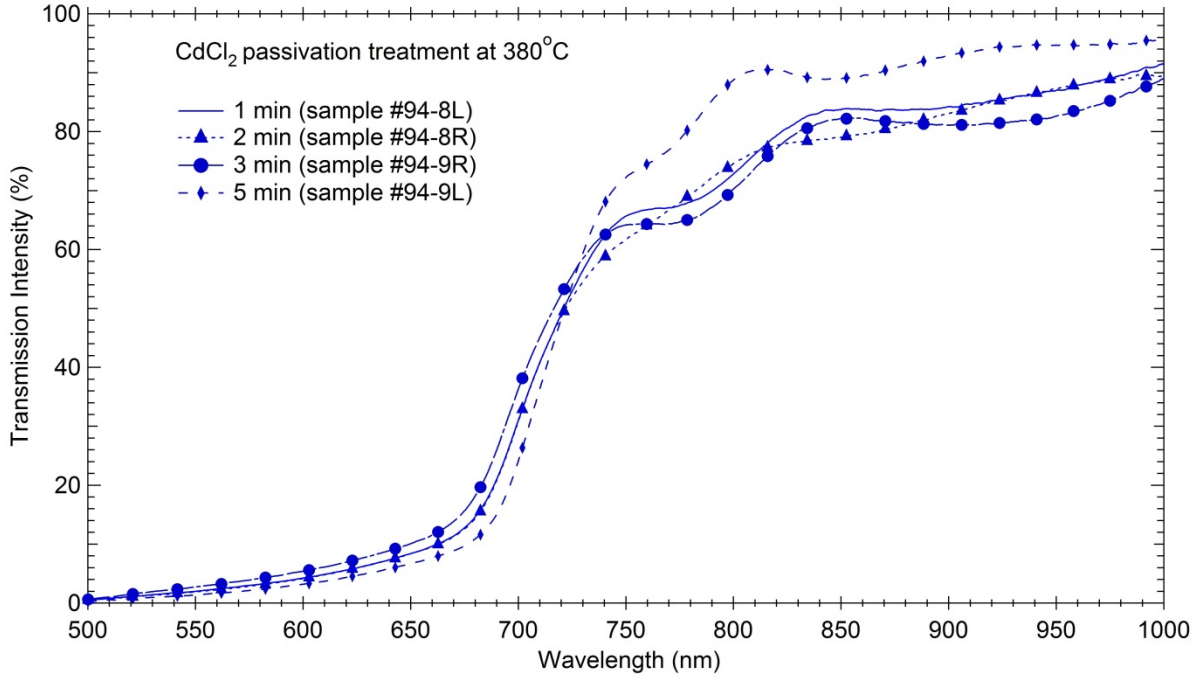

Figure 42 Transmission measurements CdS etched from RF sputtered CdZnTe that had undergone $CdCl_2$ treatment

In the JV measurements (Figure 43), the sample treated with $CdCl_2$ for 2 minutes had a better device performance. However longer $CdCl_2$ passivation time or temperature without the generation of pinholes is required for further improving the device performance From the EQE graph (Figure 44), the band edge of the RF sputtered CdZnTe was maintained after the $CdCl_2$ treatment. This is a good indication of CdS film acting as a capping for zinc loss from CdZnTe during the $CdCl_2$ treatment. The total photo generated current collected was less than 50% which may be attributed to incomplete passivation of the CdZnTe absorber. In the shorter wavelength region, photo generated current collection was observed suggesting MgZnO buffer more suitable than CdS window layer.

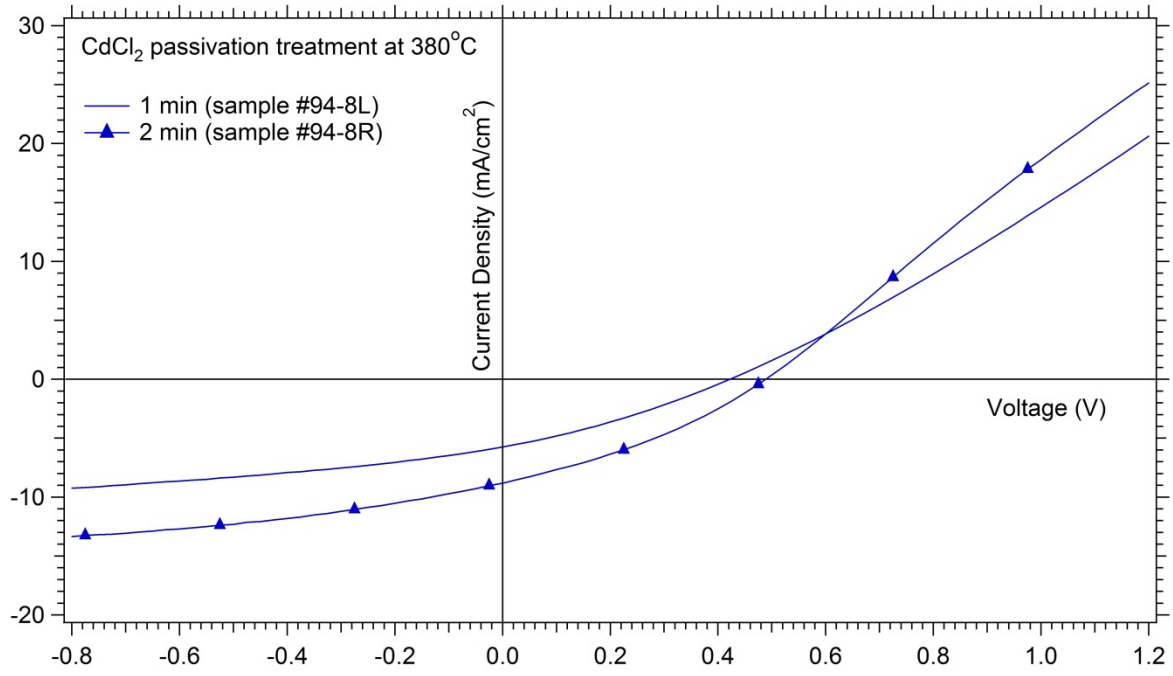

Figure 43 JV graph of devices fabrciated after etching CdS capping from RF sputtered CdZnTe treated with $CdCl_2$

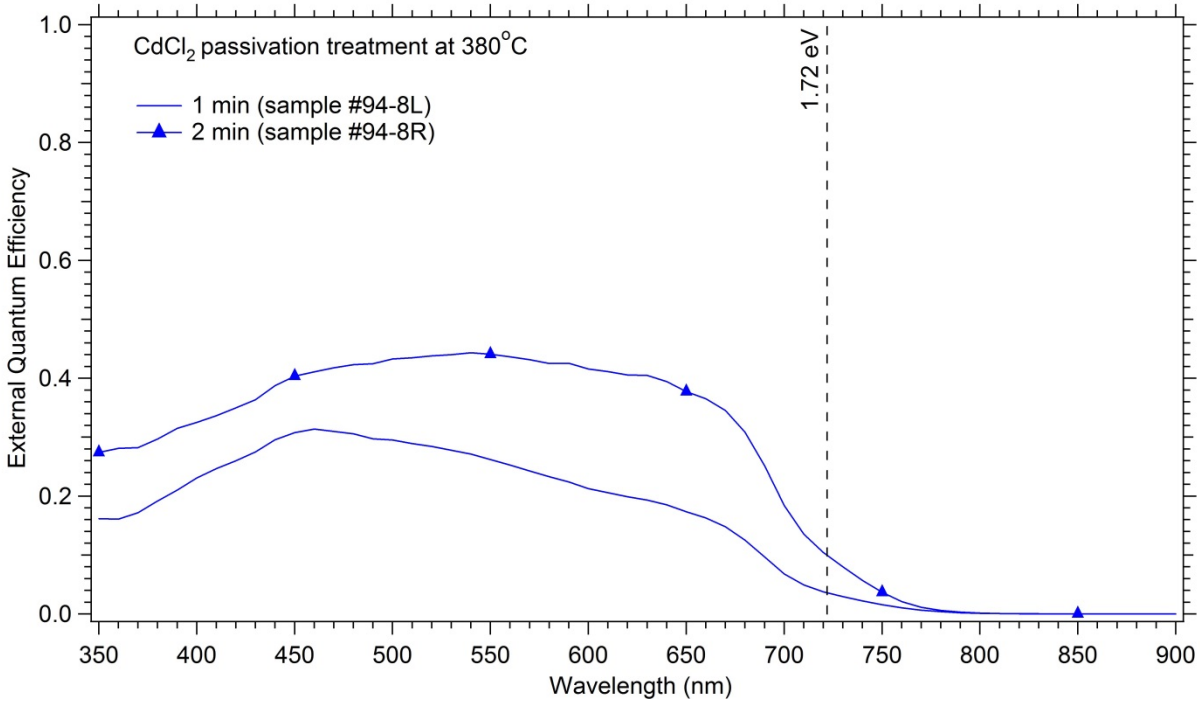

Figure 44 External quantum efficiency of devices fabrciated after etching CdS capping from RF sputtered CdZnTe treated with $CdCl_2$

4.6 $CdCl_2$ treatement on co-sublimated CdZnTe with CdS capping

As shown in theFigure 45, three samples of CdZnTe were fabricated with the co-sublimation of CdTe and Zn. The thickness of CdZnTe, band gap (1.72 eV) and the deposition process parameters were all kept the same. The $CdCl_2$ passivation treatment on the two CdZnTe samples was also the same. The as-deposited CdZnTe sample and $CdCl_2$ treated CdZnTe without CdS capping sample were used to guage the efficacy of the CdZnTe sample with CdS capping and treated with $CdCl_2$

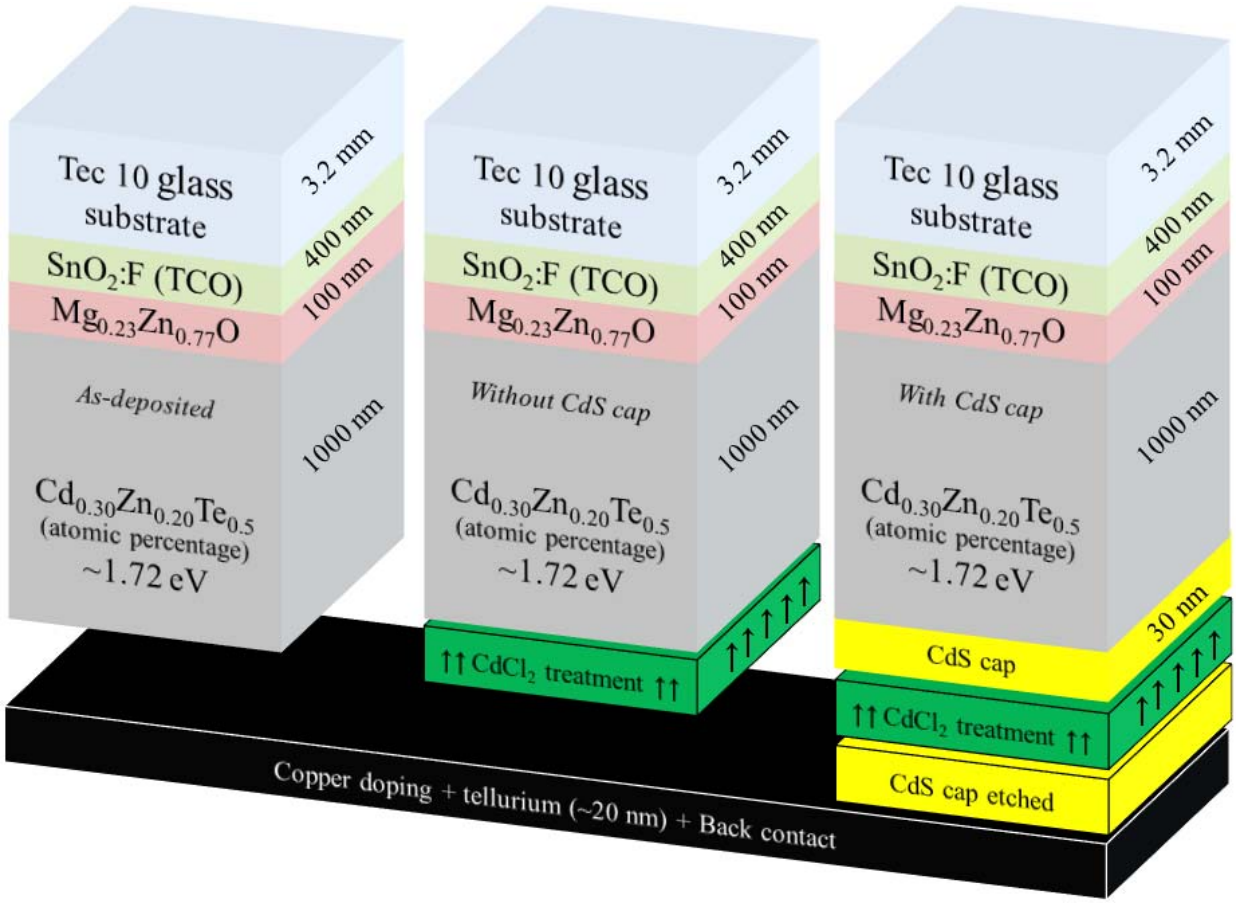

Figure 45 Co-sublimated CdZnTe samples used to test the efficacy of CdS capping layer during the $CdCl_2$ treatment

4.7 Device Performance of Co-Sublimated CdZnTe with CdS Capping Treated with $CdCl_2$

In the transmission measurements (Figure 46), CdZnTe sample with no capping layer and treated with $CdCl_2$ exhibited a clear shift in the band edge towards the longer wavelength region when compared to the as-deposited CdZnTe sample. The shift in the band edge towards the longer indicates that the CdZnTe has lost significant amount of Zn and converted to a lower band gap material closer to CdTe. The change in the band gap during the $CdCl_2$ passivation treatment points out to the fact that a capping layer on CdZnTe is necessary to prevent Zn loss.

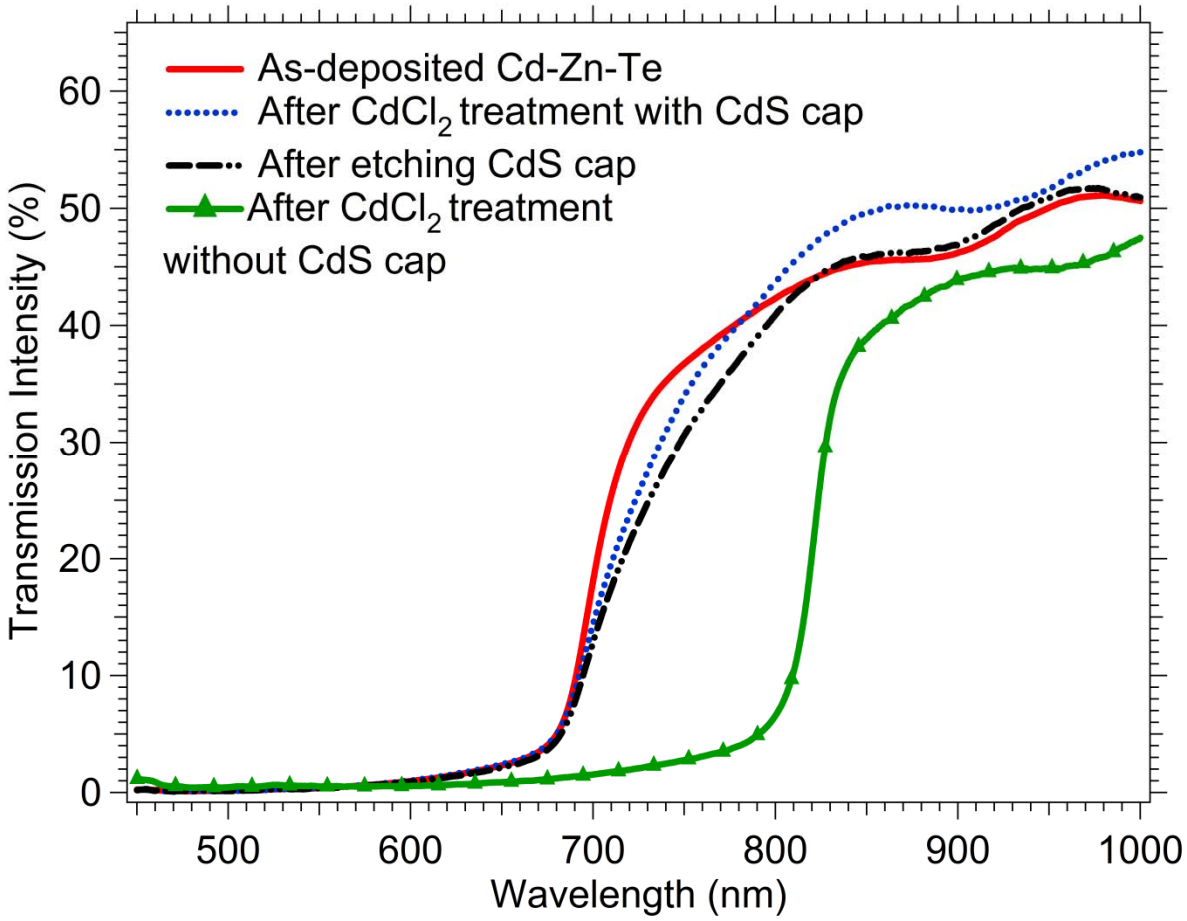

Figure 46 Transmission measurements on co-sublimated CdZnTe samples

After etching the CdS off the back surface of CdZnTe treated with $CdCl_2$, there was slight change in the transmission. The change would be due to slight loss of Zn from the back surface of CdZnTe during the $CdCl_2$ treatment in the form of $ZnCl_2$.

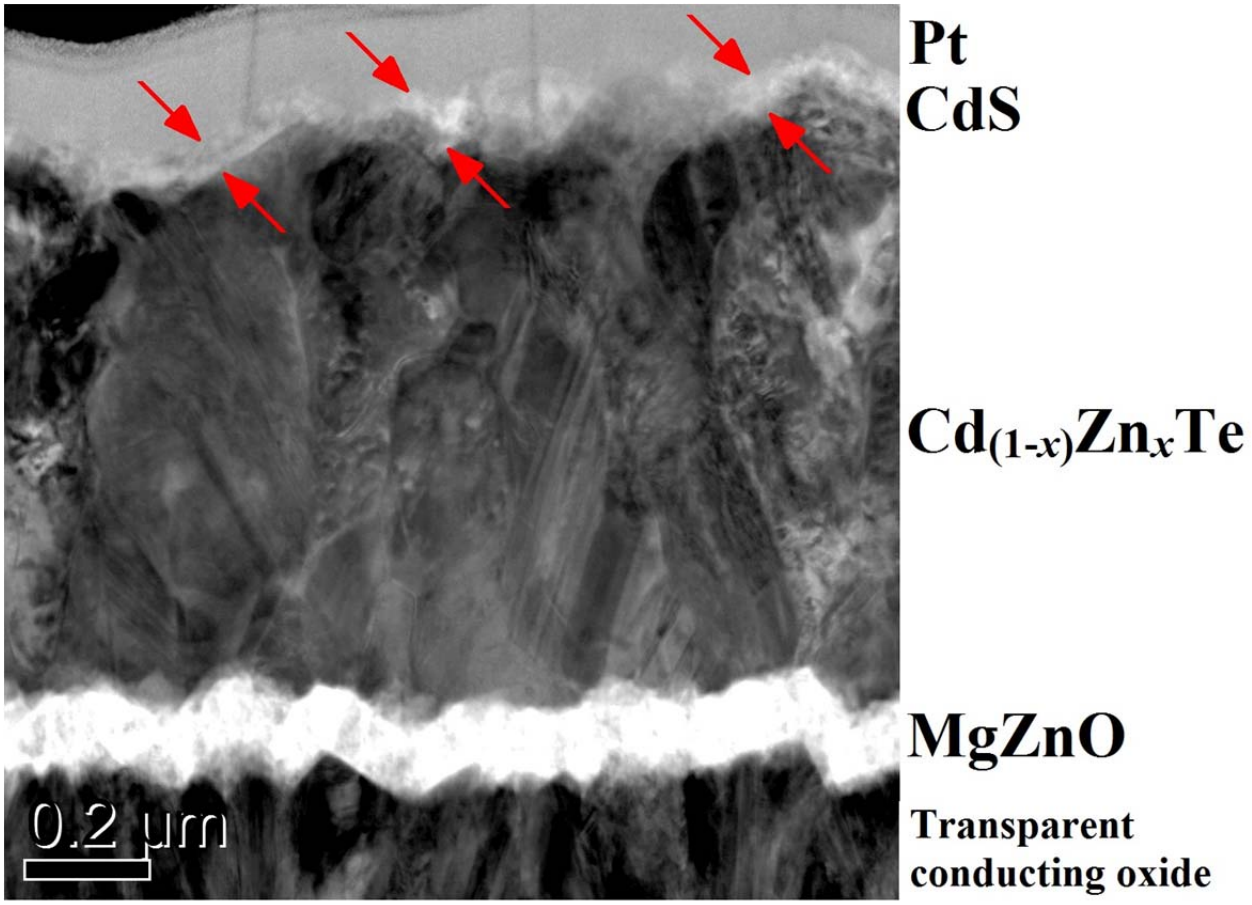

Figure 47 Bright field image of the cross section of the CdZnTe sample fitted with CdS capping layer and treated with $CdCl_2$ treatment

The cross section of the CdZnTe sample fitted with the CdS capping and treated with the $CdCl_2$ was prepared using focused ion beam and viewed under transmission electron microscope at Loughborough University (Figure 47). The deposited CdZnTe on MgZnO was close to 1 micron. In CdTe absorbers treated with the $CdCl_2$, recrystallization, grain growth to a large size grains and removal of majority of stacking faults is observed. In the bright field image, the recrystallization of CdZnTe was observed after the $CdCl_2$ treatment to some extend. The stacking faults were present in very few grains of CdZnTe which suggested that more aggressive or longer $CdCl_2$ treatment is required to completely passivate the CdZnTe absorber.

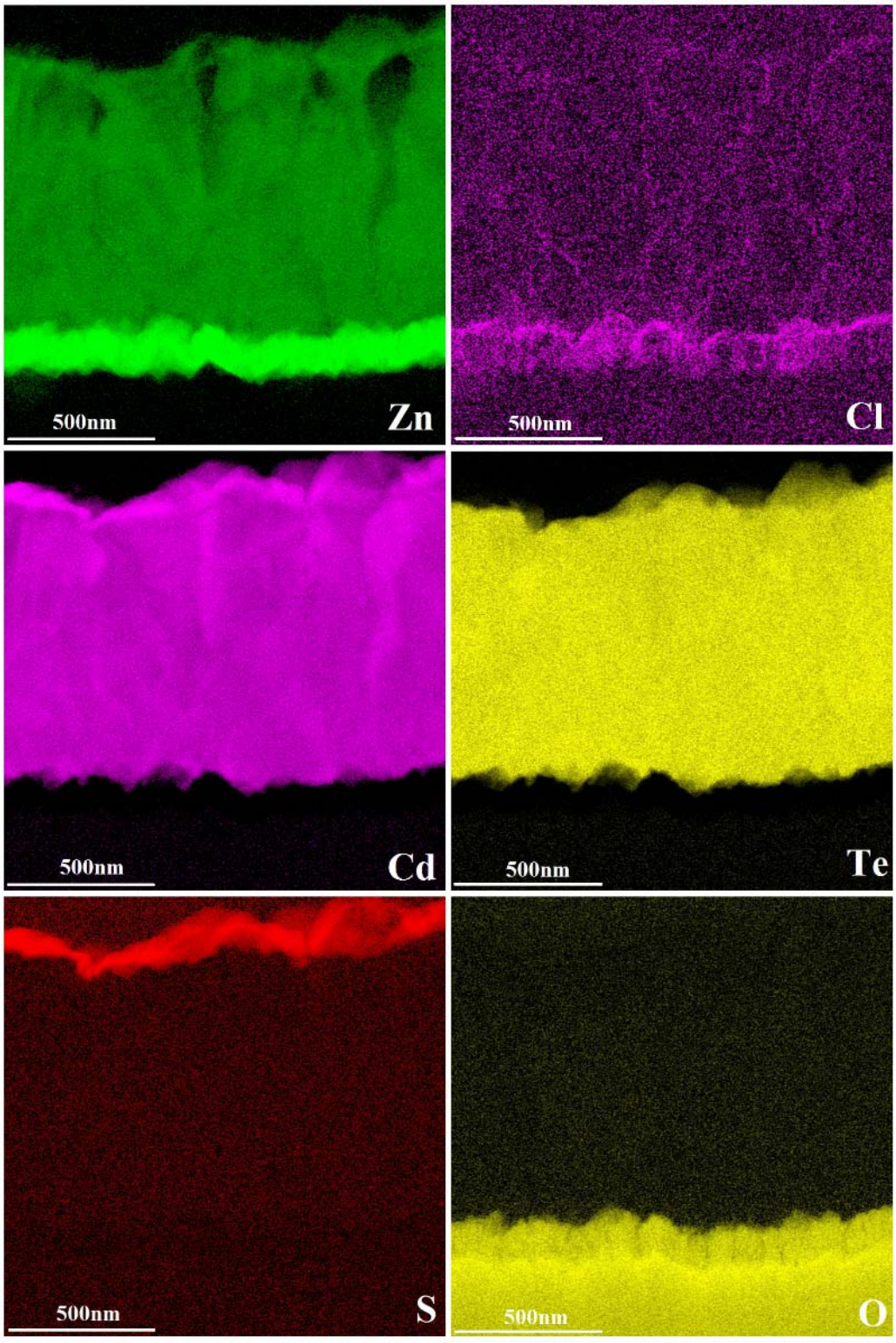

Figure 48 Elemental maps collected from the cross section of co-sublimated CdZnTe sample fitted with CdS cap and treated with $CdCl_2$

The elemental maps collected from the cross section of the co-sublimated CdZnTe sample fitted with CdS cap and treated with $CdCl_2$ is shown in the Figure 48. Most of the zinc is retained after the $CdCl_2$ treatment was observed in the bulk of CdZnTe. Minor loss of Zn was observed from the back surface of co-sublimated CdZnTe. This results is in line with the loss of Zn from the back surface of RF sputtered CdZnTe treated with the $CdCl_2$. There is an abrupt change in the concentration of Zn from MgZnO to CdZnTe. The abrupt change suggested that there was no Zn diffusion from CdZnTe to MgZnO or vice versa. No major streaks of Zn diffusion in CdS was observed.

One of the encouraging results was observed in the Cl map. The Cl decorating the CdZnTe grain boundaries without causing the loss of Zn is a major step in passivating the CdZnTe absorber. In the literature, the Cl in grain boundaries of CdTe have improved the device performance by a factor of 4 when compared to untreated CdTe [18]. The Cl accumulation observed at the interface of CdZnTe and MgZnO is considered to be detrimental to the device performance. The accumulation of Cl at the interface and no recrystallization or grain growth suggests that the $CdCl_2$ passivation treatment time is sufficient for Cl to diffuse through the CdZnTe absorber. But the thermal energy is inadequate for recrystallization or grain growth of CdZnTe. This can be resolved by increasing the substrate temperature as well as the $CdCl_2$ source temperature during the $CdCl_2$ process.

The Te map was uniform indicating that no other phases such as ZnTe or CdTe were being formed. The S map confirmed that the CdS capping layer was uniform and conformal over the back surface of CdZnTe. The formation of oxides in the CdZnTe was below the detection limit of the instrument.

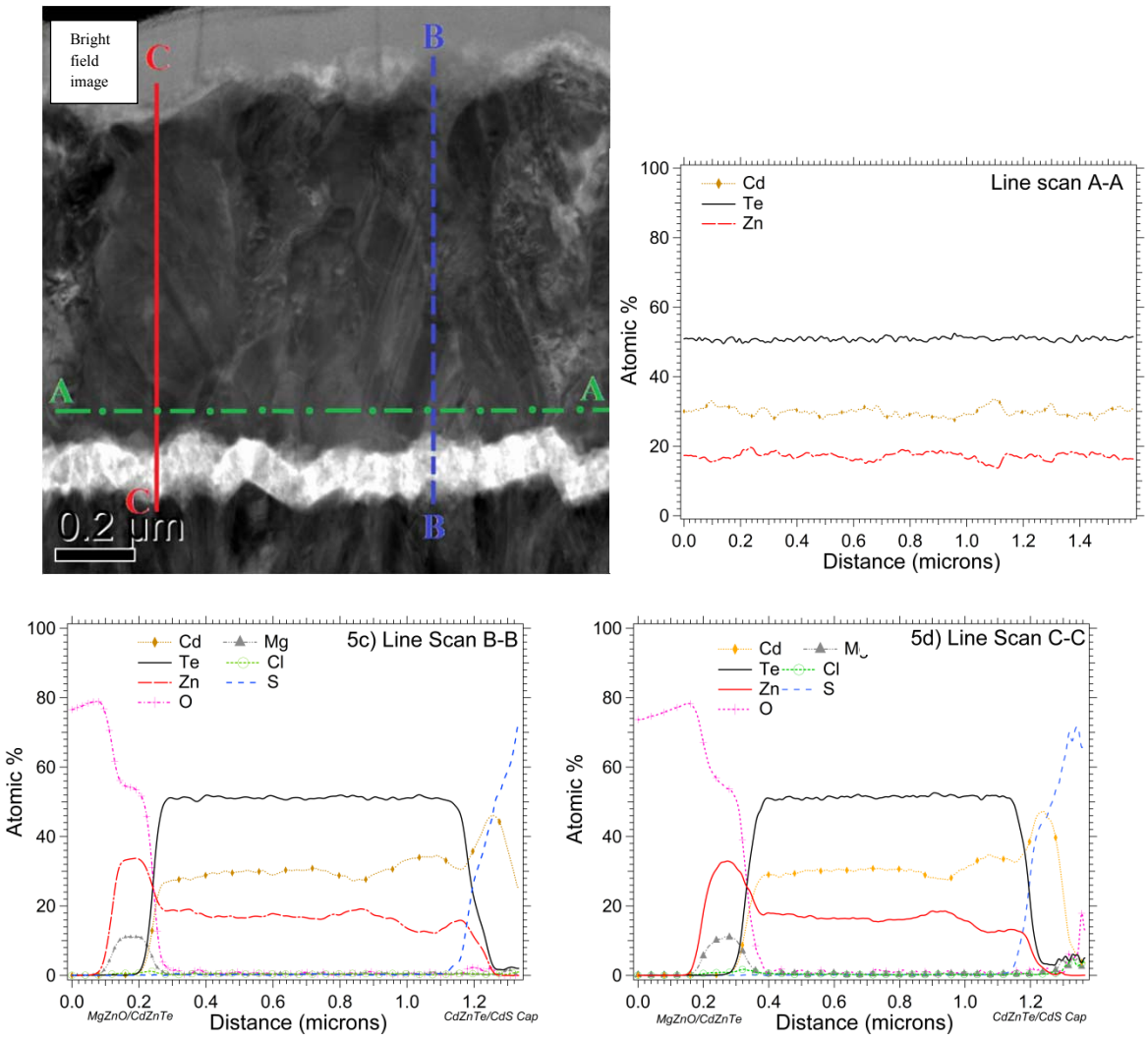

Figure 49 Line scans on the cross section of the co-sublimated CdZnTe sample fitted with CdS cap and treated with $CdCl_2$

The line scans on the cross section of co-sublimated CdZnTe with CdS capping and treated with $CdCl_2$ (Figure 49) was conducted at various locations to determine quantitatively the composition of elements present. The line scan A-A probed the bulk of CdZnTe and the composition was $Cd_{29.87}Zn_{17.14}Te_{50.85}$ by atomic percentage which equal to the $Cd_{59.74}Zn_{34.28}Te$ by weight. The corresponding band gap for the calculated composition is close to ~1.68 eV. The composition of CdZnTe unchanged after the $CdCl_2$ treatment supports the data from the elemental maps of Zn and Cl. In the line scans B-B and C-C, there is decrease in the Zn atomic

% and corresponding increase in Cd atomic % near the CdZnTe-CdS capping interface. The Te atomic % remains unchanged. The presence of Zn in a decreasing composition in the CdS capping is also observed. The average composition calculated for different regions is given in the Table 11.

Table 11 Composition of contributing elements obtained from the line scans

Composition of Cd-Zn-Te obtained from different line scans

Fig. 5	Line scan	Distance (microns)	Atomic %					
			Cd	Zn	Te	S	$Cd_{(1-x)}Zn_xTe$	Estimated bang gap of $Cd_{(1-x)}Zn_xTe$ (eV)
(a) and (b)	A-A	0 TO 1.5	29.87	17.14	50.85	-	$Cd_{29.87}Zn_{17.14}Te$	1.68
		STD. DEV.	1.86	1.53	1.73	-		
(a) and (c)	B-B	0.3 TO 0.8	29.50	17.23	51.16	-	$Cd_{29.50}Zn_{17.23}Te$	1.68
		STD. DEV.	1.41	1.12	1.33	- BELOW 0.3		
		0.9 TO 1.1	32.59	14.28	51.17	-	$Cd_{32.59}Zn_{14.28}Te$	1.63
		STD. DEV.	2.06	2.00	1.33	BELOW 0.3		
		0.44 TO 0.84	30.26	~17.00	51.32	BELOW 0.2	$Cd_{30.26}Zn_{17.00}Te$	1.68
		STD. DEV.	0.97	0.8	1.09	-		
(a) and (d)	C-C	1.0 TO 1.1	33.33	13.49	51.62	- BELOW 0.2	$Cd_{33.33}Zn_{13.49}Te$	1.62
		STD. DEV.	1.39	1.26	1.13	-		
		1.1 TO 1.3	37.97	7.24	24.90	27.06	In the CdS cap	-
		STD. DEV.	6.34	5.46	20.81	21.56		

Standard Deviation (STD. DEV.)

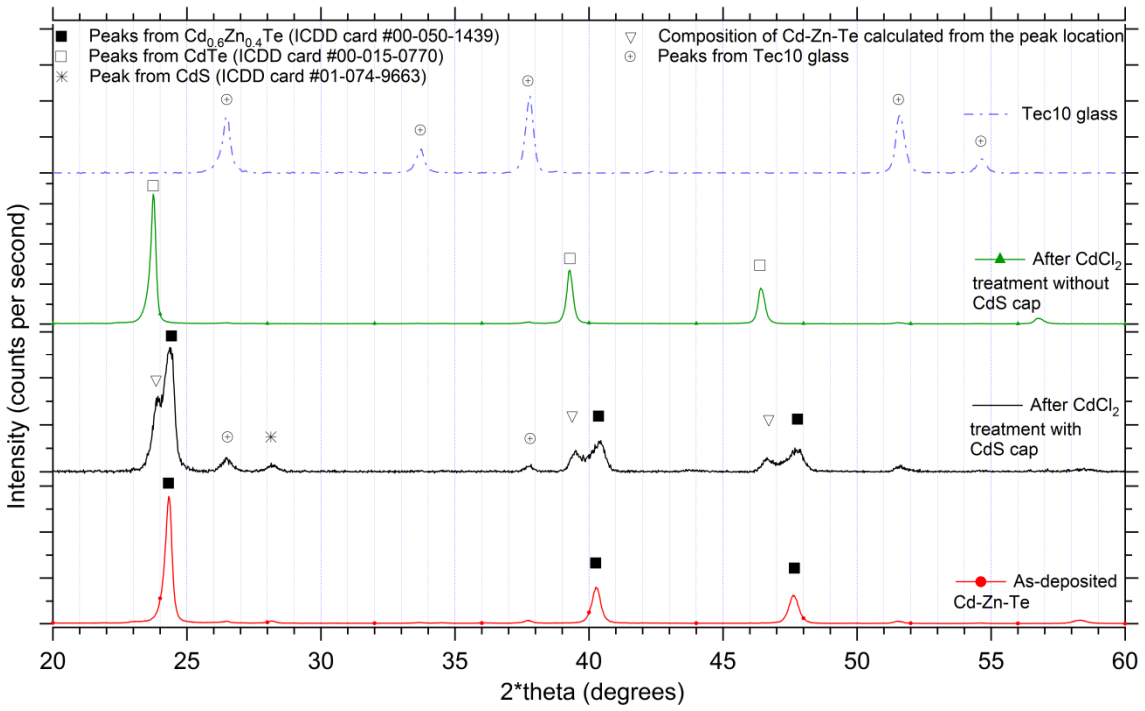

Figure 50 Glancing angle X-ray diffraction on the co-sublimated CdZnTe samples and Tec 10 glass

The glancing angle X- ray diffraction (Figure 50) was conducted on the co-sublimated CdZnTe samples to identify the composition and structural changes before and after the $CdCl_2$ treatment. From the TEM images, the zinc loss occurs from the back surface of CdZnTe. Keeping that result in mind, glancing angle of 3^o was selected to probe the CdZnTe films. At the same glacing angle, X-ray diffraction was also conducted on a bare Tec 10 glass to compare the peaks generated from the underlying SnO_2:F film.

The diffracted peaks (24.32^o, 40.26^o, 47.62^o) generated from as-deposited CdZnTe matched closely with the alloy composition of $Cd_{0.6}Zn_{0.4}Te$ by weight (ICDD card #00-015-1439). The band gap for the corresponding alloy is 1.72 eV. The as-deposited CdZnTe had a prefreed orientation along {111} corresponding to peak at 24.32^o. The peaks from other compounds such as CdTe or ZnTe wer not observed. The deposited CdZnTe film was a single phase face centered cubic structured ternary alloy of CdZnTe.

In the CdZnTe sample treated with $CdCl_2$ without any capping layer, the diffracted peaks shifted towards the lower 2*theta angle. This suggested that there is a significant change in the composition of the film after the $CdCl_2$ treatment. The peaks (23.74^o, 39.28^o and 46.4^o) closely matched to CdTe peaks given in the ICDD card# 00-015-0770. The peak at 23.74^o corresponding to plane {111} had the high intensity suggesting the prefreed orientation remained the same after the $CdCl_2$ treatment.

In the CdZnTe sample fitted with CdS capping layer and treated with $CdCl_2$ showed no major change in the alloy composition. The diffracted peaks matched with the peaks from the as-deposited CdZnTe sample. However, new low intensity peaks were identified. The composition of the alloy with the new low intensity peaks was $Cd_{0.9}Zn_{0.1}Te$ by weight [31]. The new alloy formed would be near the back surface of CdZnTe and in agreement with the observations noted in the elemental maps.

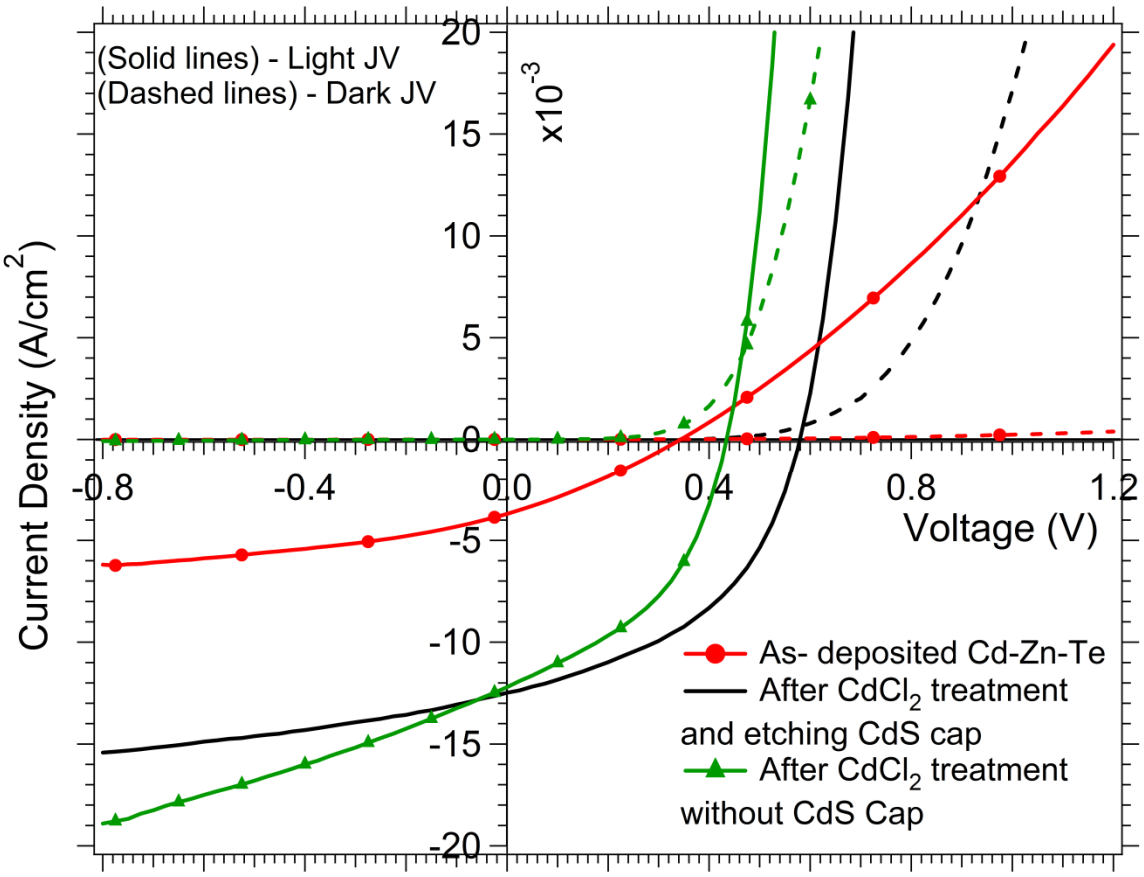

Figure 51 JV graphs of the devices fabricated from the co-sublimated CdZnTe samples.

To understand the device performance, JV testing was conducted on the three samples fabricated from co-sublimation process (Figure 51). For the as-deposited CdZnTe devices, the JV graph under zero illumination was flat which was a sign of a poor diode. In the forward bias condition, the current collection was linear with the applied voltage suggesting that as-deposited CdZnTe was a poor absorber and some post deposition treatment is required to improve the device performance.

In the rest of the two samples treated with $CdCl_2$, the devices exhibited a diodle like curve. The device with CdS cap during the $CdCl_2$ treatment had better device performance than the device without CdS cap during the $CdCl_2$ treatment. The short circuit current density measured for the device with CdS cap during the $CdCl_2$ treatment was 12.5 mA/cm^2. When

compared to the current generated by an ideal absorber with a band gap of 1.72 eV with including the estimated losses, the measured short circuit current density was more than 75% of the incident light. The kink in the JV measurement was not observed from the device with CdS cap during the $CdCl_2$ treatment suggesting that CdS was completely removed during the acid etch process.

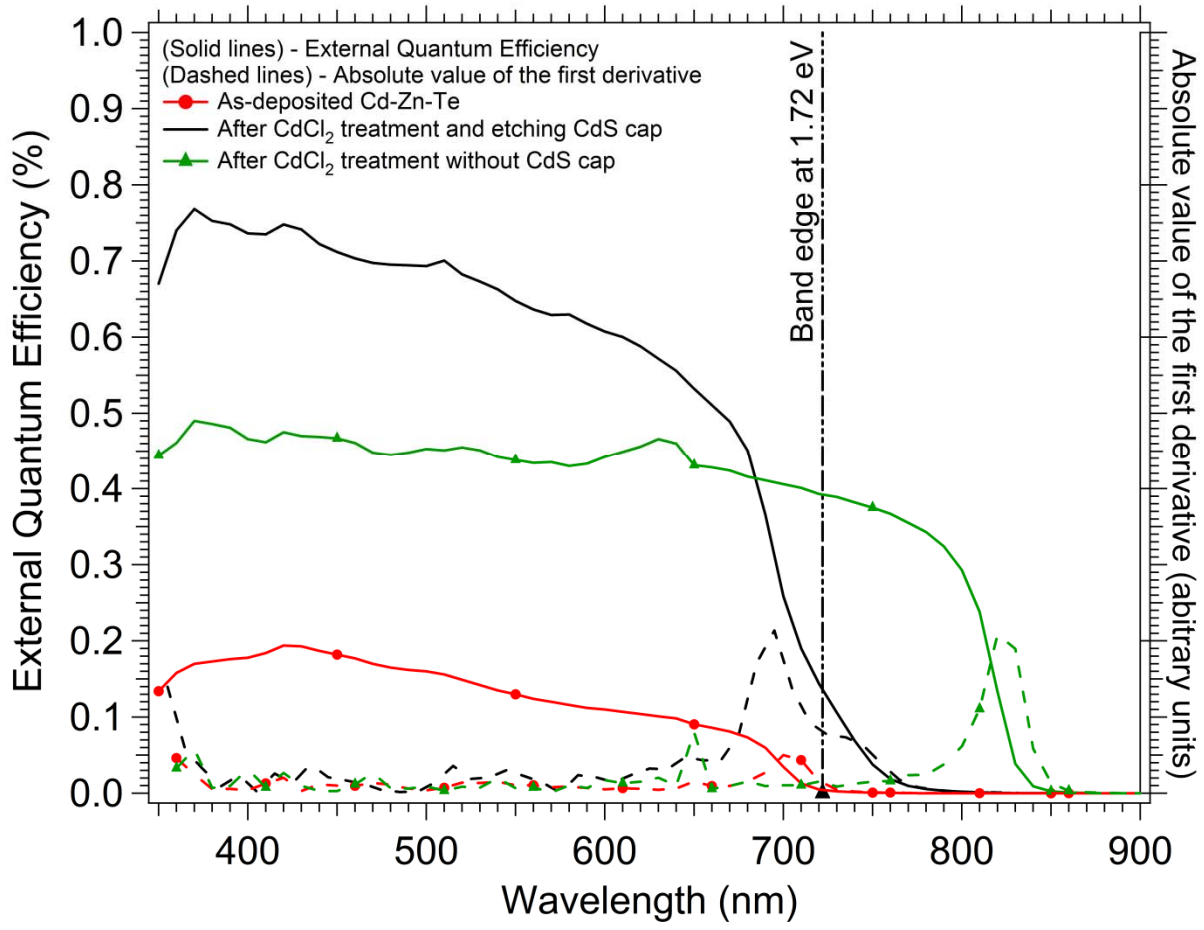

Figure 52 External quantum efficiency measurement on the devices fabricated from the co-sublimated CdZnTe samples

The external quantum efficiency measurement conducted on the fabricated devices from the co-sublimation process is shown in the Figure 52. The shift in the band edge in the device fabricated from as-deposited CdZnTe is not observed but the EQE is lower than the samples treated with $CdCl_2$. For the device with CdS cap during the $CdCl_2$ treatment, showed no shift the

band edge. This means that the composition of the CdZnTe after the $CdCl_2$ treatment is maintained. The current collection near the short wavelength region is close 0.7 where absorption occurs and lower in the range of 550 nm to 650 nm. The lower current collection may be due to the recombination at the back surface of CdZnTe. A significant shift towards the longer wavelength region was observed in the device without CdS cap during the $CdCl_2$ treatment. The shift indicates that a loss of Zn has occurred during the $CdCl_2$ treatment and the residual material is Zn depleted.

Chapter 5
$ZnCl_2$ Passivation Treatment on RF Sputtered CdZnTe

5.1 Tested Hypothesis RF Sputtered CdZnTe with $ZnCl_2$ Passivation Treatment

The initial material and electrical characterization results on RF sputtered CdZnTe treated with $ZnCl_2$ in the horizontal bell jar exhibited:

a) No loss of zinc from CdZnTe
b) In XRD, the CdZnTe film orientation changed towards more random
c) Under SEM, loosely attached fine grain structure with large grains randomly distributed was observed.
d) Delamination occurred at CdS/CdZnTe interface due to the condensation of $ZnCl_2$
e) The devices exhibited low current density and break down was observed in the reverse bias condition
f) The condensation occurred due to the lower substrate temperature during the $ZnCl_2$ Treatment
g) Accumulation of melted $ZnCl_2$ at one edge of the source was observed after the $ZnCl_2$ treatment

Based on the intial results, it was concluded that

a) The substrate temperature was lower than the source and top plate temperature during the $ZnCl_2$ treatment and likely the cause of $ZnCl_2$ condensation
b) For uniform treatment, a new source to hold the $ZnCl_2$ uniformly during and after the treatment was required

5.2 Source Modification in the Horizontal Bell Jar

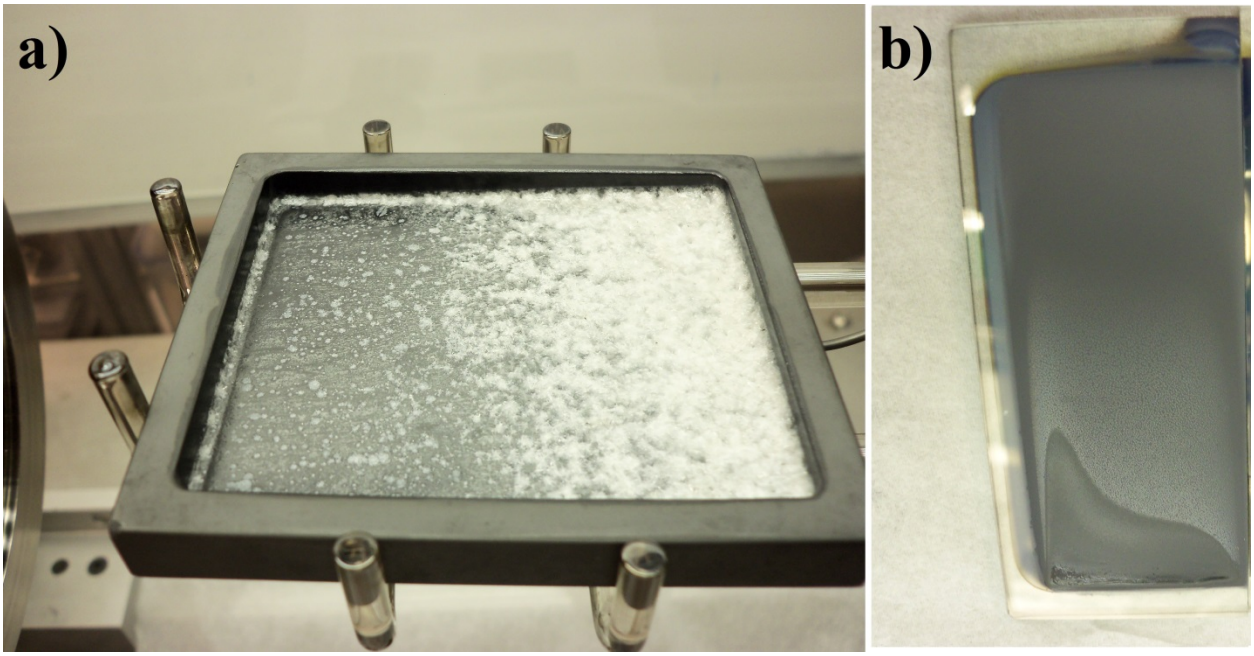

Figure 53 a) Accumulated $ZnCl_2$ after the treatement in the grapite source without any pockets. b) non-uniform $ZnCl_2$ treatment on the substrate

The $ZnCl_2$ melting temperature is at 296^oC [42]. The $ZnCl_2$ treatment is conducted at 380^oC. So during the $ZnCl_2$ treatment, the $ZnCl_2$ powder in the source melts and some of it sublimates. Due to a slight angle in the source holder, the melted $ZnCl_2$ accumulates at edge of the source. After cooling to room temperature, the $ZnCl_2$ solidifies near the edge (Figure 53a). The flowing of $ZnCl_2$ towards the edge affected the passivation treatment process on the samples. As shown in the Figure 53b, the treatment was aggressive at the edge where $ZnCl_2$ was accumulated. Few attempts were made to levelised the source holder before the treatment. But after the treatment, the $ZnCl_2$ was still getting accumulated at one of the edges of the source.

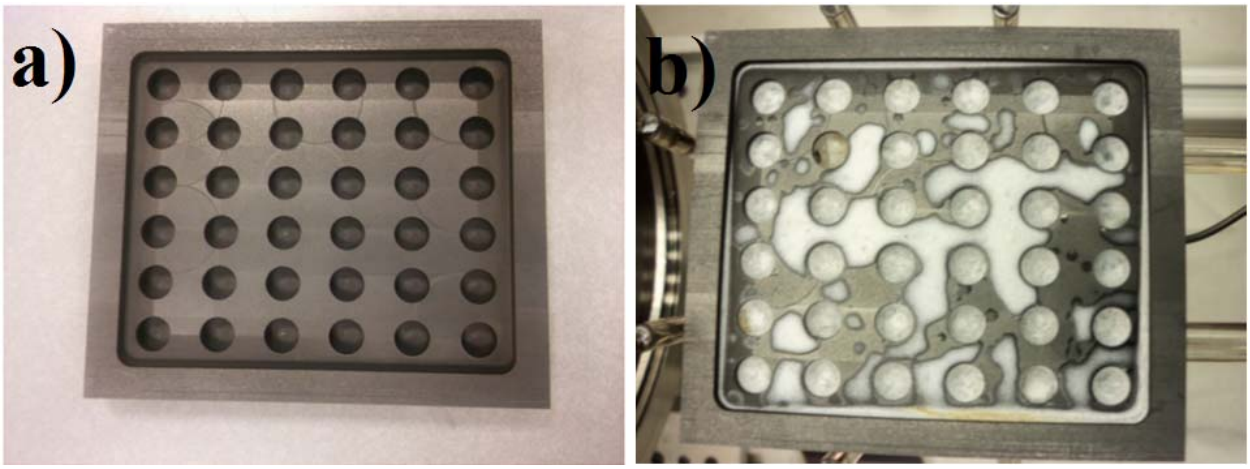

Figure 54a) New graphite source with pockets was fabricated. b) $ZnCl_2$ was contained in the pockets after the treatment

To prevent the accumulation of $ZnCl_2$, a new source was designed and fabricated at Electro-Tech Machining shop, California. The new source had pockets fabricated so that the melted $ZnCl_2$ is contained in the pockets during the treatment (Figure 54). The dimensions of the pockets were 0.25 inches in diameter and $ZnCl_2$ was loaded in all the pockets before the treatment. The overall dimensions of the new source with pockets was same as the one without pockets.

5.3 Graphite Source and Substrate Temperature Measurements

For the temperature measurements, a thermocouple was cemented to the center of the substrate on the TCO side. The temperature output of the top plate, the graphite source plate and the thermocouple attached to substrate were measured. The assumption was made that the substrate temperature without any CdZnTe film would be comparable with the substrate temperature with CdZnTe layer under similar heating conditions. The graphite source did not contain any $ZnCl_2$ material for the temperature measurement experiments.

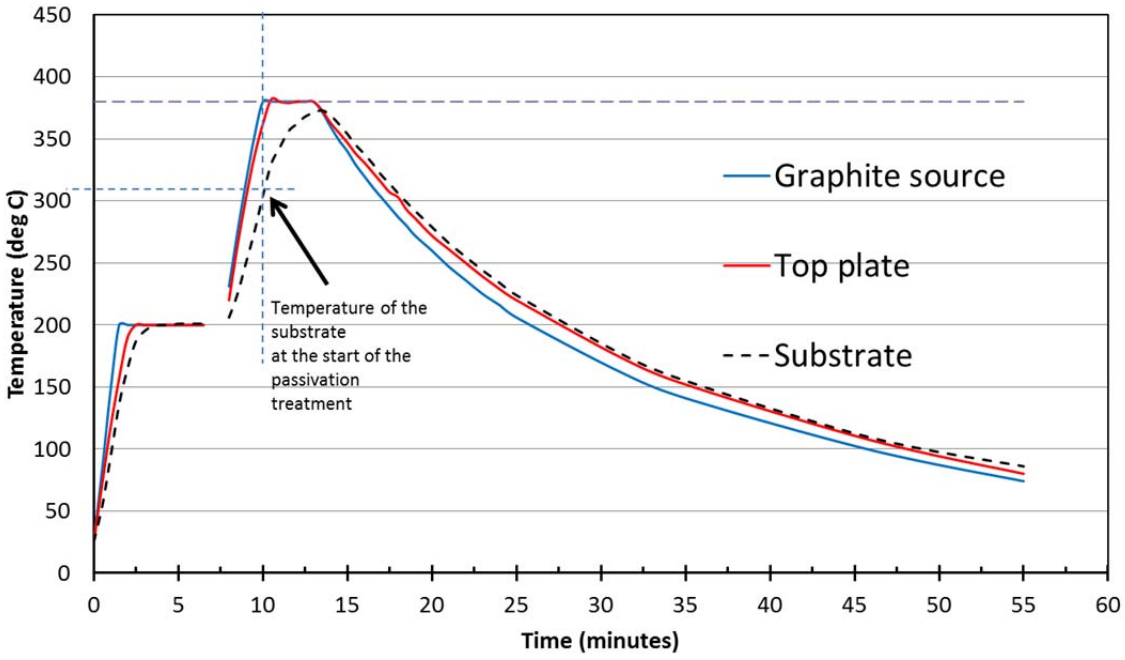

Figure 55 Temperature measurements using the parameters in section 2.3

In first set of the temperature measurements, the parameters in the section 2.3 were used and Temperature vs Time was plotted (Figure 55). The top plate and the graphite source reached 380^{o}C after ~10 minutes of heating. But the substrate temperature measured was 310^{o}C which is colder than the top plate and the graphite source. The colder substrate leads to the condensation of the $ZnCl_2$ and would be the possible cause for delamination of the films.

In the next three sets of temperature measurements, the top plate temperature was fixed to 400^{o}C. A dwell time of 5 minutes was given to stabilize the temperature and also heat the substrate. After 5 minutes, the graphite source temperature was set to 340^{o}C (set II), 360^{o}C (set III) and 380^{o}C (set IV).

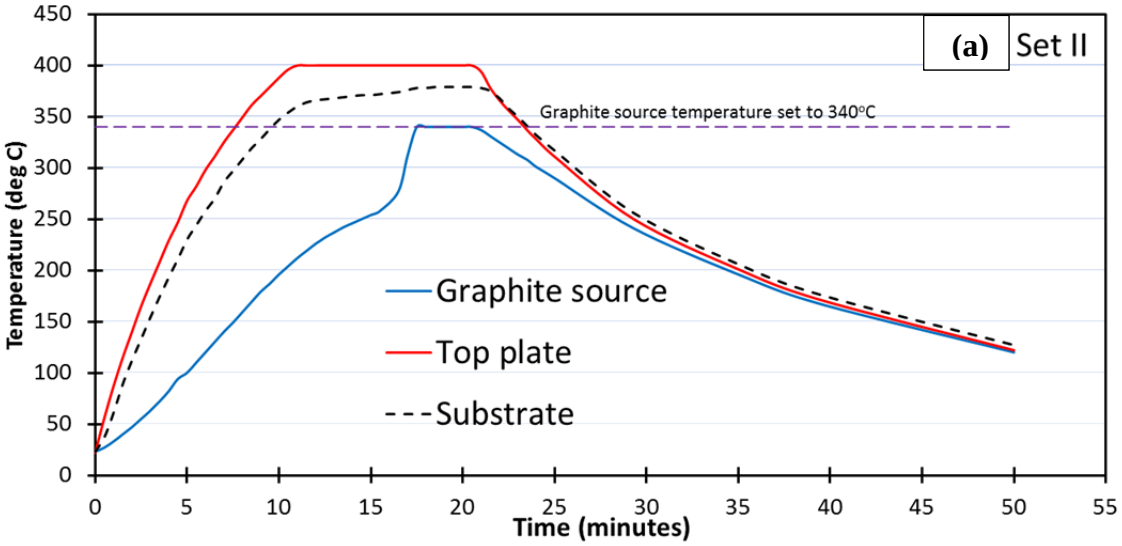
(a)
Set II
Graphite source temperature set to 340°C
Graphite source
Top plate
Substrate
Temperature (deg C)
Time (minutes)
0
50
100
150
200
250
300
350
400
450
0
5
10
15
20
25
30
35
40
45
50
55

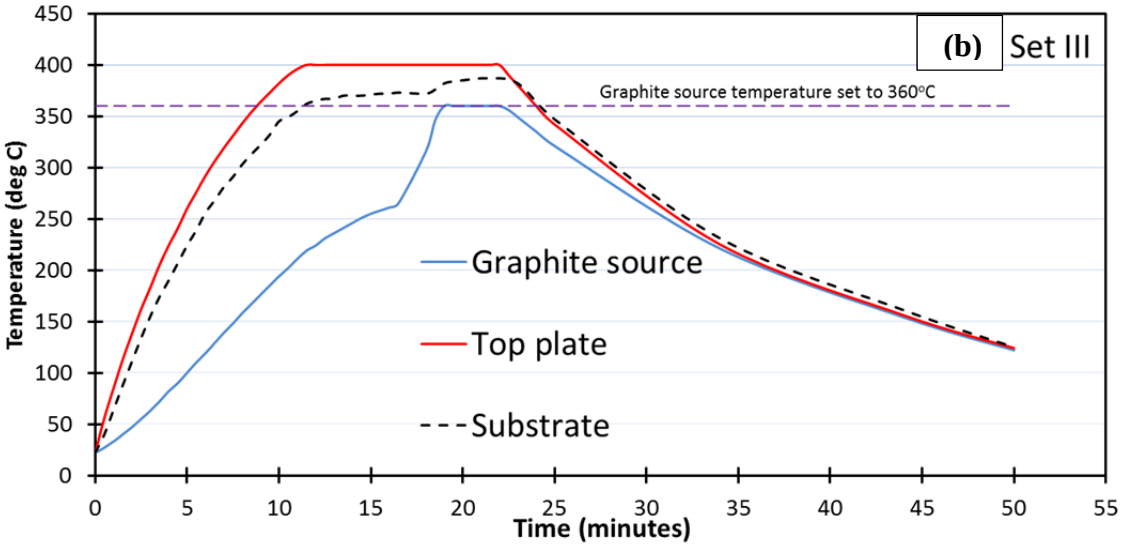
(b)
Set III
Graphite source temperature set to 360°C
Graphite source
Top plate
Substrate
Temperature (deg C)
Time (minutes)
0
50
100
150
200
250
300
350
400
450
0
5
10
15
20
25
30
35
40
45
50
55

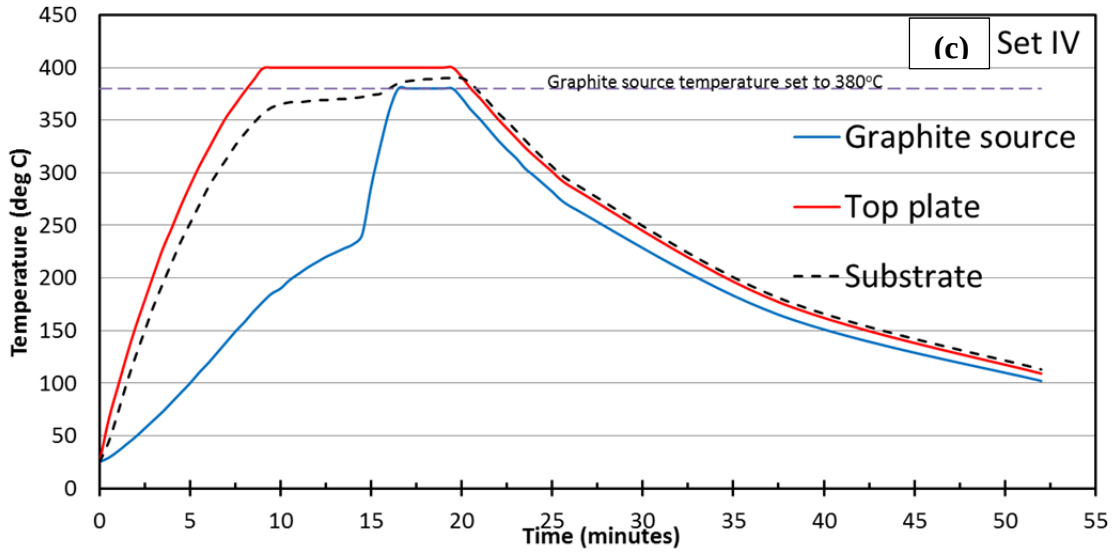

Figure 56 Temperature measurements with fixed top plate temperature fixed and the temperature of the graphite source was varied to a) 340°C, b) 360°C and c) 380°C.

The temperature measured from the three sets is shown in the Figure 56. In all the mentioned sets, it took ~10 minutes for the top plate to reach to a temperature of 400°C. After the 5 minutes of dwell time, the substrate reached 380°C which was suitable for the $ZnCl_2$ experiments. The substrate temperature was always greater than the graphite source temperature which would avoid any condensation of $ZnCl_2$ during the passivation treatment.

5.4 $ZnCl_2$ Passivation Treatment on RF Sputtered CdZnTe with New Source and Higher Substrate Temperature

The $ZnCl_2$ passivation treatment on RF sputtered CdZnTe was performed using the parameters described in the section 5.3. The objective was to keep the substrate temperature greater than the graphite source temperature to prevent $ZnCl_2$ condensation on the substrate. The $ZnCl_2$ of 10 grams in total was loaded in the different pockets of the newly fabricated graphite source. Instead of CdS layer, MgZnO was used. The thickness of the RF sputtered CdZnTe was 1 micron. The details about the passivation time and temperature are given in the table .

Table 12 $ZnCl_2$ passivation treatment conditions with new graphite source

Passivation Temperature *(deg C)*	Top Graphite Plate Temperature *(deg C)*	Time *(minutes)*
Control	-	-
340	400	3
360	400	3
380	400	3
380	400	5

5.5 Transmission Measurements on RF Sputtered CdZnTe After $ZnCl_2$ Passivation Treatment with New Source and Higher Substrate Temperature

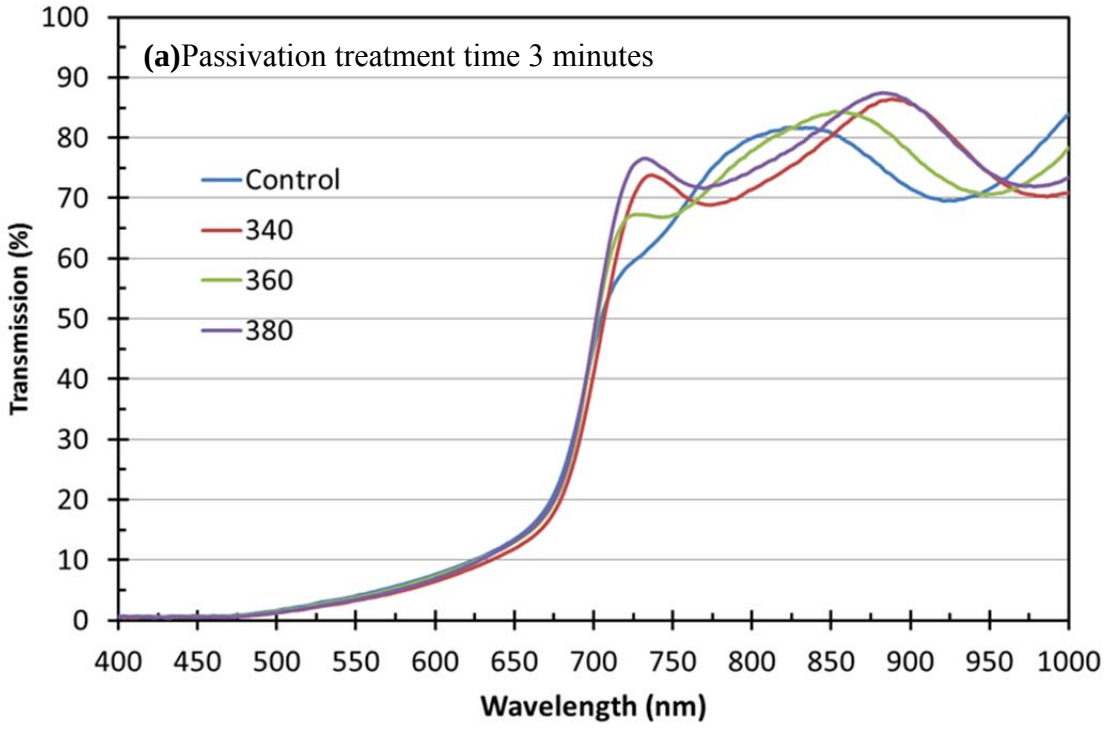

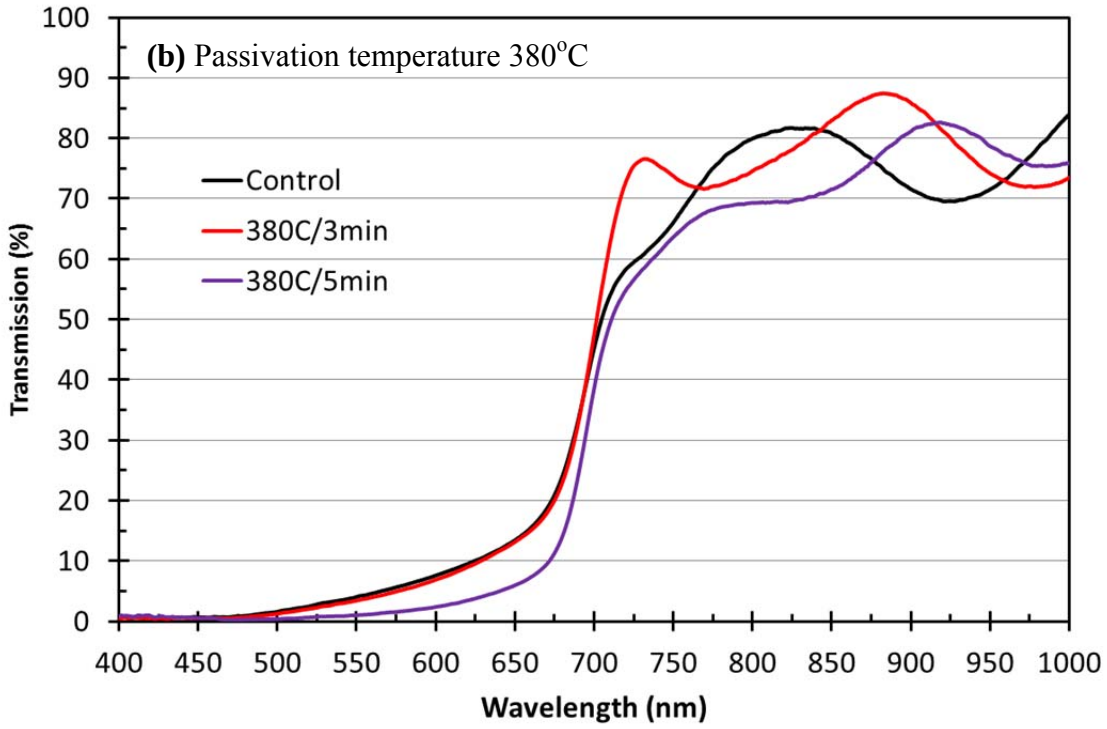

Figure 57 Transmission measurements on RF sputtered CdZnTe after $ZnCl_2$ passivation in the new graphite source and at higher substrate temperature. a) passivation treatment temperature varied. b) passivation treatment time varied

As shown in the Figure 57(a) and (b), after the $ZnCl_2$ passivation treatment, the shift in the band edge is not detected. This implies that the composition of the CdZnTe after the treatment is same as before the treatment. The substrate at the higher temperature during the treatment does not affect the change in the composition of CdZnTe.

5.6 Tape Test on RF Sputtered CdZnTe after the $ZnCl_2$ Passivation Treatment with New Source and Higher Substrate Temperature

The tape test was performed on all the samples after the $ZnCl_2$ passivation treatment. The delamination of the CdZnTe film was not observed which suggested that $ZnCl_2$ condensation on the CdZnTe film did not occur due to higher substrate temperature.

5.7 Device Performance of RF Sputtered CdZnTe after $ZnCl_2$ Passivation Treatment with New Source and Higher Substrate Temperature

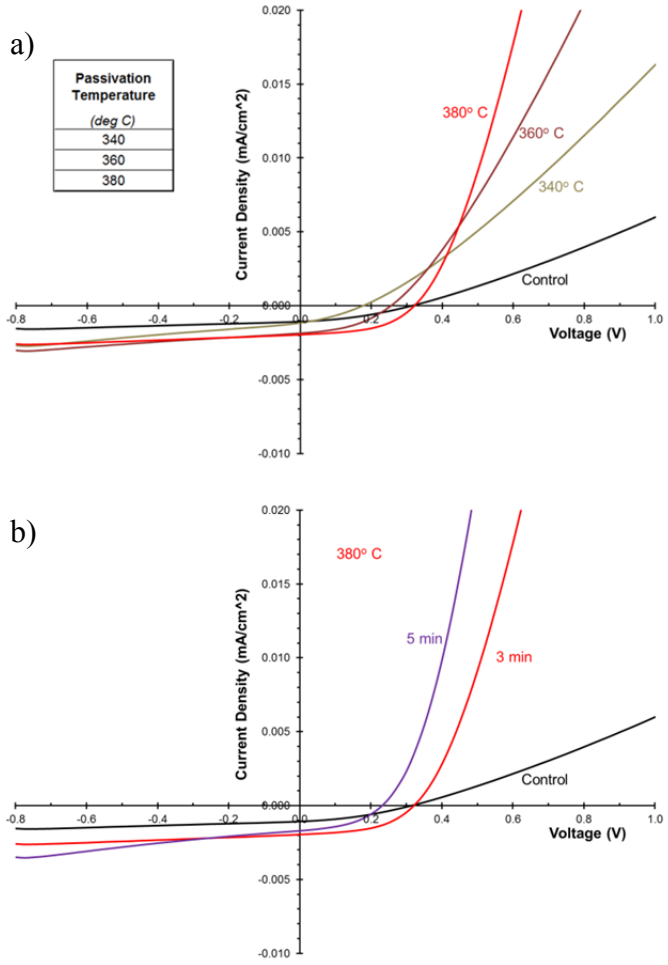

Figure 58 JV device performance of RF sputtered CdZnTe after $ZnCl_2$ passivation in the new graphite source and at higher substrate temperature. a) passivation treatment temperature varied. b) passivation treatment time varied

As shown in the Figure 58(a) and (b), there is improvement in the device performance after the $ZnCl_2$ treatment when compared with the control sample. The device performance improved with the increasing passivation temperature. With the longer $ZnCl_2$ passivation time at same passivation temperature, there was a decrease in the device performance suggesting that longer time would be detrimental to the device performance.

5.8 SEM Images of RF Sputtered CdZnTe after the $ZnCl_2$ Passivation Treatment with New Source and Higher Substrate Temperature

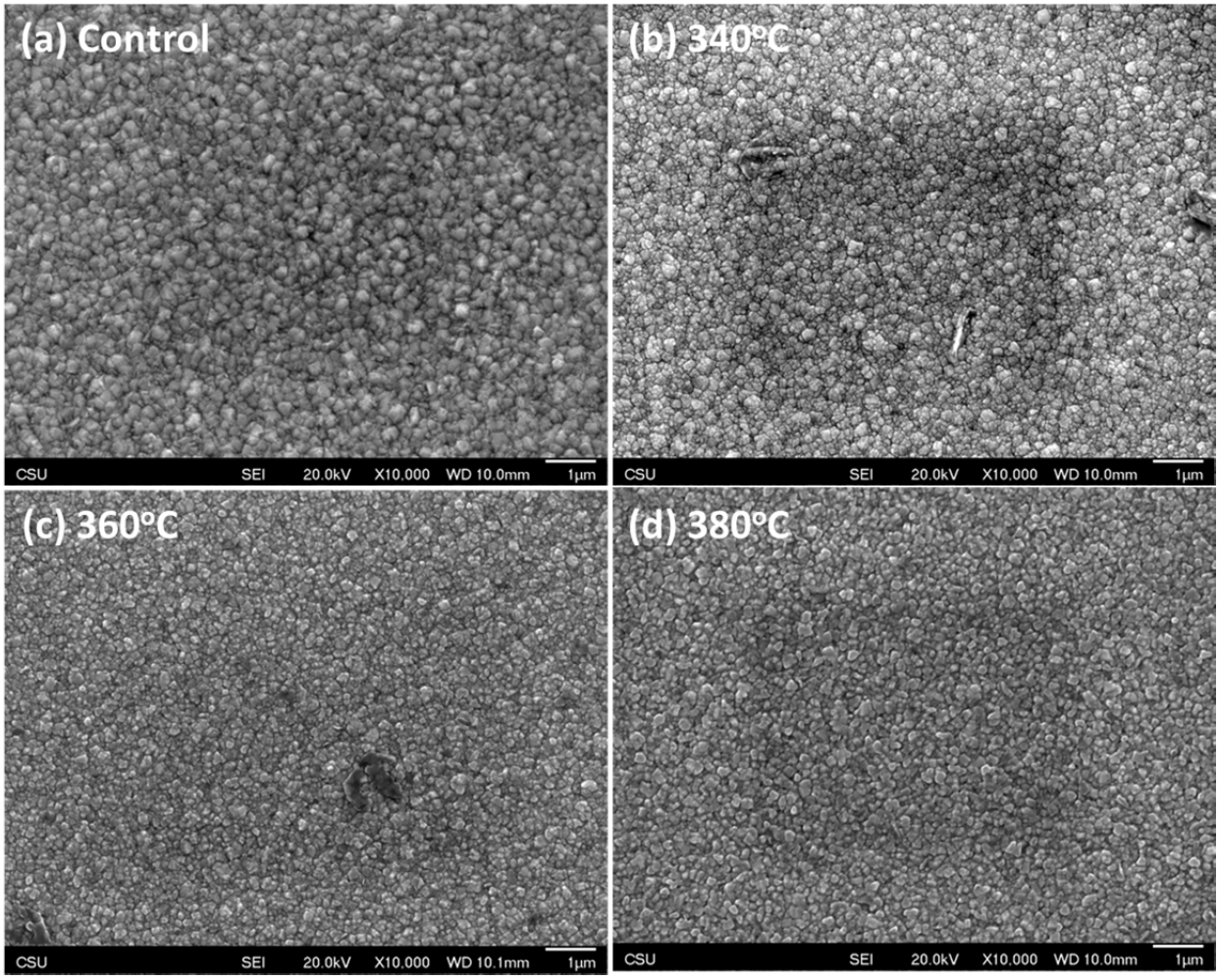

Figure 59 SEM images of CdZnTe (a) before and (b)(c)&(d) after the $ZnCl_2$ passivation treatment at for 3 minutes with the new source and higher substrate temperature

The SEM images of RF sputtered CdZnTe before and after the $ZnCl_2$ passivation treatment at 380^{o}C for 3 minutes is shown in the Figure 59. After the treatment, increase in the grain size of the CdZnTe was not observed but morphology of the grains changed from round shaped to flat and more faceted with the increase in the passivation temperature. No delamination of the films was observed under SEM.

Chapter 6
Conclusions and Future Work

6.1 Summary

The passivation of polycrystalline CdZnTe films is an essential step to improve the absorber quality and device performance. In this study, CdZnTe films with different structures were passivated with different chloride compounds ($CdCl_2$, $MgCl_2$, and $ZnCl_2$) individually. The objective was to check whether the passivation had occurred without any significant change in the composition of the CdZnTe films. The metrics for passivation were:

a) Chlorine along the grain boundaries
b) Removal of stacking faults in the grains
c) Recrystallization and grain growth
d) Diode-like behavior in JV measurements
e) Current collection in EQE
f) No shift in the band edge towards the longer wavelength region observed in the transmission and EQE
g) Change in the composition detected in the GAXRD

6.2 $CdCl_2$ Treatment of RF Sputtered CdZnTe

In the RF sputtered CdZnTe films treated with $CdCl_2$ showed that the Zn loss initiated at the back surface and proceeded towards the front junction through the grains. The grain growth was observed in the zinc depleted region. The chlorine signal in the bulk of CdZnTe was below the detection limit with stacking faults visible. The shift in the band edge towards the longer wavelength was observed in the transmission. The diffracted peaks in the GAXRD suggested the formation of alloy close to CdTe. The fabricated devices did not exhibit the diode like behavior.

6.3 $CdCl_2$ Treatment on RF Sputtered CdZnTe with CdTe Cap Acting as a Capping

With a CdTe capping on the back of RF sputtered CdZnTe film, zinc retention was observed in the sample treated with lower passivation temperature (380^{o}C). The grain growth and the prescence of chlorine along the grain boundaries was observed. The improvement in the device performance with the shift in the band edge towards the longer wavelength region was also observed. The shift in the band edge would be due to the current collection from the CdTe cap and CdTe formed due to the loss of zinc. This suggests that the CdTe cap is not suitable for the passivation treatment with $CdCl_2$.

6.4 . $CdCl_2$ Treatment on RF Sputtered CdZnTe and Co-Sublimated CdTe and Zn with CdS Cap Acting as a Capping

At passivation temperature 380^{o}C and treatment times between 1 to 5 minutes, no shift in the band edge was observed in the RF sputtered CdZnTe films. The diode like behavior was observed in the devices treated for 2 minutes. However longer treatment times generated pinholes in the CdZnTe films which were detrimental to device performance.

For co-sublimated CdZnTe fitted with CdS cap during the $CdCl_2$ treatment had chlorine along the grain boundaries. The stacking faults were present in few CdZnTe grains which suggested that more aggressive or longer $CdCl_2$ treatment is required. But more aggressive or longer $CdCl_2$ treatment will increase the zinc diffusion in the CdS cap. The diffracted peaks closely match the alloy composition of the as-deposited CdZnTe film. The fabricated device had the best performance in this study. In the EQE, the band edge was retained with the current collection close 0.7 near the short wavelength region.

6.5 $MgCl_2$ Treatment on RF Sputtered CdZnTe

Under SEM, the change in the morphology of CdZnTe films from spherical shaped grains to a faceted was observed. No loss zinc was observed in the transmission. But the photogenerated current was low indicating that the devices were not completely passivated.

6.6 $ZnCl_2$ Treatment on RF Sputtered CdZnTe

There was no loss of zinc from RF sputtered CdZnTe in all the $ZnCl_2$ passivation treatments conducted in this study. The delamination of CdZnTe films did not occur when the substrate temperature was higher than the source during the $ZnCl_2$ passivation treatment. However, grain size did not change which led to poor performing devices.

6.7 Overall Conclusions

$CdCl_2$ and $ZnCl_2$ are found to be effective for passivating CdZnTe films. A capping is required at the back of CdZnTe films to prevent zinc from escaping during the $CdCl_2$ passivation treatment. For $ZnCl_2$ passivation treatment to be effective, higher substrate temperature is required to prevent the delamination of CdZnTe films.

6.8 Future Work

The zinc diffusion in the CdS cap during the $CdCl_2$ passivation treatment is one of the disadvantages. Moreover acidic solution is required to etch CdS cap which may harm the underlying MgZnO window layer. To minimize zinc diffusion in the capping layer, an oxide layer instead of CdS should be used. Recently, high lifetimes in CdTe devices have been achieved by depositing alumina on the back of CdTe and then treating with the $CdCl_2$ [43]. The alumina layer can be easily etched off by using a basic solution without harming the underlying MgZnO. The device configuration with CdZnTe capped with alumina should be tried to improve the passivation.

Bibliography

[1] G. Martin, *Solar Cells: Operating Principles, Technology and System Applications*. 1985.

[2] K. Zweibel, *Harnessing Solar Power: The Photovoltaics Challenge*. Springer US, 1990.

[3] W. Shockley and H. J. Queisser, "Detailed balance limit of efficiency of p-n junction solar cells," *J. Appl. Phys.*, vol. 32, no. 3, pp. 510–519, 1961.

[4] NREL, "Best Research Cell Efficiencies." [Online]. Available: http://www.nrel.gov/ncpv/images/efficiency_chart.jpg. [Accessed: 01-Mar-2016].

[5] First Solar, "CdTe Efficiency 22.1%." [Online]. Available: www.firstsolar.com. [Accessed: 07-May-2018].

[6] L. C. Hirst and N. J. Ekins-Daukes, "Fundamental losses in solar cells," *Prog. Photovoltaics Res. Appl.*, vol. 19, no. 3, pp. 286–293, May 2011.

[7] A. Smets, "ET3034x Solar Energy Course." edX, 2015.

[8] G. F. Brown and J. Wu, "Third generation photovoltaics," *Laser Photonics Rev.*, vol. 3, no. 4, pp. 394–405, 2009.

[9] "Tandem solar cells." [Online]. Available: http://www.superstrate.net/pv/limit/tandem.html.

[10] C. B. Bremner, S. P., Levy, M. Y. and Honsberg, "Analysis of Tandem Solar Cell Efficiencies Under AM1.5G Spectrum Using a Rapid Flux Calculation Method," *Prog. Photovoltaics Res. Appl.*, vol. 16, no. 1, pp. 225–233, 2008.

[11] J. D. Major, R. E. Treharne, L. J. Phillips, and K. Durose, "A low-cost non-toxic post-growth activation step for CdTe solar cells," *Nature*, vol. 511, no. 7509, pp. 334–337, 2014.

[12] C. Li, Y. Wu, J. Poplawsky, T. J. Pennycook, N. Paudel, W. Yin, S. J. Haigh, M. P. Oxley, A. R. Lupini, M. Al-Jassim, S. J. Pennycook, and Y. Yan, "Grain-Boundary-Enhanced Carrier Collection in CdTe Solar Cells," *Phys. Rev. Lett.*, vol. 112, no. 15, p. 156103, 2014.

[13] M. Terheggen, H. Heinrich, G. Kostorz, A. Romeo, D. Baetzner, A. N. Tiwari, A. Bosio, and N. Romeo, "Structural and Chemical Interface Characterization of CdTe Solar Cells by Transmission Electron Microscopy," *Thin Solid Films*, vol. 431–432, no. 3, pp. 262–266, 2003.

[14] B. E. McCandless, L. V. Moulton, and R. W. Birkmire, "Recrystallization and sulfur diffusion in CdCl2-treated CdTe/CdS thin films," *Prog. Photovoltaics Res. Appl.*, vol. 5, no. March, pp. 249–260, 1997.

[15] M. Rami, E. Benamar, M. Fahoume, F. Chraibi, and a Ennaoui, “Effect of heat treatment with CdCl 2 on the electrodeposited CdTe / CdS heterojunction (A),” vol. 3, no. 1, pp. 66–70, 2000.

[16] A. Abbas, B. Maniscalco, J. W. Bowers, P. M. Kaminski, G. D. West, and J. M. Walls, “Initiation of the cadmium chloride assisted re-crystallization process of magnetron sputtered thin film CdTe,” *Conf. Rec. IEEE Photovolt. Spec. Conf.*, pp. 1930–1934, 2013.

[17] J. Lee, “Effects of heat treatment of vacuum evaporated CdCl2 layer on the properties of CdS/CdTe solar cells,” *Curr. Appl. Phys.*, vol. 11, no. 1 SUPPL., pp. S103–S108, 2011.

[18] A. Abbas, G. D. West, J. W. Bowers, P. Isherwood, P. M. Kaminski, B. Maniscalco, P. Rowley, J. M. Walls, K. Barricklow, W. S. Sampath, and K. L. Barth, “The effect of cadmium chloride treatment on close-spaced sublimated cadmium telluride thin-film solar cells,” *IEEE J. Photovoltaics*, vol. 3, no. 4, pp. 1361–1366, 2013.

[19] J.-H. Yang, S. Chen, W.-J. Yin, X. G. Gong, A. Walsh, and S.-H. Wei, “Electronic structure and phase stability of MgTe, ZnTe, CdTe, and their alloys in the *B* 3, *B* 4, and *B* 8 structures,” *Phys. Rev. B*, vol. 79, no. 24, p. 245202, 2009.

[20] K. S. Rahman, F. Haque, N. A. Khan, M. A. Islam, M. M. Alam, Z. A. Alothman, K. Sopian, and N. Amin, “Effect of CdCl2 Treatment on Thermally Evaporated CdTe Thin Films,” *Chalcogenide Lett.*, vol. 11, no. 3, pp. 129–139, 2014.

[21] B. E. McCandless, “Cadmium zinc telluride films for wide band gap solar cells,” *Conf. Rec. Twenty-Ninth IEEE Photovolt. Spec. Conf. 2002.*, pp. 488–491, 2002.

[22] T. J. Coutts, J. S. Ward, D. L. Young, K. A. Emery, T. A. Gessert, and R. Noufi, “Critical issues in the design of polycrystalline, thin-film tandem solar cells,” *Prog. Photovoltaics Res. Appl.*, vol. 11, no. 6, pp. 359–375, 2003.

[23] S. H. Lee, A. Gupta, and A. D. Compaan, “Polycrystalline sputtered Cd(Zn, Mn)Te films for top cells in PV tandem structures,” *Phys. Status Solidi*, vol. 1, no. 4, pp. 1042–1045, 2004.

[24] S. H. Lee, A. Gupta, S. Wang, A. D. Compaan, and B. E. McCandless, “Sputtered Cd1-xZnxTe films for top junctions in tandem solar cells,” *Sol. Energy Mater. Sol. Cells*, vol. 86, no. 4, pp. 551–563, 2005.

[25] R. . Sudharsanan, S. . Ringel, and A. . Rohatgi, “High Efficiency Cadmium and Zinc Telluride Based Thin Film Solar Cells,” 1991.

[26] A. Rohatgi, S. A. Ringel, J. Welch, E. Meeks, K. Pollard, A. Erbil, C. J. Summers, P. V Meyers, and C. H. Liu, “Growth and Characterization of CdMnTe and CdZnTe Polycrystalline Thin Films For Solar Cells,” vol. 24, pp. 185–194, 1988.

[27] P. S. Kobyakov, R. Geisthardt, T. Cote, and W. S. Sampath, “Growth and Characterization of Cd 1-x Mg x Te Thin Films for Possible Application in High-Efficiency Solar Cells,” pp. 160–163, 2011.

[28] B. E. Mccandless, W. A. Buchanan, and G. M. Hanket, “Thin Film Cadmium Zinc Telluride Solar Cells,” pp. 483–486, 2006.

[29] R. Dhere, T. Gessert, J. Zhou, S. Asher, J. Pankow, and H. Moutinho, “Investigation of CdZnTe for Thin-Film Tandem Solar Cell Applications,” *MRS Online Proc. Libr. Arch.*, vol. 763, p. null-null, 2003.

[30] J. Gaduputi, “Characterization Of Cadmium Zinc Telluride Films And Solar Cells On Glass And Flexible Substrates By RF Sputtering,” University of South Florida, 2004.

[31] S. A. Ringel, R. Sudharsanan, A. Rohatgi, and W. B. Carter, “A Study of Polycrystalline Cd (Zn, Mn) Te/CdS Films and Interfaces,” *J. Electron. Mater.*, vol. 19, no. 3, pp. 259–263, 1989.

[32] A. Rohatgi, R. Sudharsanan, S. Ringel, and M. MacDougal, “Growth and Process Optimization of Cdte and Cdznte Polycrystalline Films for High-Efficiency Solar-Cells,” *Sol. Cells*, vol. 30, no. 1–4, pp. 109–122, 1991.

[33] E. Yilmaz, E. Tuğay, A. Aktağ, I. Yildiz, M. Parlak, and R. Turan, “Surface morphology and depth profile study of Cd1−xZnxTe alloy nanostructures,” *J. Alloys Compd.*, vol. 545, pp. 90–98, Dec. 2012.

[34] S. Subramanian, “Characterization of cadmium zinc telluride solar cells by RF sputtering,” 2003.

[35] R. Dhere, T. Gessert, J. Zhou, J. Pankow, S. Asher, and H. Moutinho, “Development of CdxZn1−xTe alloy thin films for tandem solar cell applications,” *Phys. Status Solidi*, vol. 241, no. 3, pp. 771–774, 2004.

[36] G. Sivaraman, “Characterization of cadmium zinc telluride solar cells,” University of South Florida, 2003.

[37] D. E. Swanson, J. M. Kephart, P. S. Kobyakov, K. Walters, K. C. Cameron, K. L. Barth, W. S. Sampath, J. Drayton, and J. R. Sites, “Single vacuum chamber with multiple close space sublimation sources to fabricate CdTe solar cells,” *J. Vac. Sci. Technol. A Vacuum, Surfaces, Film.*, vol. 34, no. 2, p. 21202, 2016.

[38] M. Ohring, *Materials science of thin films*. Academic press, 2001.

[39] ICDD, “© 2014 International Centre for Diffraction Data. All rights reserved.,” *00-050-1439 Cd0.6Zn0.4Te*, no. I, p. 2014, 2014.

[40] ICDD, “© 2014 International Centre for Diffraction Data. All rights reserved.,” *00-015-0770 CdTe*, no. I, p. 2014, 2014.

[41] ICDD, “© 2012 International Centre for Diffraction Data. All rights reserved.,” *00-015-0746 ZnTe*, p. 2012, 2012.

[42] Sigma-Aldrich, “Zinc chloride 99.999% trace metals basis _ Sigma-Aldrich.” [Online]. Available:

http://www.sigmaaldrich.com/catalog/product/aldrich/229997?lang=en&region=US. [Accessed: 08-Jan-2016].

[43] J. M. Kephart, A. Kindvall, D. Williams, D. Kuciauskas, P. Dippo, A. Munshi, and W. S. Sampath, "Sputter-Deposited Oxides for Interface Passivation of CdTe Photovoltaics," *IEEE J. Photovoltaics*, vol. 8, no. 2, pp. 587–593, 2018.